

THE HUMUS/SWAT NATIONAL WATER QUALITY MODELING SYSTEM

OCTOBER 2010

Authors: J.G. Arnold*, Santhi Chinnasamy**, M. Di Luzio**, E.B. Haney**, N. Kannan**, M. White*

*Grassland, Soil and Water Research Laboratory, USDA-ARS, Temple, TX 76502

**Blackland Research Center, Temple, TX 76502

CONTENTS

CHAPTER 1	
OVERVIEW OF THE HUMUS SYSTEM	1
<hr/>	
CHAPTER 2	
LAND-USE DELINEATION	3
<hr/>	
2.1 WATERSHED DELINEATION	4
2.2 HRU DEVELOPMENT	7
2.3 REFERENCES	24
CHAPTER 3	
MODEL INPUT DATA	25
<hr/>	
3.1 WEATHER	26
3.2 ATMOSPHERIC DEPOSITION	35
3.3 POINT SOURCES	42
3.4 PONDS, RESERVOIRS	45
3.5 REFERENCES	45

CHAPTER 4

UN-CULTIVATED MANAGEMENT SYSTEMS	59
4.1 PASTURE	60
4.2 HAY	61
4.3 URBAN	62
4.4 FOREST	69
4.5 WETLAND	70
4.6 BARREN LAND	71
4.7 REFERENCES	71

CHAPTER 5

APEX INTEGRATION	73
5.1 STATISTICAL SAMPLING AND MODELING APPROACH	74
5.2 MODELING CONSERVATION PRACTICES	76
5.3 REFERENCES	83

CHAPTER 6

WATERSHED DELIVERY RATIOS	85
6.1 DEVELOPMENT OF DELIVERY RATIO	86
6.2 DELIVERY RATIO FOR UN-CULTIVATED LAND	89
6.3 COMPUTATION OF TIME OF CONCENTRATION OF THE HRU	92
6.4 REFERENCES	93

CHAPTER 7

CALIBRATION AND VALIDATION	95
7.1 FLOW CALIBRATION AND VALIDATION PROCEDURE	96
7.2 CALIBRATION OF AVERAGE ANNUAL RUNOFF AT 8-DIGIT WATERSHEDS	98
7.3 OBSERVED/ESTIMATED DATA USED FOR SPATIAL CALIBRATION	102
7.4 DEMONSTRATION OF THE SWAT AUTOMATED FLOW CALIBRATION PROCEDURE	104
7.5 NUTRIENT CALIBRATION	112
7.6 REFERENCES	134

ABBREVIATIONS

CAFO	Confined Animal Feeding Operation
CASTNET	Clean Air Status and Trends Network
CEAP	Conservation Effects Assessment Project
CONUS	Conterminous United States
COOP	National Weather Service Cooperative Observer
CREP	Conservation Reserve Enhancement Program
CRP	Conservation Reserve Program
EPA	Environmental Protection Agency
GIS	Geographic Information Systems
HLR	Hydrologic Landscape Regions
HRU	Hydrologic Resources Unit
HUC	Hydrologic Unit Code
HUMUS	Hydrologic Unit Model for the United States
IADN	Integrated Atmospheric Deposition Network
IDW	Inverse Distance Weighted
LAI	Leaf Area Index
LULC	Land Use/Land Cover
NADP	National Atmospheric Deposition Program

NASIS	National Soil Information System
NASS	National Agricultural Statistics Service
NCDC	National Climatic Data Center
NCSS	National Cooperative Soil Survey
NDDN	National Dry Deposition Network
NLCD	National Land Cover Database
NPS	National Park Service
NRCS	Natural Resources Conservation Service
NRI	National Resources Inventory
NSSL	National Soil Survey Laboratory
NTN	National Trends Network
ONRL	Oak Ridge National Laboratory
PRISM	Parameter-elevation Regressions on Independent Slopes Model
QA/QC	Quality Assurance/Quality Control
RCA	Resources Conservation Act
RFF	Resources for the Future
RUSLE	Revised Universal Soil Loss Equation
STATSGO	State Soil Geographic Database
SWAT	Soil Water Assessment Tool
USGS	United State Geological Survey
USGS SPARROW	USGS Spatially Referenced Regressions on Watershed Attributes

CHAPTER 1

OVERVIEW OF THE HUMUS SYSTEM

The HUMUS (Hydrologic Unit Model for the United States) system improves on existing technologies for making national and regional water resource assessment considering both current and projected management conditions. The major components of the HUMUS system are: 1) a basin scale Soil and Water Assessment Tool (SWAT) to model the surface and sub-surface water quality and quantity, 2) a Geographic Information Systems (GIS) to collect, manage, analyze and display the spatial and temporal inputs and outputs, and 3) relational databases needed to manage the non-spatial data and drive the models. The HUMUS project simulates and validates approximately 2,150 8-digit hydrologic unit areas that have been delineated by the USGS for the 18 major river basins in the continental U.S. This report discusses the data integration, calibration and validation of the SWAT/HUMUS project.

The Resources Conservation Act of 1977 (RCA), as amended, required the Department of Agriculture to appraise the status, condition, and trends in the uses and conservation of non-federal soil and water related natural resources. The HUMUS project was initially designed to provide the technical basis for conducting the appraisal of water resources for the 1997 RCA Appraisal Report. It was intended to provide better information than has ever been obtained before about the uses of water on irrigated and non-irrigated agricultural lands and of the physical and economic effects of changing agricultural practices and cropping patterns on future water needs and supplies.

The integrated HUMUS system components include: 1) Simulation Models; 2) Spatial Database System (GIS); and 3) Relational Database System. For approximately 2,150 watershed areas (the 8-digit hydrologic accounting units delineated by the Water Resources Council in the Second National Assessment), the HUMUS project includes information about local weather, soil properties, topography, natural vegetation, cropped areas, runoff, erosion, groundwater, irrigation, and agricultural practices.

CHAPTER 2

LAND-USE DELINEATION

2.1 WATERSHED DELINEATION

The following information was adapted from <http://water.usgs.gov>.

The Nation is divided into 21 major geographic areas or regions (Figure 2-1). The contiguous 48 states consist of 18 regions, while Alaska, Hawaii, and Puerto Rico and other Caribbean areas comprise regions 19, 20, and 21, respectively. Each region contains either the watershed of a major river or the combined watershed of a series of rivers. Each hydrologic unit is identified by a unique hydrologic unit code (HUC) consisting of two to eight digits based on the four levels of classification in the hydrologic unit system.



Figure 2-1. Water Resource Regions

The 21 regions are further divided into 221 subregions. Each subregion includes the area drained by a river system, a reach of a river and its tributaries in that reach, a closed basin(s), or a group of streams forming a coastal drainage area. The subregions of the Texas-Gulf Region are depicted in Figure 2-2.

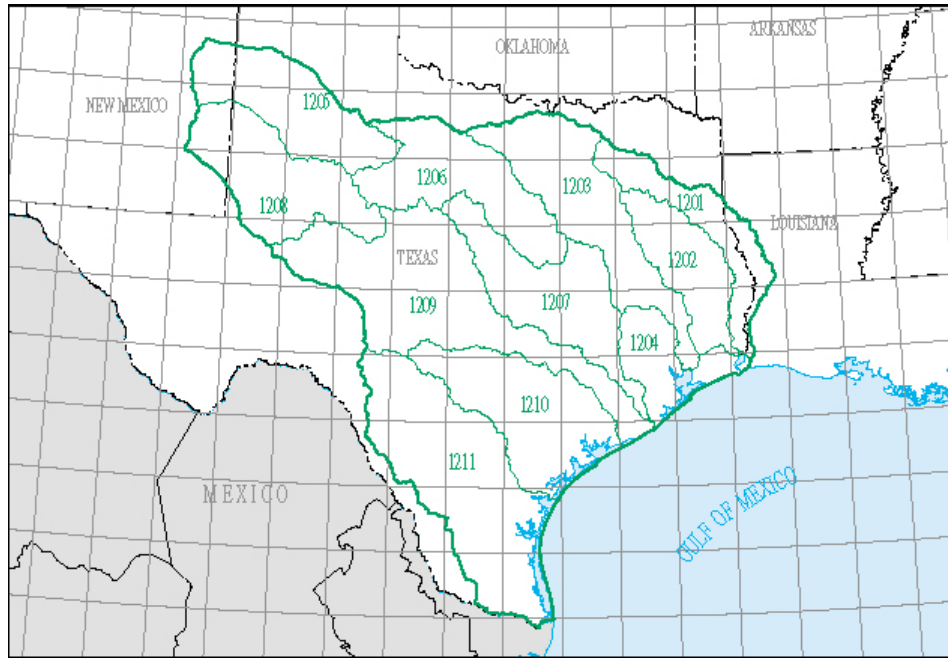


Figure 2-2. Subregions of the Texas-Gulf Region (source: <http://water.usgs.gov>)

The subregions are divided into 378 hydrologic accounting units. These 378 hydrologic accounting units are nested within or are equivalent to the subregions. The accounting units within the *1211* subregion are depicted in Figure 2-3.

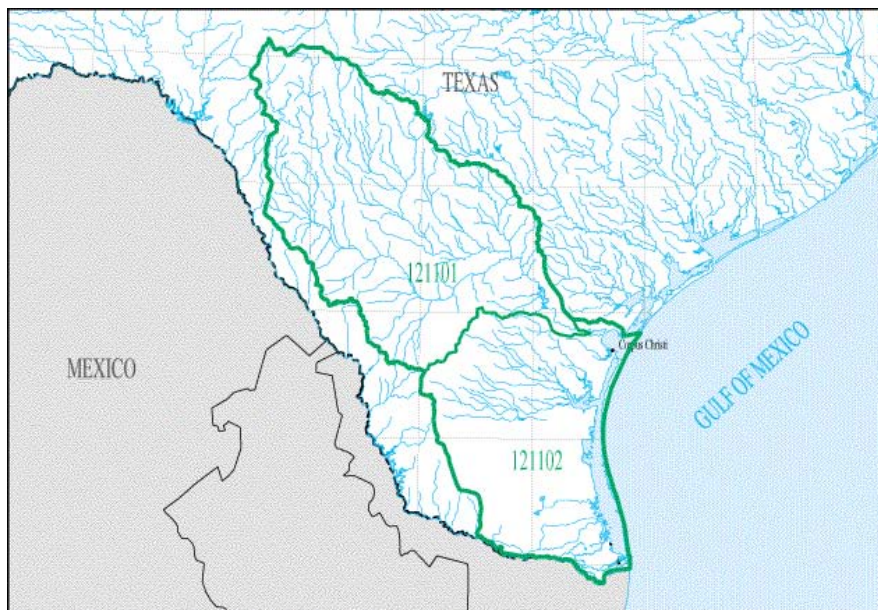


Figure 2-3. Accounting units within the *1211* subregion (source: <http://water.usgs.gov>)

The smallest subdivision of the hydrologic units is the 2264 cataloging units. A cataloging unit is a geographic area representing part of all of a surface drainage basin, a combination of drainage basins, or a distinct hydrologic feature. The cataloging units are identified by 8-digit hydrologic unit codes. For modeling purposes, each 8 digit HUC is represented as a single subbasin in SWAT. The 8-digit HUCs within the 121102 accounting unit are depicted in Figure 2-4.



Figure 2-4. 8-digit hydrologic unit codes (source: <http://water.usgs.gov>)

In the HUMUS set up each 8-digit HUC is subdivided into hydrologic response units (HRUs) that consist of homogeneous land-use, management, and soil characteristics. The HRUs represent percentages of the subwatershed area and are not identified spatially within a SWAT simulation. Alternatively, a watershed can be subdivided into only subwatersheds that are characterized by dominant land-use, soil type, and management.

2.2 HRU DEVELOPMENT

2.2.1 LAND-USE

The HRUs definition and aggregation/disaggregation are fundamental in the CEAP national modeling assessment because they define distinct biophysical/hydrological features of the basin and indirectly establish the areal weight of the simulating components within the total loading. A GIS-based procedure for HRU definition and aggregation/disaggregation was developed to associate the proper land-use/land-cover/soil units and area (acres) to the respective simulation categories within each basic watershed feature (8-digit HUC) and sub-watershed (hydrologic landscape unit). The development of such procedure is described below.

2.2.1.1 DEFINITION OF THE HYDROLOGIC RESPONSE UNITS FOR CEAP HUMUS

Table 2-1 lists the digital data used to establish the areas of the simulation units (HRUs) relative to each watershed feature (HUC) and composing landscape features.

Table 2-1. Data sets applied for the definition of the HRUs

Data Set	Reference
Hydrologic Units of the United States (1:250,000-scale)	USGS, 1994
United States Geological Survey (USGS) National Land-Cover Data Sets (NLCD) 2001 GIS grid (30 m resolution)	Homer et al., 2007
State Soil Geographic Database (STATSGO)	USDA-NRCS, 1992
Hydrologic Landscape Regions (HLR) of the United States (1 km resolution).	USGS, 2003
NRI (Natural Resources Inventory) 1997	USDA-NRCS, 1997
AgCensus 2003 Farm and Ranch Irrigation Survey	USDA NASS, 2004

Figure 2-1 outlines the entire HRU computation flowchart.

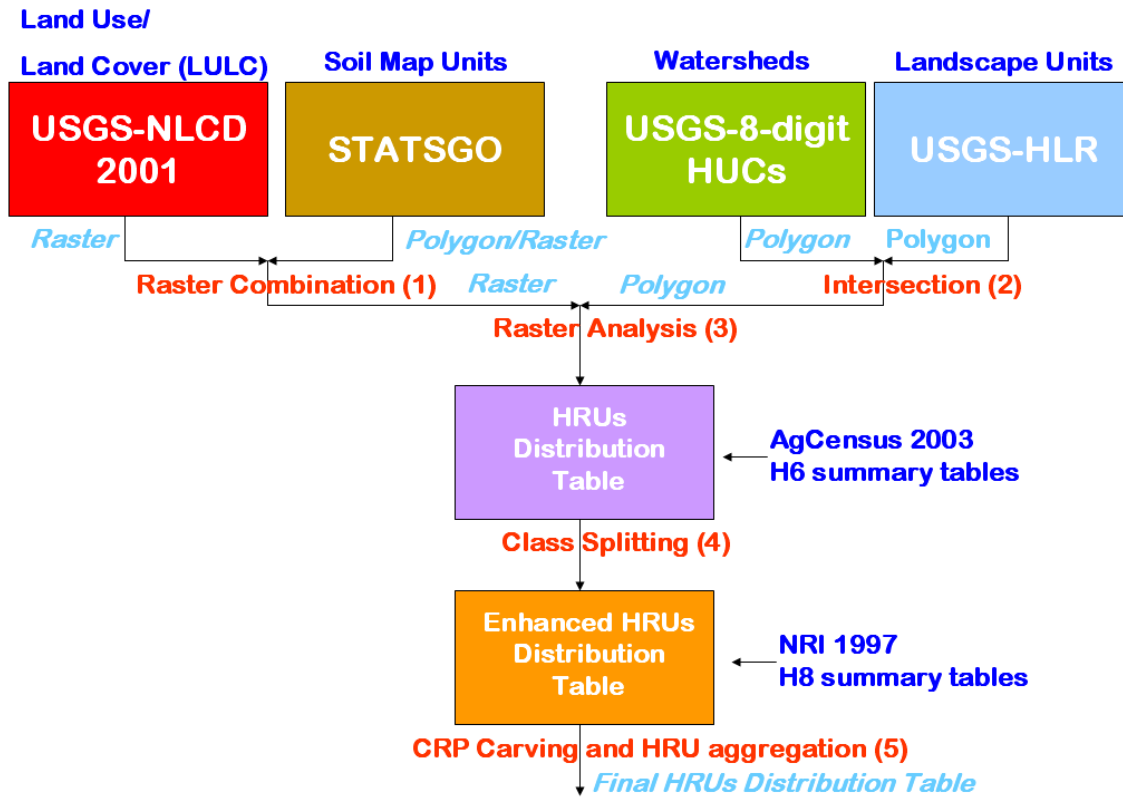


Figure 2-5. Data flowchart for the definition of the HRUs

The developed GIS analysis procedure includes the following tasks: a) combination of the spatial information from the Land Use/Land Cover (LULC) map, the National Land Cover Database (NLCD) 2001 data set; and the soil map units, the State Soil Geographic Database (STATSGO) polygons (Task 1 in Figure 2-5); b) outline of significant elementary portions of the basin area by intersecting the hydrologic landscape regions (HLR) polygon features with the respective HUC polygons (Task 2); and c) definition of the unique combination of LULC and soil classes (HRUs) within them (Task 3). The HRU distribution tables were additionally refined using AgCensus derived summary tables at the 6-digit level (Task 4) and NRI derived summary tables at the 8-digit level (Task 5).

The steps used to process and merge this input information are described in sections 2.2.1.2 through 2.2.1.6.

2.2.1.2 USGS NLCD 2001 AND STATSGO GIS DATA PROCESS

Inputs to Task 1 are the USGS National NLCD 2001 and STATSGO maps. The NLCD, in grid format, is provided by USGS for each 14-production-zone (Figure 2-6). The NLCD data is derived from spring, summer and fall imagery, ancillary DEM (digital elevation models) data, and image derivatives of percent imperviousness and percent tree canopy estimates. Example NLCD land use/land cover data is presented in Figure 2-7.

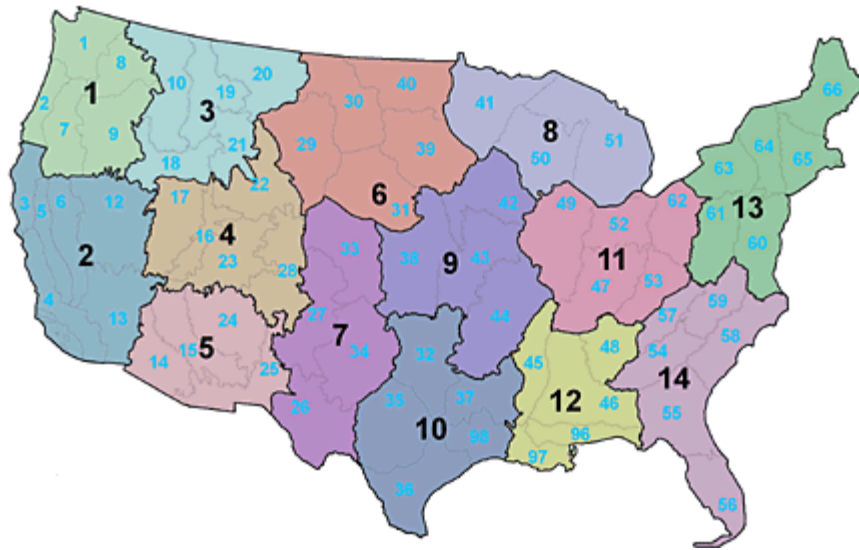


Figure 2-6. Multi-zone for the NLCD 2001 Download Site (obtained from <http://www.mrlc.gov>)

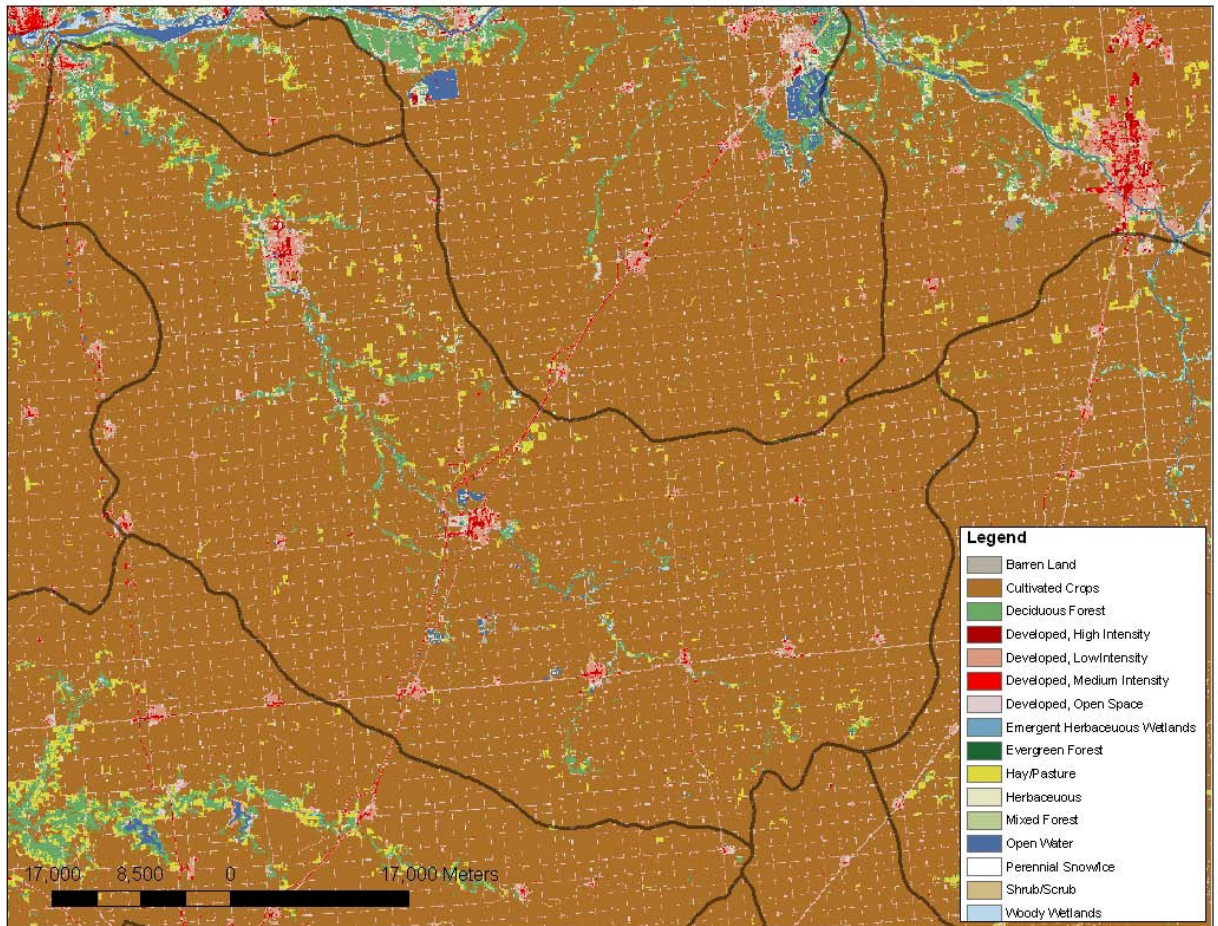


Figure 2-7. Example Land Use/Land-Cover Raster Data for HUC 07130002.

The coordinate system (NAD83 and an Albers Equal Area projection) and resolution (30 m) of these data sets were set as the raster working environment for the remainder of the GIS tasks. The value attribute table for the NLCD grids includes the LULC class code as listed in the first column of Table 3-2.

LULC classes were spatially aggregated following the rules depicted in the second column of Table 2-2.

Table 2-2. United States Geological National Land-Cover Data Sets 2001 (USGS NLCD2001) original and grouped classes.

NLCD 2001 Code. LULC Classes	NLCD Grouped (codes)
11. Open Water	Water (11, 12)
12. Perennial Ice/Snow	
21. Developed, Open Space	Urban (21, 22, 23, 24)
22. Developed, Low Intensity	
23. Developed, Medium Intensity	
24. Developed, High Intensity	
31. Barren Land (Rock/Sand/Clay)	Barren (31)
32. Unconsolidated Shore*	
41. Deciduous Forest	Deciduous Forest (41)
42. Evergreen Forest	Evergreen Forest (42)
43. Mixed Forest	Mixed Forest (43)
51 Dwarf Scrub*	
52. Shrub/Scrub	Range Brush (52)
71. Grassland/Herbaceous.	Range Grasses (71, 72)
72. Sedge/Herbaceous	
72. Lichens*	
74. Moss*	
81. Pasture/Hay	Pasture and Hay (81)
82. Cultivated Crops	Cultiv. Cropland and Horticulture (82)
90. Woody Wetlands	Forested Wetland (90, 91, 93)
91. Palustrine Forested Wetland.	
93. Estuarine Forested Wetland.	
92. Palustrine Scrub/Shrub Wetland.	
94. Estuarine Scrub/Shrub Wetland.	Non-Forest Wetland (92, 94, 95, 96, 97)
95. Emergent Herbaceous Wetlands.	
96. Palustrine Emergent Wetland (Persistent)	
97. Estuarine Emergent Wetland	
98. Palustrine Aquatic Bed	
99. Estuarine Aquatic Bed.	Water (98, 99)

*These LULC classes was absent in the CONUS area.

For computational convenience a raster version (1 km resolution) of the entire set of STATSGO map unit polygons was used (Miller and White, 1998). An example of the STATSGO map unit data is presented in Figure 2-8. The value attribute table for the grid dataset includes the mapunit ID (MUID) for each grid cell. The data set has been re-projected from the original NAD27 to the target NAD83.

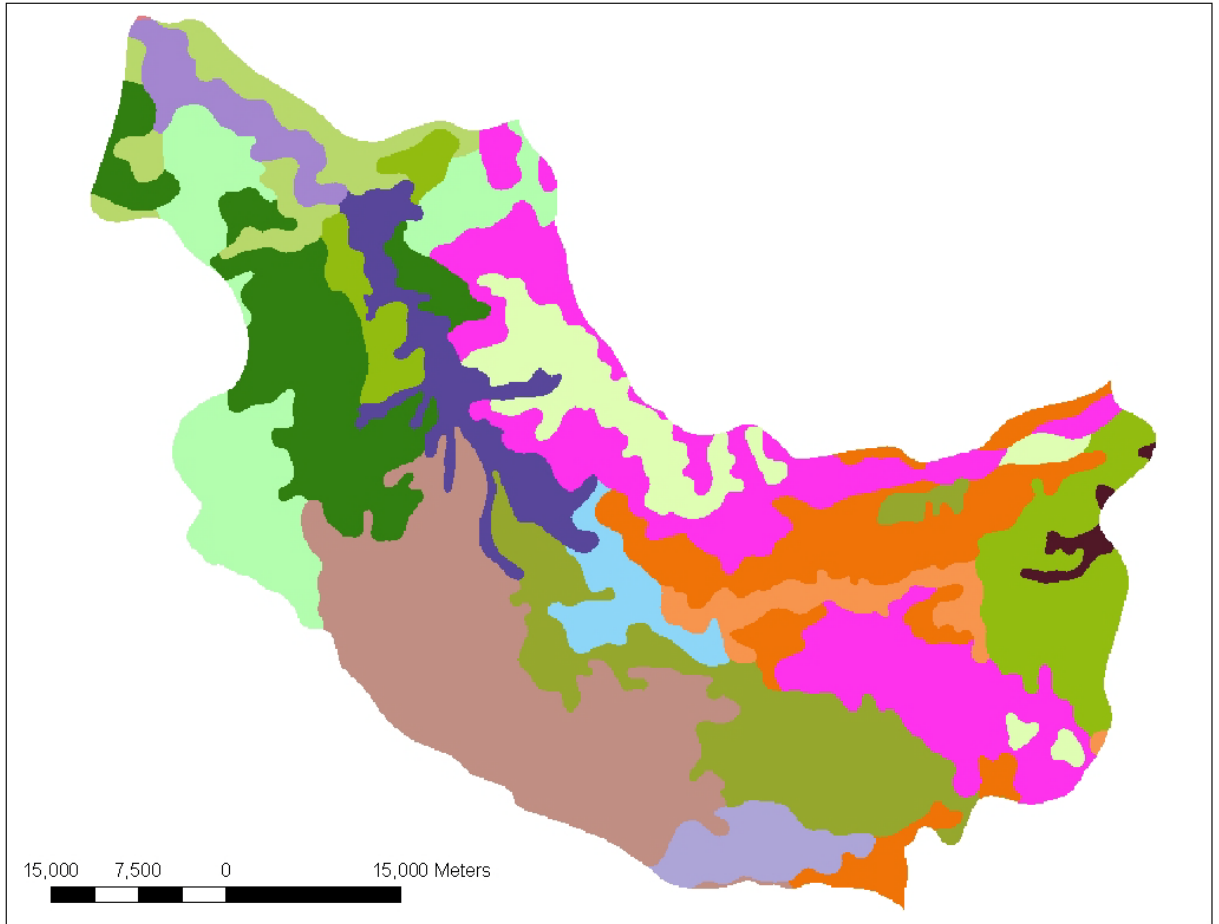


Figure 2-8. STATSGO soils data for HUC 07130002.

The raster combination of the NLCD grouped grid and STATSGO grid, is the output of this task. This grouped data set will be identified as HRU grid for the remainder of the report.

2.2.1.3 USGS HUCs AND HYDROLOGIC LANDSCAPE REGIONS GIS DATA PROCESS.

In CEAP the basic watershed units are outlined by the Hydrologic Units of the United States (USGS, 1994). A significant segmentation of these polygon units was obtained by their intersection with the Hydrologic Landscape Regions (HLR) of the United States (USGS, 2003). The HLRs and the composing watersheds reflect fundamental hydrologic processes that are expected to affect water quality and other environmental characteristics (Winter, 2001). The composing watersheds (43,931 polygons in the United States) extend roughly 200 square kilometers and are distinguished by land-surface form (i.e. slope and relief), geologic texture (permeability of the soil and bedrock), and climate variables.

The data set was re-projected from the original Lambert Azimuthal Equal Area to the target Albers Equal Area projection. Task 2 includes the intersection of the HUC polygons and the HLR ones. For example, the Upper Mississippi basin counts 131 HUC polygons and 2,689 HLR watersheds overlapping/intersecting them (Figure 2-9).

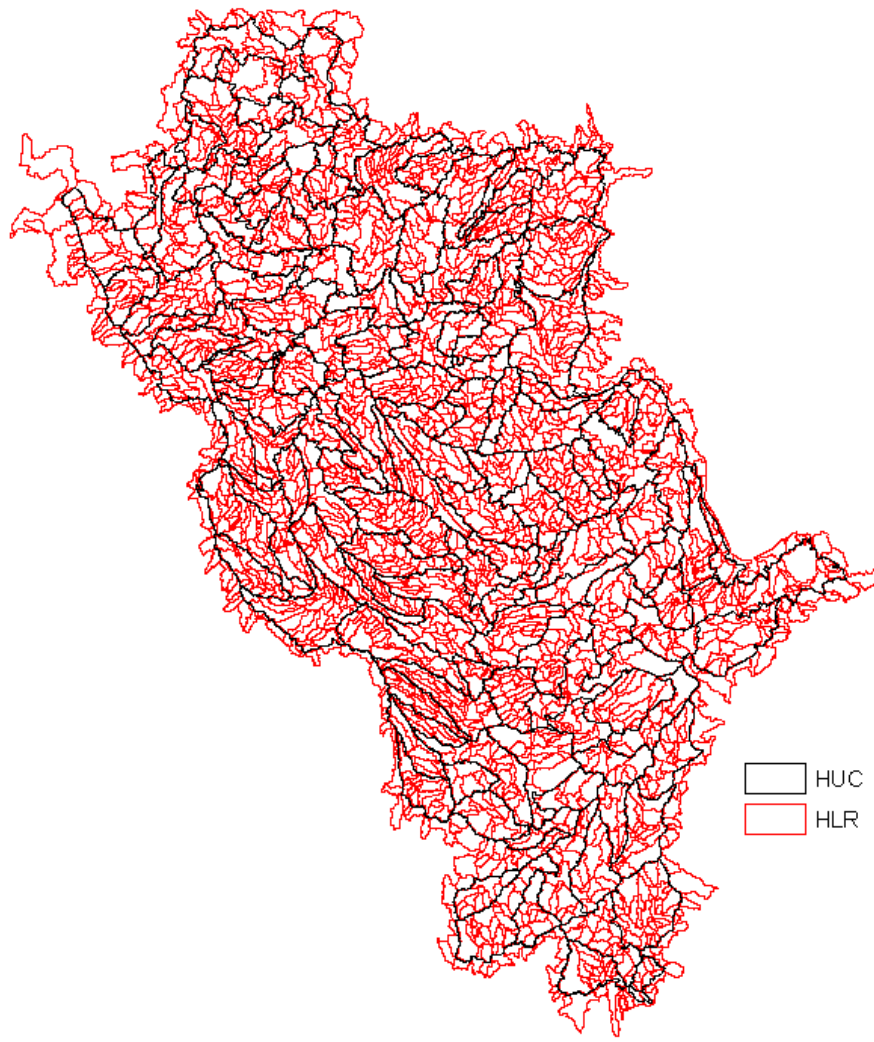


Figure 2-9. USGS HUCs and Hydrologic Landscape Regions (HLR) Watersheds in the Upper Mississippi Basin

2.2.1.4 HRU GRID PROCESS

The HRU grid (combined NLCD and STATSGO data) was spatially analyzed within each HLR watershed composing the respective HUC polygon. The developed procedure included:

- a) Raster extraction over the HLR polygon;
- b) Raster analysis over the extracted data;
- c) Creation of HRU distribution table.

The output of this step is the distribution (reported as percent of the HLR polygon area within the HUC) of the grouped NLCD class/soil association (HRU). The NLCD classes are listed in the second column of Table 2-2. The resulting output spatial data is depicted in Figure 2-10.

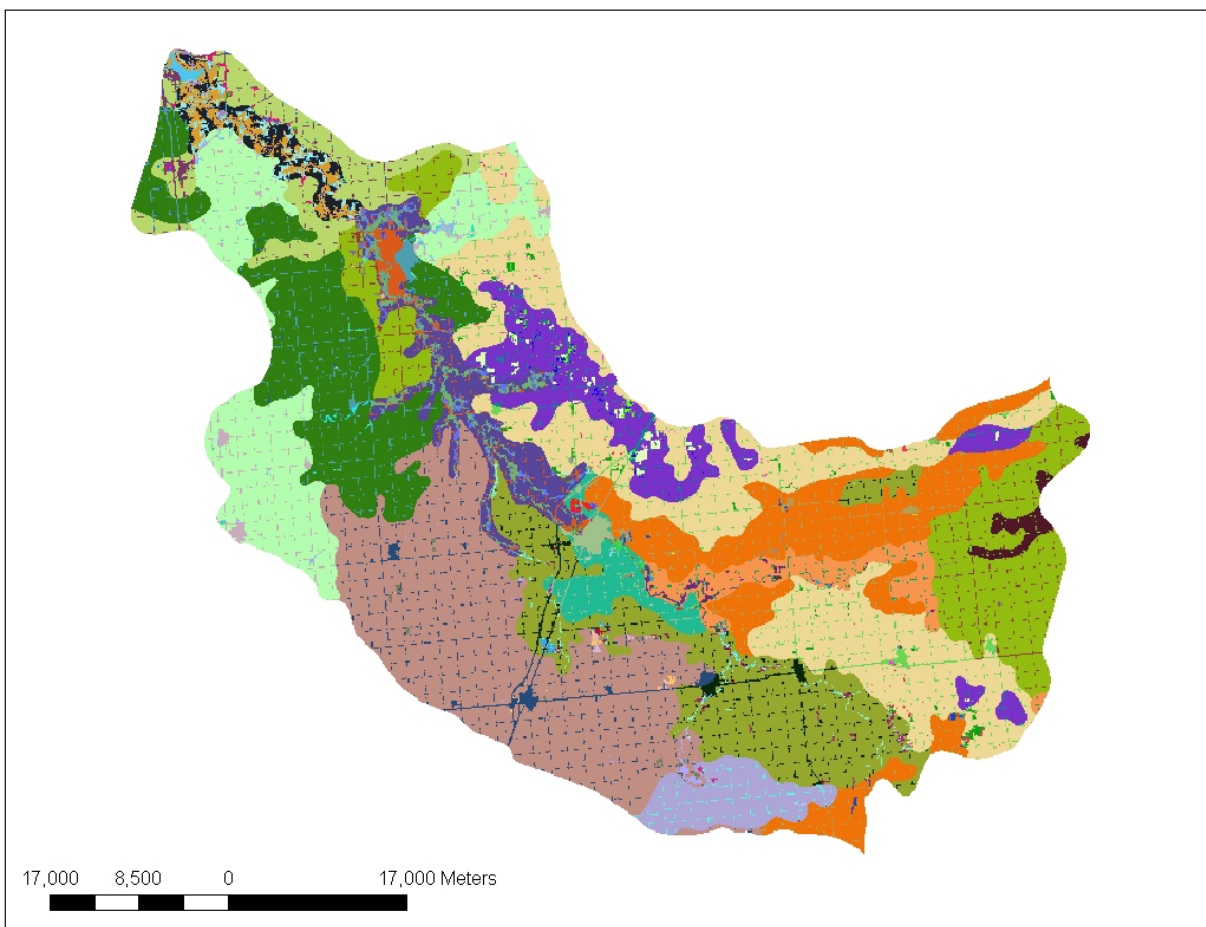


Figure 2-10. Example of the combination output data for HUC 07130002.

In addition:

- a) A single soil, identified by the map unit ID, was assigned to each NLCD group within a distinct HLR watershed. Among the various soils associated to each group, the areal dominant was selected as the most representative of the composing HRU.
- b) The slope of the HLR watershed was associated to the respective HRU. The slope data is inherent in the USGS, 2003 HLR data.

For example, for the Upper Mississippi basin, 24,276 HRUs were defined with the methodology described above (Task 1-3).

2.2.1.5 ASSIMILATION OF AGCENSUS AND NRI INFORMATION

Task 4, class splitting, focuses on two of the land-use classes, Pasture/Hay (original NLCD code 81) and Cultivated Cropland and Horticulture (code 82), highlighted in the second column of Table 2-2. The development of this procedure was necessary to estimate the Cultivated Pasture/Hay and Cultivated Cropland and Horticulture land-use items not specifically identified by the NLCD product, and to distinguish these portions simulated, which are simulated by the APEX model from those designed to be simulated with the SWAT model.

In order to achieve this goal, data from the AgCensus 2003 Farm and Ranch Irrigation Survey and NRI 1997 record acreages summarized at the 6-digit watershed level (USGS accounting unit) were integrated into the previous NLCD analysis. NRI 1997 data are founded on statistically-based survey information from 800,000 sample points throughout the United States and Puerto Rico. The NRI data includes land cover and use, soil erosion, prime farmland soils, wetlands, habitat diversity, selected conservation practices, and related resource attributes (USDA, 2000). The AgCensus 2003 Farm and Ranch Irrigation Survey provides irrigation data for farm practices in 2003, including acres of irrigated land for each land use, yields of irrigated and nonirrigated crops, water application quantity and distribution information (USDA NASS, 2004).

Because the NLCD data is based on imagery, pastureland/hay that has been in rotation (cultivated) or that was actually CRP land were not distinguishable from other pasture/hay and

were identified as pastureland hay (NLCD 81). Since these cultivated portions of hay and pasture are simulated with APEX, NRI data was used to identify the proportion (percent area) of these lands that must be segregated from the NLCD 81 land use, which are simulated with SWAT. In addition, the NLCD 82 classification includes Horticulture, which is simulated with SWAT, and Cropland, which is simulated with APEX. NRI data was utilized to segregate the area that is cropland from the area that is horticulture as identified in NLCD 82.

The AgCensus 2003 Farm and Ranch Irrigation Survey records at the 6-digit level were used to split the pastureland categories (the portion not in rotation simulated by SWAT). These pastureland components (irrigated, I., and non-irrigated, N.-I.) were further subdivided into the respective cultivated (CL.) and un-cultivated (N.-CL) categories again using the proportions estimated using the AgCensus 2003 Farm and Ranch Irrigation Survey records at the 6-digit level.

All portions of the HUMUS Horticulture and HUMUS Hay & Pasture categories were designed to be simulated with the SWAT model. All the categories associated with HUMUS Cropland component are actually designed to be simulated with the APEX model. The output from APEX is assimilated into the SWAT routing modeling framework composing the CEAP national assessment as described in Chapter 5. *APEX Integration*.

HUMUS HORTIC.	HUMUS CROPLAND						HUMUS HAY&PASTURE					
Hortic.	Cropland		CRP Non-Hay & Pastureland	Hay & Past.	APEX Hayland		APEX Pastureland		Hayland		Pastureland	
					Legum.	Grass.			Legum.	Grass.		
					I.	N.-I.	I.	N.-I.	I.	N.-I.	I.	N.-I.
NLCD 82				NLCD 81								

Figure 2-11. Composition of the Cropland, Horticulture, Hayland and Pastureland HUMUS categories (I. = Irrigated, N.-I. = Non-Irrigated)

As depicted in Figure 2-11, the CRP (Conservation Reserve Program) Non-Hay and Pastureland class was not directly associated to any of the other NLCD LULC classes. A procedure was developed to complete the assimilation of the actual CRP acres as accounted by the NRI 1997 records reported at the 8-digit level (NRI code = 410).

The procedure was based on the logic that if the CRP was reported (non-zero) on the specific 8-digit level (and proportionally on all the HRL subwatersheds) the Non-Hay and Pastureland part of the CRP, was accounted for by adjusting the area of the following LULC categories: Range Brush, Range Grasses, Deciduous Forest, Evergreen Forest, Mixed Forest, Forested Wetland, and Non- Forested Wetland. The CRP non-hay and pastureland now comprise the “Other Humus (1)” and “Other Humus (2)” groups in Figure 2-12, which summarizes the results of the overall procedure (Task 1-5).

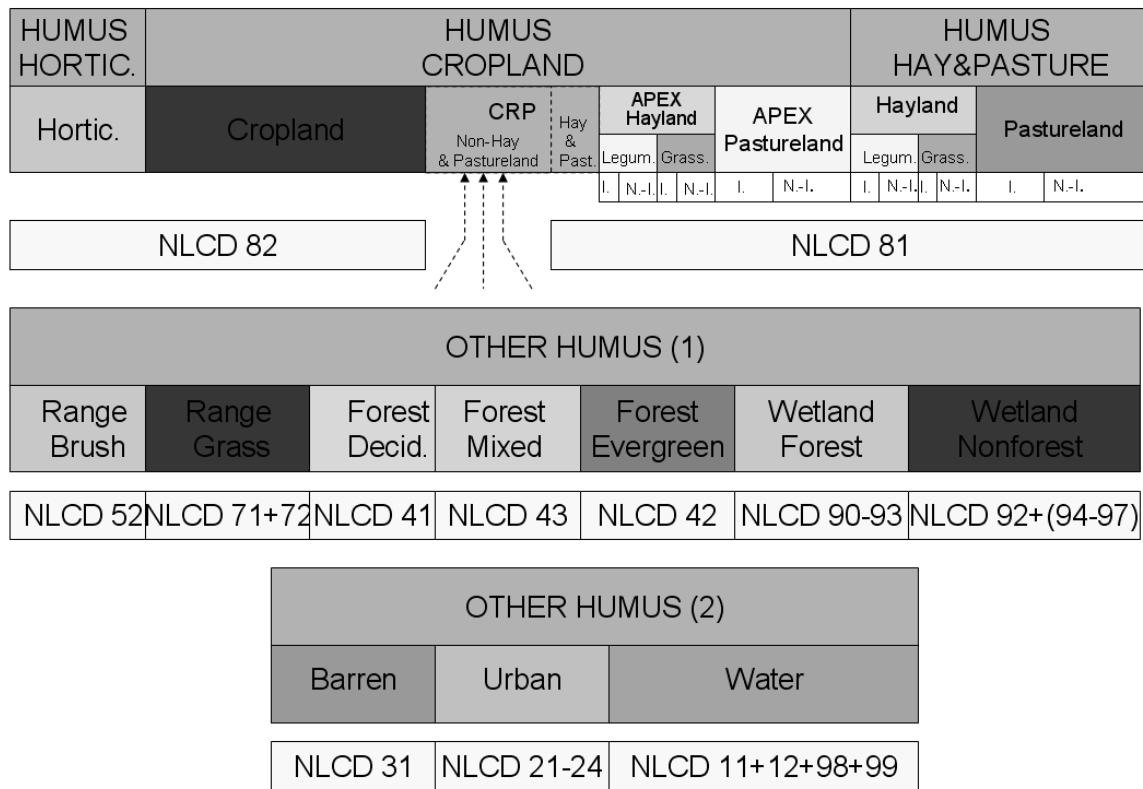


Figure 2-12. Final Land-Use/Land-Cover spectrum in the CEAP simulations (I. = Irrigated; N.-I. = Non-Irrigated)

Following the schema depicted in Figure 2-4, the proportions just illustrated, were applied to the 8-digit level distribution elaborated at Task 3. The results of this task are the enhanced/more detailed HRUs, which were completed using the methodology described in section 2.2.3.

2.2.3 HRU REDUCTION

The new HUMUS model, like previous versions, represents each 8-digit HUC as a single subbasin in SWAT. In an effort to improve model accuracy, the number of hydrologic response units (HRUs) within each subbasin was significantly increased. The development of all potential HRUs was described in the previous section as an overlay of HRL, soils and land use. The result of each unique combination was considered a potential HRU. Due to limited computational resources, it is not possible to represent every potential HRU as an actual HRU in the final SWAT model. For example, within the Upper Mississippi (Region 07) there were 58,000 potential HRUs. The HUMUS team generally agreed on an upper limit of 5,000 HRUs per region, to prevent excessive model execution times. The goal of this procedure is to reduce the number of HRUs to this level while maintaining the best possible representation of the region being simulated. The procedure was based on the following rule items:

- a) Preserve the representation of all the HLR watersheds;
- b) Simplify small size HRUs at the HLR watershed level;
- c) Preserve the land-use distribution at the 8-digit level.

Several criteria are used to assess the significance of each potential HRU. The fulfillment of any one of the following criteria results in the inclusion of an HRU in the final model.

- **Exceeds Threshold Area**

A user defined threshold area is used to preferentially include larger potential HRUs in the final model. If the fractional coverage area of a particular HRU exceeds the designated threshold value, it is included. The threshold value varies by landcover type. Landcovers of greater perceived importance or with greater pollutant contributions, such as pastures receiving animal manures, were subject to smaller threshold values. Threshold values ranged from 1% to 0.1% of the total subbasin area and are given in Table 2-3.

Table 2-3: Threshold fractional areas used to define HRUs.

Land use	Threshold
Cultivated Cropland	-
Horticulture	0.005
Legume hayland irrigated	0.005
Legume hayland not irrigated	0.005
Other hayland irrigated	0.005
Other hayland not irrigated	0.005
Pastureland irrigated with no-manure applied	0.005
Pastureland irrigated with manure Applied	0.001
Pastureland not-irrigated with no-manure applied	0.005
Pastureland not-irrigated with manure Applied	0.001
Range Brush	0.01
Range Grasses	0.01
Deciduous Forest	0.01
Evergreen Forest	0.01
Mixed Forest	0.01
Barren	0.01
Urban	0.005
Forested Wetland	0.01
Non-Forest Wetland	0.01
Water	0.01
Legume hayland irrigated	0.001
Legume hayland not irrigated	0.001
Other hayland irrigated	0.001
Other hayland not irrigated	0.001
Urban Construction	0.005

- **Dominant HRU**

Within each HUC, potential HRU were defined by hydrologic region. The largest potential HRU within each hydrologic region was included in the final model to ensure the representation of each group of hydrologic conditions.

- **Single Representative**

Within each subbasin it is critical that each landcover type be represented at least once. If a particular landcover type is not represented through either of the previous criteria, the largest potential HRU of that landcover type within each subbasin is included in the final model.

- **Area Correction**

The inclusion of some potential HRUs and exclusion of others results in a misrepresentation of land use distribution in the final model. In general, small fragmented land use types are underrepresented. To overcome this issue, the areas of each HRU were modified such that the land use-area distribution of the original data was preserved in the final model.

2.2.4 CONCLUSION

The Land Use / Land Cover (LULC) categories, which bounded with the soil categories compose the HRUs deployed in the simulation, were defined from the development and application of the methodology described above are summarized and illustrated by Figure 2-12. These newly obtained categories univocally associated the proper soil and also distinguished them by land-surface form, geologic texture, and climate variables settings. A more manageable number of HRUs was obtained by developing and applying a procedure to retain only the most representative and significant one characterizing the hydrology of the basin and composing features.

Table 2-4 shows example data for estimated Land Use /Land Cover acreage elaborated for a single HUC (02010001). Note that some of the less relevant sub-classes are not shown in order to allow the table to fit the page.

Table 2-4. Estimated land use areas, HLR soils, percent HUC area, and associated slopes

HUC	HLR	HLR FRACTION	SLOPE	SOIL1	SOIL2	SOIL3	SOIL4	SOIL5	CROP	HORT	LEGUME HAY IRRIGATED NO MANURE	OTHER HAY IRRIGATED	OTHER HAY IRRIGATED NO MANURE	PASTURE IRRIGATED NO MANURE	PASTURE IRRIGATED MANURE	PASTURE IRRIGATED NO MANURE	PASTURE NOT IRRIGATED MANURE
02010001	1	18.70	2.92	VT014	VT014	VT014	NY150	NY150	10.49	0.26	4.43	0.00	6.13	0.00	0.00	5.34	0.14
02010001	2	4.05	4.25	NY152	NY085	NY150	NY150	NY150	3.00	0.08	0.93	0.00	1.29	0.00	0.00	1.12	0.03
02010001	3	2.10	4.68	NY085	NY085	VT014	NY154	NY154	13.69	0.35	3.31	0.00	4.58	0.00	0.00	3.99	0.11
02010001	4	1.72	7.05	NY085	NY085	NY154	NY085	NY154	5.87	0.15	0.60	0.00	0.83	0.00	0.00	0.72	0.02
02010001	5	6.78	4.75	VT014	VT014	VT014	NY147	NY147	2.55	0.05	4.31	0.00	5.96	0.00	0.00	5.19	0.14
02010001	6	2.07	2.26	VT014	VT014	VT010	VT010	VT010	2.88	0.06	5.80	0.00	8.03	0.00	0.00	6.99	0.18
02010001	7	6.84	5.22	VT010	VT010	VT010	VT010	VT010	3.03	0.07	1.96	0.00	2.71	0.00	0.00	2.36	0.06
02010001	8	10.46	7.31	NY138	NY147	NY147	NY147	NY147	0.64	0.02	0.27	0.00	0.38	0.00	0.00	0.33	0.01
02010001	9	2.53	2.63	VT014	VT014	VT010	VT014	VT010	4.22	0.10	5.11	0.00	7.07	0.00	0.00	6.15	0.16
02010001	10	3.19	6.28		NY147		NY154	NY147	0.00	0.00	0.00	0.00	0.00	0.00	0.00	0.00	0.00
02010001	11	3.59	2.52	NY159	NY064	NY156	NY174	NY156	3.16	0.06	6.28	0.00	8.68	0.00	0.00	7.56	0.20
02010001	12	6.52	4.36	VT010	VT008	VT010	VT091	VT010	5.10	0.12	3.34	0.00	4.61	0.00	0.00	4.02	0.11
02010001	13	2.70	7.10	NY147	NY147	NY147	NY147	NY147	0.09	0.00	0.23	0.00	0.32	0.00	0.00	0.28	0.01
02010001	14	4.08	5.48	NY149	NY064	NY064	NY064	NY157	4.59	0.11	4.13	0.00	5.71	0.00	0.00	4.98	0.13
02010001	15	4.22	6.25	NY149	NY147	NY147	NY147	NY147	0.48	0.01	0.08	0.00	0.10	0.00	0.00	0.09	0.00
02010001	16	3.05	2.84	NY098	NY156	NY156	VT091	VT010	7.01	0.18	3.36	0.00	4.64	0.00	0.00	4.04	0.11
02010001	17	2.99	6.97	VT007	VT008	VT008	VT008	VT010	4.71	0.11	4.39	0.00	6.07	0.00	0.00	5.28	0.14
02010001	18	4.25	1.85	NY085	NY085	NY156	NY156	NY156	8.37	0.19	9.21	0.00	12.73	0.00	0.00	11.09	0.29
02010001	19	2.96	3.97	VT010	NY156	NY156	VT001	VT001	7.50	0.18	5.56	0.00	7.69	0.00	0.00	6.70	0.18
02010001	20	2.73	4.28	NY085	NY085	NY085	NY158	NY147	9.16	0.24	2.73	0.00	3.78	0.00	0.00	3.29	0.09
02010001	21	2.66	9.17	VT002	VT002	VT001	VT002	VT004	3.30	0.08	3.19	0.00	4.41	0.00	0.00	3.84	0.10
02010001	22	1.81	3.27	NY085	NY085	NY085	NY156	NY156	7.21	0.17	7.94	0.00	10.98	0.00	0.00	9.56	0.25

Table 2-5. Redefined HRU based on representative soil type, land use and associated slope.

HUC8	subbasin	HRU#	LULC	SOIL	SLOPE	Original Component Area (SKM)	HUC 8 Area (SKM)	Apex area (SKM), Included Crop and CRP	SWAT Area (SKM)	Fraction of HUC8	Reason Included	Corrected HUC Fraction	LULC Total (SKM)	Represented area Total (SKM)	Corrected Area (SKM)
2010001	2000000	1	HORT	VT014	2.92	1.75	3542.17	182.13	3362.22	0.00	lulc Dom	0.00	4.45	1.75	4.45
2010001	2000000	2	LEGHANIR	VT014	2.92	29.36	3542.17	182.13	3362.22	0.01	lulc Dom	0.04	119.16	29.36	119.16
2010001	2000000	3	OTHANIR	VT014	2.92	40.60	3542.17	182.13	3362.22	0.01	lulc Dom	0.03	164.78	59.78	111.92
2010001	2000000	4	PASTNIRNM	VT014	2.92	35.36	3542.17	182.13	3362.22	0.01	lulc Dom	0.04	143.50	35.36	143.50
2010001	2000000	5	PASTNIRYM	VT014	2.92	0.93	3542.17	182.13	3362.22	0.00	lulc Dom	0.00	3.79	0.93	3.79
2010001	2000000	6	RNGGRASS	NY150	2.92	1.23	3542.17	182.13	3362.22	0.00	lulc Dom	0.00	6.55	1.23	6.55
2010001	2000000	7	FRSTDECID	NY150	2.92	96.95	3542.17	182.13	3362.22	0.03	Ex Treshold	0.03	1116.55	1089.55	99.35
2010001	2000000	8	FRSTEVER	NY150	2.92	86.40	3542.17	182.13	3362.22	0.02	lulc Dom	0.05	592.47	287.29	178.19
2010001	2000000	9	FRSTMIXED	NY150	2.92	82.72	3542.17	182.13	3362.22	0.02	lulc Dom	0.07	345.42	121.38	235.40
2010001	2000000	10	BARREN	NYW	2.92	1.87	3542.17	182.13	3362.22	0.00	lulc Dom	0.00	4.61	1.87	4.61
2010001	2000000	11	URBAN	NY150	2.92	26.50	3542.17	182.13	3362.22	0.01	lulc Dom	0.05	169.40	26.50	169.40
2010001	2000000	12	WETLFRST	NY150	2.92	32.36	3542.17	182.13	3362.22	0.01	lulc Dom	0.06	214.24	32.36	214.24
2010001	2000000	13	WATER	VTW	2.92	136.08	3542.17	182.13	3362.22	0.04	lulc Dom	0.05	336.62	256.95	178.28
2010001	2000000	14	LEGHANIRYM	VT014	2.92	0.15	3542.17	182.13	3362.22	0.00	lulc Dom	0.00	0.62	0.15	0.62
2010001	2000000	15	OTHANIRYM	VT014	2.92	3.38	3542.17	182.13	3362.22	0.00	lulc Dom	0.00	13.70	3.38	13.70
2010001	2000000	16	CONST	NY150	2.92	0.87	3542.17	182.13	3362.22	0.00	lulc Dom	0.00	5.17	0.87	5.17

2.3 REFERENCES

- Singh, A., Rudra, R., Yang, W., Gharabaghi, B., Lowrance, R.R., Diluzio, M. 2007. Swat-remm interface for modeling effects of riparian buffer system on sub-basin hydrology. Transactions of the ASABE.
- USDA-NRCS, US Department of Agriculture-Natural Resource Conservation Service, 1992. State Soil Geographic Database (STATSGO) Data Users' Guide. Publication 1492, US Government Printing Office, Washington, DC.
- USGS, 1994: 1:250,000-scale Hydrologic Units of the United States. USGS Open-File Rep. 94-0236 [Available on line at <http://water.usgs.gov/GIS/metadata/usgswrd/XML/huc250k.xml>].
- USDA-NASS, Farm and Ranch Irrigation Survey. 2004. Farm and Ranch Irrigation Survey, Volume 3, Special Studies Part 1.
- USDA, 2000. *Summary Report: 1997 National Resources Inventory (revised December 2000)*, Natural Resources Conservation Service, Washington, DC, and Statistical Laboratory, Iowa State University, Ames, Iowa, 89 pages. USGS, 2003: Hydrologic landscape regions of the United States. U.S. Geological Survey Open-File Rep. 03-145.

CHAPTER 3

MODEL INPUT DATA

3.1 WEATHER

Precipitation and temperature are driving variables in the simulation of physical and biological processes occurring in the landscape. In the CEAP Project, the large spatial domain of the application project prevents using detailed on-site collection of near-surface data, which are only available for traditional large station networks and only recently from remote sensors (radars and satellites). For CEAP, a pattern based method for the development of daily total precipitation and temperature (daily maximum and minimum) gridded data sets which are ultimately needed to meet the following modeling requirements: (a) seamless spatial coverage of the entire project application area (the CONUS, Conterminous United States); (b) representation of sequential daily values; (c) serially complete over an extended historical period; (d) an adequate resolution to support the applied hydrologic models at the current (and most probably becoming finer in the near future) spatial hydrologic segmentation; and (e) provision of orographic adjustment. The first requirement is dictated by the geographic scope of the model simulations along with the necessity, also related to the rest of the requirements, of their calibration using observed data (stream flows, sediment loads, etc.), which are expected to be correlated to the implementation of the conservation practices, thereby excluding the usage of generated weather records. In addition, as described above, the model simulations require daily input time series. Their historical extent, and spatial and temporal variability are fundamental for the achievement of the project goals and any water resource management plan. The inclusion of the strong variation of climate with elevation is obviously important and in addition provides background data for the concurrent estimation of the atmospheric deposition loads.

3.1.1 PROCEDURE FOR DATA GRIDDING

In developing the CEAP data sets, the station observations are considered the true values on a surface component dominated by the prevailing weather systems determined by large-scale synoptic forcing (atmospheric pattern) acting at the monthly base, mixed with a modulating daily component determined by local forcing. The precipitation field, $P(x,y,t)$ is considered equivalent to the cumulative topography-based sum, $P_c(x,y,t)$, modulated by a second component, such as pointwise time-varying ratios, $P_r(x,y,t)$, defined by the daily pattern, such as:

$$P(x, y, t) = P_c(x, y, t) P_r(x, y, t) \quad (1)$$

$P_r(x, y, t)$ was derived from the interpolation of ratios calculated using station records and the procedure described in the next section. In place of $P_c(x, y, t)$, for each month we used the distinct PRISM (Parameter-elevation Regressions on Independent Slopes Model, Daly et al. 1994, 1997, 2002) cumulative precipitation fields at the full resolution (4 km). A similar approach to obtain daily temperature fields (maximum and minimum), decomposed in its monthly mean $\bar{T}(x, y, t)$ and additive daily anomaly $T_a(x, y, t)$ was used, such as:

$$T(x, y, t) = \bar{T}(x, y, t) + T_a(x, y, t) \quad (2)$$

The anomaly-average ratio $T_r(x, y, t)$ was defined as:

$$T_r(x, y, t) = \frac{T_a(x, y, t)}{T(x, y, t)} \quad (3)$$

$T_r(x, y, t)$ was derived from the interpolation of fractions calculated using station records and the procedure described in the next section. In place of $\bar{T}(x, y, t)$, for each month we used the distinct PRISM average temperature (maximum and minimum) fields at the full resolution (4 km) that combined with $T_r(x, y, t)$ allowed the spatial distribution of the daily values representing the estimated daily fields (see implementation details below).

A deterministic interpolation method (the Inverse Distance Weighted, IDW; Watson and Philip 1985) was implemented to specifically assign fraction values to missing locations based on the surrounding measured values. IDW, although lacking in optimality criteria, is in general recognized as more appropriate than the classic nearest-neighbor method (Thiessen 1911), which in turn introduces discontinuous surfaces and is traditionally used for large area hydrological assessments. For a given estimation point, IDW technique provides a set of weights that sum to unity and that are inversely related to the distances to the data points. The $IDW(x, y)$ estimation at (x, y) is a linear combination of the observed values, such as:

$$IDW(x, y) = \sum_j w_j f(x_j, y_j) \quad (4)$$

with the weights w_j defined as follow:

$$w_j = \frac{d_j^{-p}}{\sum_k d_k^{-p}} \quad (5)$$

where d_k is the distance from (x,y) to (x_k,y_k) and $f(x_k,y_k)$ is the observed value at (x_k,y_k) ; p is a positive real number that influences the character of the interpolation, from local to global: the higher the value the stronger the influence of the closer sample points. $p = 2$ has been used (inverse square interpolation), which still determines a local dominating weight to a particular measurement when it is located near the estimation point, and in addition returns a smooth transition of the interpolated surface (the first derivative is zero at the data point). The input set of data points (stations) for calculating each interpolated point have been limited to 12. Using IDW, the range of interpolated values is limited to the range of the measured variable. In general this is considered a major disadvantage because the interpolation is not fully responsive to local trends (e.g. for unsampled hill tops and valley bottoms). The importance of this issue is minimized here since the fractional values are interpolated and the local trends are accounted for at the monthly level.

The implementation for the CONUS used the following precompiled data sets: (a) corrected and quality controlled National Weather Service Cooperative Observer (COOP)'s daily observations from the National Climatic Data Center (NCDC); and (2) the PRISM monthly grid estimates; which are here briefly described along with the national segmentation currently adopted in the project.

a) Daily precipitation and temperature data and the Hydrologic Units map

A serially complete (no missing values) daily total precipitation and maximum-minimum temperature time series developed initially for the Western United States (Eischeid et al. 2000), and extended to the entire United States, is the data set used in this project. It was compiled, purging and/or correcting extreme errors and/or missing values traditionally included in observation records, creating quality controlled, serially complete data in support of natural resource modeling. The source records were from the COOP stations, namely the NCDC Summary of Day (TD3200). In the creation of the final serially complete data sets the following refinement steps were applied: (1) quality control identifying unreliable reporting stations and records which had been flagged as missing values; (2) replacement of missing daily values based on the use of simultaneous values at nearby stations along with six different, seasonally and geographically dependent, methods of spatial interpolation to calculate estimated

values for those specific days (Eischeid et al. 1995); and (3) final data consistency check and eventual correction.

The total number of distinct stations in the serially complete data set, operative in the period 1895-2001, are 12,540 and 7,998 respectively for precipitation and maximum-minimum temperature. The number of operative stations and their distribution results changes over the years. Our target period (1960-2001) avoids high temporal data inhomogeneities in the COOP data prior to 1950 noted by Hamlet et al. (2005). These persistent temporal inhomogeneities are due to undocumented changes in stations and station locations. In order to limit this problem, while Eischeid et al. (2000) retained the stations with at least 10 years of data and with no more than 48 missing months, a procedure has been applied to remove a few spatially redundant stations (with the same coordinates), retaining only the longest recording station. The number of distinct stations recording at any time within our target period (1960-2001) is 11,680 and 7,565 for precipitation and temperature respectively. The spatial distribution of the stations is shown in Figure 3-1a and Figure 3-1b (maximum and minimum temperature stations share identical locations) with reference to the USGS water-resources regions shown in Figure 3-1c.

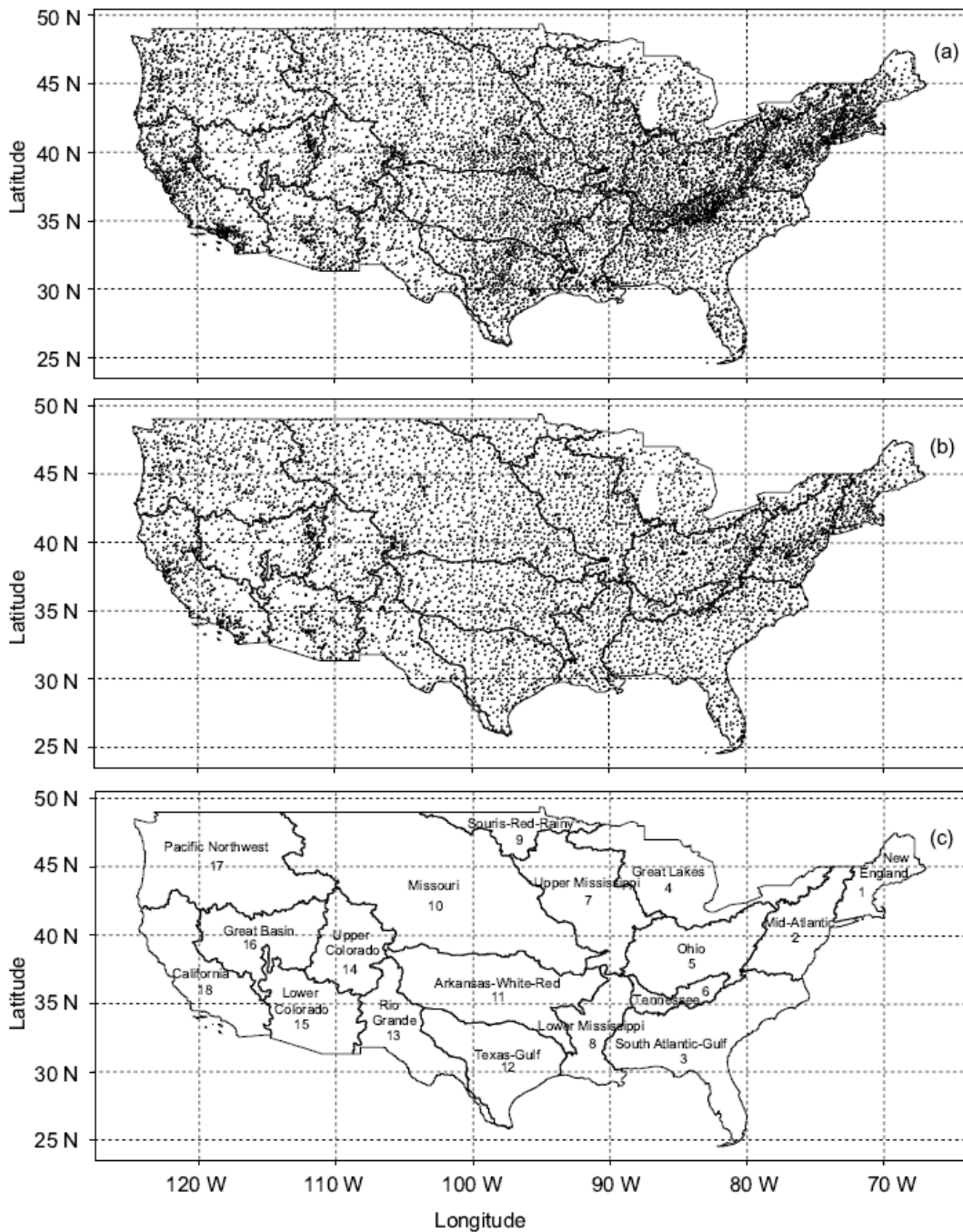


Figure 3-1. (a) Spatial distribution of the 11,680 Cooperative Observer (COOP) stations measuring precipitation in the period 1960-2001. (b) Spatial distribution of the 7,565 Cooperative Observer (COOP) stations measuring temperature in the period 1960-2001. (c) USGS Water Resources Regions in the CONUS.

The supporting digital spatial data set used in this project is the 1:250,000-scale Hydrologic Units of the US (USGS, 1994), which counts 2,150 HUCs for the entire Nation. After some minor simplifications and aggregations, the revised data set contains 2,108 units.

b) PRISM grids

The PRISM climate mapping system was used to create the gridded climate data sets described in this study. PRISM is a knowledge-based system that uses point data, a DEM (digital elevation model), and many other geographic data sets to generate gridded estimates of monthly and event-based climatic parameters (Daly et al. 1994, 2001, 2002, 2003; Daly 2006). PRISM has been used extensively to map precipitation, temperature, dew point, weather generator parameters, and other climate elements over the United States, Canada, China, and other countries (USDA-NRCS 1998; Daly and Johnson 1999; Johnson et al. 2000; Plantico et al. 2000; Daly et al. 2001; Gibson et al. 2002; NOAA-NCDC 2002; Daly et al. 2003; Zhu et al. 2003; Daly and Hannaway 2005; Hannaway et al. 2005; Simpson et al. 2005).

3.1.2 IMPLEMENTATION

Daily precipitation and maximum-minimum temperature spatial data sets were created by linking and combining the data sources outlined above (daily station records and PRISM monthly grids). The implementation, illustrated in Figure 3-2, relies on the input PRISM grids to reproduce the climate patterns as well as to fasten the accumulated values on the monthly base (total precipitation and average daily temperatures). The linkage is established by defining, for each station in the database and for each day of the analyses, the daily fractional contribution to the total monthly precipitation and the fractional daily anomaly with respect to the average monthly values for daily maximum and minimum temperature (see points 1 and 2 below). An IDW interpolation function is applied to expand these point-sample-ratios (fractional anomalies) over the spatial scope, such as the CONUS territory (see point 3 below). The spatial combination (see point 4 below) of the resulting grids with the PRISM grids returns the new spatial data set at the daily time step, which is expected to be consistent with the monthly precipitation totals

(monthly average daily temperatures) provided by the PRISM grids. An additional spatial function was applied to obtain records at the HUC level (see point 5).

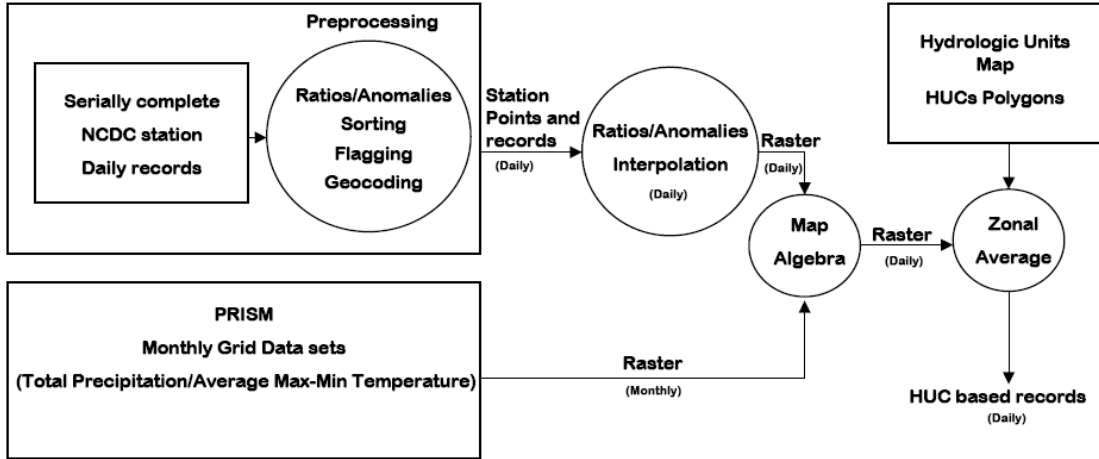


Figure 3-2. Scheme of the input-output data elaboration

The method was applied to the project target period (1960-2001) incorporating the following specific procedures:

1. Processing of the serially complete station records.

This procedure included the following tasks: (a) identification and extraction of the stations operating any time within the target period, (b) flagging of the station-days in which the respective station had not been operative (this is for the days outside the gapless station specific serially complete period), (c) for each selected precipitation station, computation of the monthly precipitation total (*Monthly P_c*) and ultimately the daily ratio (*Daily P_r*) of the monthly total precipitation as follows:

$$Daily P_r = Daily P / Monthly P_c \quad (8)$$

Where:

Daily P = Daily recorded precipitation.

For each selected temperature station, computation of monthly average *Monthly \bar{T}* (independently for maximum and minimum temperature) are calculated as:

$$Monthly \bar{T} = \sum_{i=1}^N Daily T_i / N \quad (9)$$

Where:

Daily T_i = Daily recorded temperature at the day *i*.

N = number of days in the respective month.

The daily anomaly-average ratio (*Daily T_r*) from the average monthly temperature is calculated as follows:

$$Daily T_r = \frac{Daily T - Monthly \bar{T}}{Monthly \bar{T}} \quad (10)$$

In order to avoid problematic zeros, all the temperature computations were operated on a shifted dominion, in which a value equal to 100 was added to all the variables.

2. Data arrangement by date.

Derived data were reorganized into a comprehensive sequence of daily records, such as a database table. Each record (line of the database) contained all station data for a single day. Data included the daily ratios, the anomalies and flags calculated for all available stations. This time indexing procedure was made and applied to facilitate the following computations.

3. Sequence of interpolations for the time series of daily ratios.

Following geo-coding of the station location points, this procedure provided a day by day sequential interpolation of the daily ratios, dynamically associated only with the stations operative on the currently analyzed day. The resulting IDW continuous surfaces are the daily grids (raster data), covering the target period, and representing the spatial extension from the sampled locations to all the locations where measures are not available of the daily ratios or anomalies on the monthly bases. The spatial analysis environment used for this procedure was adopted from the PRISM data sets, namely a Geographic, World Geodetic Spheroid 1972 (WGS72) coordinate system, and the 2.5-min (around 4 km) cell resolution.

4. Daily spatial combination.

This procedure included the application of map algebra functions for combining the surface interpolation maps and the respective PRISM monthly grids. The map algebra functions combine data on a cell-by-cell basis to derive the final target information grid data set. In this way, operating on each cell, the target daily precipitation grid was obtained as the result of the following combination:

$$\text{Daily } P(i) = \text{Daily } I_r(i) * \text{Monthly } P_c(i) \quad (11)$$

Where:

Daily P(i) = Precipitation grid at day *i*;

Daily I_r(i) = Grid of IDW interpolated station ratios (see Eq. 8) at day *i*;

Monthly P_c(i) = PRISM total precipitation grid for the respective month.

The daily temperature grid (maximum and minimum) was obtained using the following combination:

$$\text{Daily } T(i) = \text{Monthly } \bar{T}(i) * \text{Daily } I_r(i) + \text{Monthly } \bar{T}(i) \quad (12)$$

Where:

Daily T(i) = Temperature grid at day *i*;

Daily I_r(i) = Grid of IDW interpolated station anomaly-average ratios (see Eq. 10) deviation from the monthly average) at day *i*;

Monthly $\bar{T}(i)$ = PRISM average temperature grid for the respective month.

5. Hydrologic Unit Average.

A further step was required to provide the CEAP models with daily time series over each computation unit (HUC watersheds). For this aim, each of the previous grids was spatially averaged (simple average of all HUC-contained grid cells) within each HUC.

3.1.3 VERIFICATION AND APPLICATION IN CEAP

The daily grids (precipitation and maximum-minimum temperature in the period 1960-2001 at the 2.5 min resolution) were verified as described in Di Luzio et al. (2008). A subsequent implementation of the same methods provided the extension of the data up to end of the 2006. The grids values, averaged on each HUC polygon and for the period 1960-2006, represent the time series of daily records applied in CEAP as input to the models, APEX and SWAT respectively. Figure 3-3 shows the annual average predicted precipitation accumulated in the period 1960-2001.

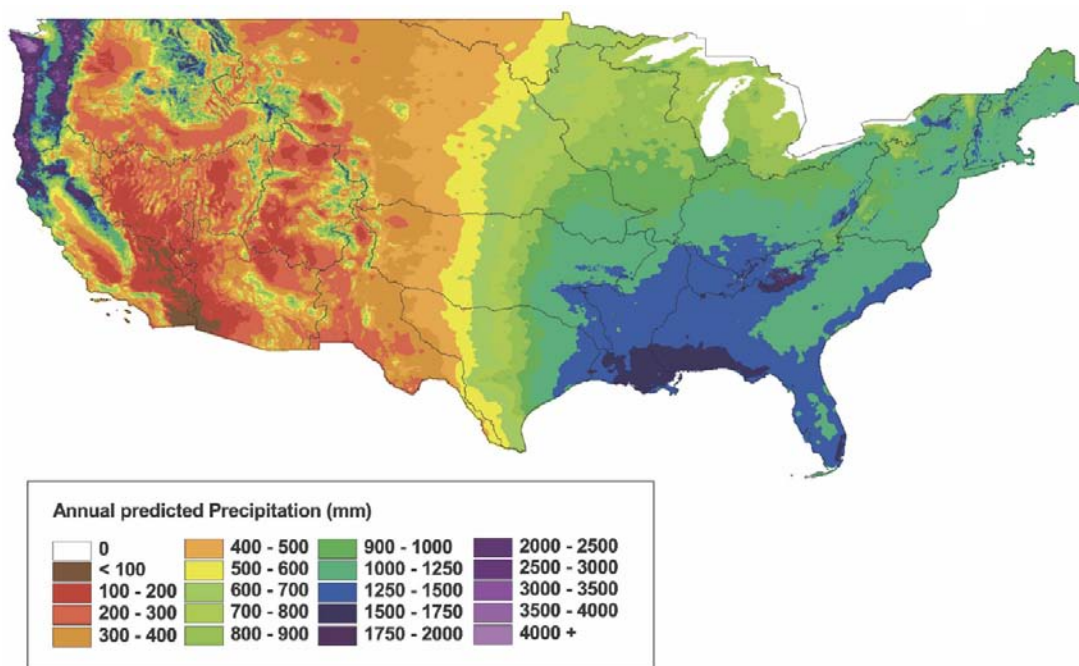


Figure 3-3. Annual average predicted precipitation accumulated in the period 1960-2001.

3.2 ATMOSPHERIC DEPOSITION

Atmospheric deposition occurs when airborne chemical compounds settle onto the land or water surface. Some of the most important chemical pollutants are those containing nitrogen or phosphorus. Nitrogen compounds can be deposited onto water and land surfaces through both wet and dry deposition mechanisms. Wet deposition occurs through the absorption of

compounds by precipitation as it falls carrying mainly nitrate (NO_3^-) and ammonium (NH_4^+). Dry deposition is the direct adsorption of compounds to water or land surfaces and involves complex interactions between airborne nitrogen compounds and plant, water, soil, rock, or building surfaces.

The relative contribution of atmospheric deposition to total nutrient loading is difficult to measure or indirectly assess and many deposition mechanisms are not fully understood. Most studies and relatively extended data sets are available on wet deposition of nitrogen, while dry deposition rates are not well defined. Phosphorus loadings due to atmospheric deposition have not been extensively studied and nation-wide extended data set were unavailable at the time of data preparation for the CEAP project. While research continues in these areas, data records generated by modeling approaches appear to be still under scrutiny.

A number of regional and local monitoring networks are operating in the U.S. mainly to address information regarding regional environmental issues. For example, the Integrated Atmospheric Deposition Network (IADN) (Galarneau et al., 2006) that estimates deposition of toxic organic substances to the Great Lakes. Over the CONUS (conterminous United States), the National Atmospheric Deposition Program (NADP) National Trends Network (NTN) (NADP/NTN, 1995; NADP/NTN, 2000; Lamb and Van Bowersox, 2000) measures and ammonium in one-week rain and snow samples at nearly 240 regionally representative sites in the CONUS (Figure 3-4) and is considered the nation's primary source for wet deposition data.

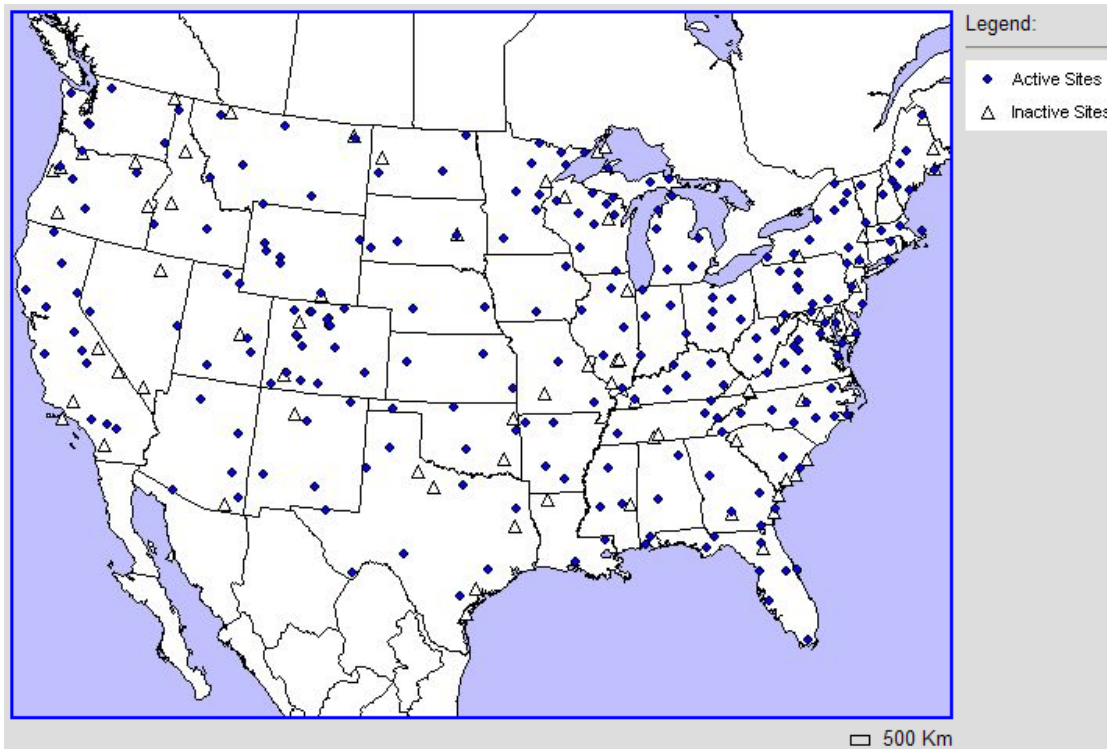


Figure 3-4. Location of NADP/NTN wet deposition sites

The U.S. EPA Clean Air Status and Trends Network (CASTNET), developed from the National Dry Deposition Network (NDDN), operates a total of 86 operational sites (as of December 2007) located in or near rural areas and sensitive ecosystems (see Figure 3-4) collecting data on ambient levels of pollutants where urban influences are minimal (CASTNET, 2007). As part of an interagency agreement, the National Park Service (NPS) sponsors 27 sites which are located in national parks and other Class-I areas designated as deserving special protection from air pollution.

Appendix 3-1 reports the averaged data and some spatial distribution statistics for each 8-digit area within the Upper Mississippi Basin.

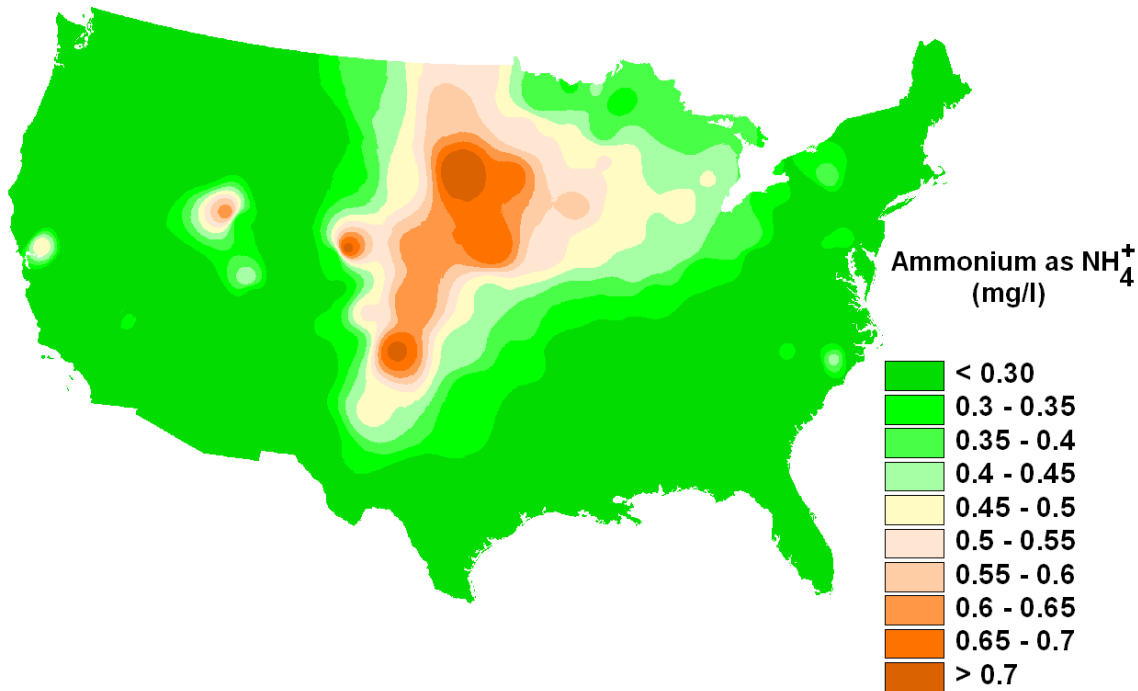


Figure 3-5. Average annual ammonium (NH_4^+) concentration (mg/l) in the period 1994-2006. Derived from National Atmospheric Deposition Program/National Trends Network <http://nadp.sws.uiuc.edu>.

Figure 3-6 plots the annual average estimated concentration of the nitrate ion for the period 1994-2006. Appendix 3-1 reports the same information and some spatial distribution statistics for each 8-digit area within the Upper Mississippi Basin.

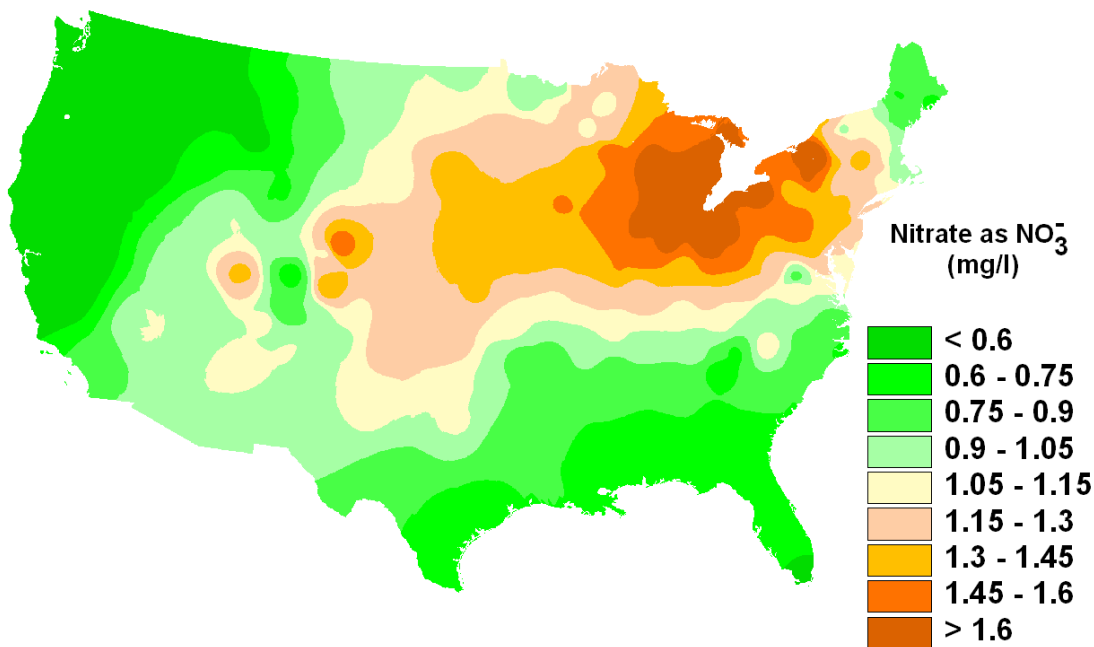


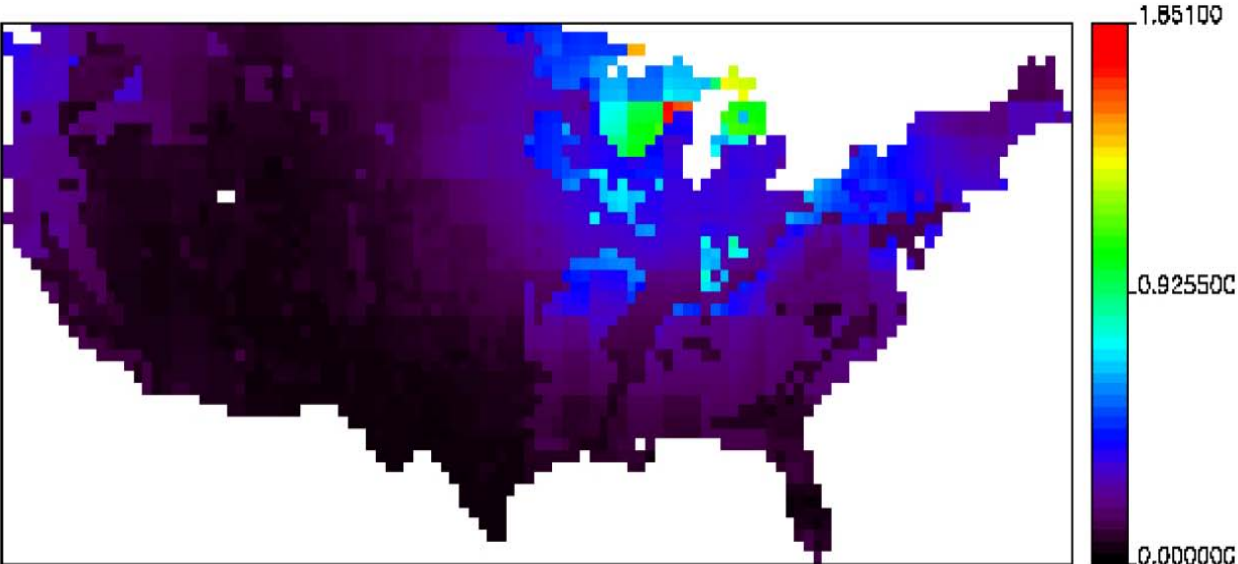
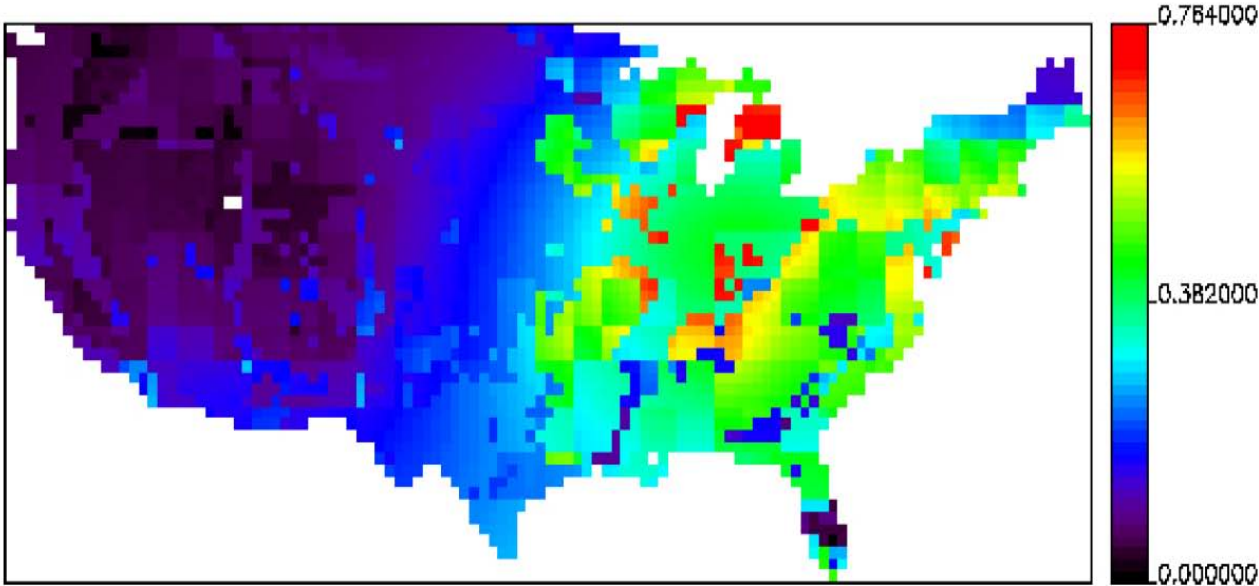
Figure 3-6. – Average annual nitrate (NO₃⁻) concentration (mg/l) in the period 1994-2006. Derived from National Atmospheric Deposition Program/National Trends Network <http://nadp.sws.uiuc.edu>.

3.2.2 NITROGEN DRY DEPOSITION FLUX RECORDS FOR CEAP

Oak Ridge National Laboratory (ORNL) publishes maps of N deposition fluxes from site-network observations for the U.S. and Western Europe (Holland et al., 2005a). Observations from monitoring networks in the U.S. and Europe were compiled in order to construct 0.5 x 0.5 degree resolution maps of N deposition by species. In the United States, measurements of ambient air concentrations, used to calculate dry deposition fluxes, were provided by the Clean Air Status and Trends Network (CASTNET) (CASTNET, 2007). The source data period extends from 1989 to 1994. The maps are necessarily restricted to the network measured quantities and consist of statistically (kriging) interpolated fields of particulate, ammonium (NH₄⁺), nitrate (NO₃⁻), and gaseous nitric acid (HNO₃). A number of gaps remain in the data set including organic N and NH₃ deposition. The dry N deposition fluxes were estimated by multiplying

interpolated surface air concentrations for each chemical species by model-calculated, spatially explicit deposition velocities (Holland et al., 2005b).

Figure 3-7a, 3-7b, and 3-7c shows the annual average dry Nitrogen, NH_4 , NO_3 , and HNO_3 flux, as published by ORNL.



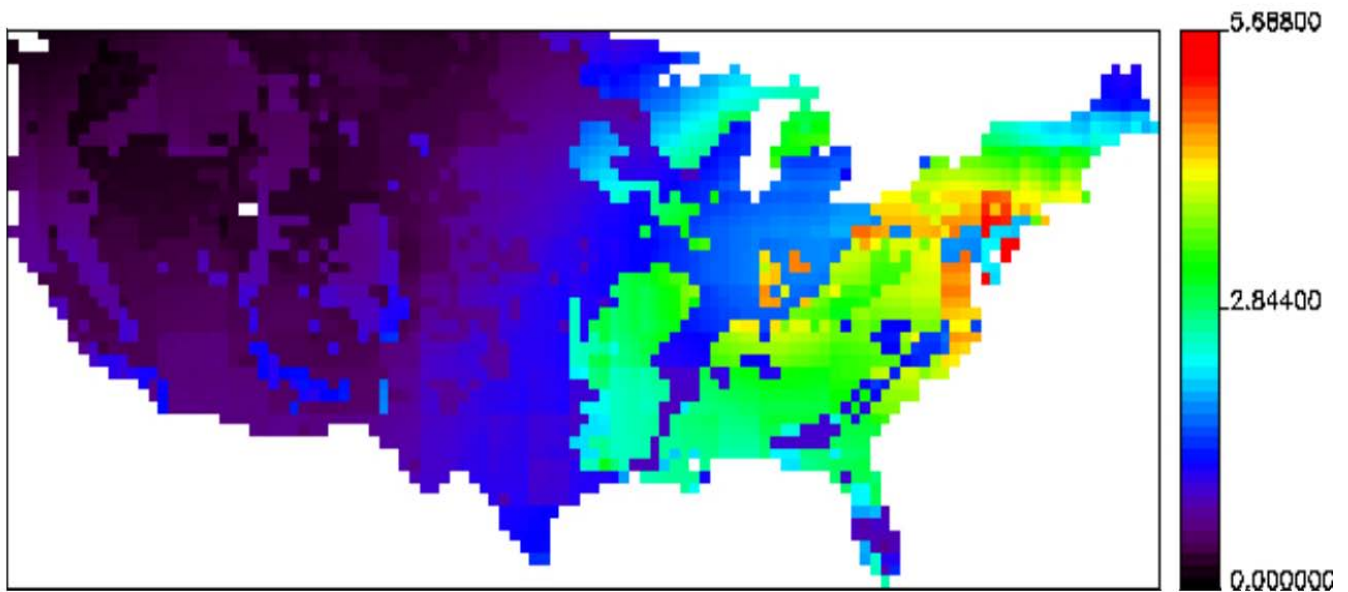


Figure 3-7. (a) Annual average dry NH_4 flux over the CONUS (kg N/ha/yr), (b) Annual average dry NO_3 flux over the CONUS (kg N/ha/yr), (c) Annual average dry HNO_3 flux over the CONUS (kg N /ha/yr)

In a Geographic Information System (GIS) environment, the spatially continuous annual average fields (NH_4 , NO_3 , and HNO_3) were spatially averaged on each Hydrologic Units of the CONUS (USGS, 1994). Appendix 3-2 reports the averaged data for each 8-digit area and some spatial distribution statistics for each 8-digit area within the Upper Mississippi Basin.

3.3 POINT SOURCES

Point-source load records for CEAP were estimated adjusting a former county-based national inventory of wastewater discharges. These records of point-source load estimates (mass/time) for 16 chemical constituents are developed from a Resources for the Future (RFF) assessment from 32,000 facilities, including industries, municipal wastewater treatment plants, and small sanitary waste facilities for the years 1977-1981 (Gianessi and Peskin, 1984).

For CEAP, the following fluxes of point-source discharges were considered: water flow, total suspended sediment, total phosphorus and Kjeldahl nitrogen. Data, single values for

municipal and industrial sources for each county, are stored by the United States Geological Survey SPATIally Referenced Regressions On Watershed Attributes (USGS SPARROW) modeling team and were downloaded from <http://water.usgs.gov/nawqa/sparrow/wrr97/point/point.html>.

The following section describes the methodology applied to update and adapt the estimates for the CEAP national modeling system.

3.3.1 ADJUSTMENT OF A NATIONAL INVENTORY OF WASTEWATER DISCHARGES

Point sources records input for the CEAP national modeling system are required for the year 2000 and for each 8-digit (HUC) Hydrologic Unit of the CONUS (USGS, 1994).

We assumed a proportion between the temporal variation of population density and the temporal variation of fluxes of discharges from point sources. Based on this assumption, the steps followed to process and merge the county-based estimates records referred in the previous section are described below.

3.3.2 CENSUS DATA PROCESS

The U.S. Census Bureau conducts a census of population every 10 years, as mandated by the United States Constitution. The United States Census Database, 1980 and 2000 includes population information from the year 1980 and 2000 census for the United States and Puerto Rico. The information is presented by county and includes statistics on total population; population under age 18; population by age, gender, race, and ethnic group; and change in population between in the previous decade.

County-based census data for this analysis were obtained from the National Atlas at www.nationalatlas.gov/people.html and process in a GIS environment as described right below:

- i) Census data tables for year 1980 and 2000 were associated (joined) to standard county boundaries to obtain county-based maps of population.

- ii) Continuous surfaces (grids at the 0.01 degree resolution) were obtained by raster conversion of the previously created maps.
- iii) Using map algebra (cell by cell computation), a grid surface (ratio of population change) was obtained as ratio of the two population grids previously created (see point ii)

3.3.3 LOADING DATA PROCESS

Source data for water flow, total suspended sediment, total phosphorus and Kjeldahl nitrogen records (see section 1) are county based. Final loading estimates, one value for each HUC, were obtained as described right below:

- 3.1 Using a procedure similar to the one described in the previous section, continuous surfaces (grids at the 0.01 degree resolution) were obtained for each of the loading variables and for municipal and industrial sources.
- 3.2 Using map algebra, each of the loading variables grids (associated to the year 1980) were reported to the respective grid relative to the year 2000 by multiplication to the ratio of population change surface (see section 2.1 point iii).
 - iii) Using a GIS procedure, the newly adjusted grids (see point ii) were aggregated (municipal and industrial source) and analyzed over each HUC area to create the final areal average summary table records at the required daily units.

3.3.4 CONCLUSION

A GIS-based procedure was developed to report county-based national inventory of wastewater discharges for the years 1977-1981 to the HUC level and to the year 2000. Appendix 3.4 reports the tabulated estimates (water flow, total Kjeldahl nitrogen, total phosphorus, and total suspended solids) for each HUC in the Upper Mississippi Basin.

3.4 PONDS, RESERVOIRS

Data on ponds and reservoirs was taken from the US Army Corps of Engineers National Inventory of Dams (<http://nid.usace.army.mil>). The inventory contains records for nearly 80,000 dams collected through 2002. Data from the inventory included drainage area and storage volumes and surface areas at both principle and emergency spillway elevations. For the HUMUS project, ponds and reservoirs were divided into dams that were on the main routing channel and those that were on tributaries within each 8-digit HUC. The dams on 8-digit tributaries were lumped into one conceptual storage area and a percentage of the 8-digit HUC draining into the reservoirs was determined. If the dams were in series on a tributary, the drainage area was adjusted so the areas were not counted twice.

3.5 REFERENCES

- Clean Air Status and Trends Network (CASTNET), 2007. http://www.epa.gov/castnet/docs/CASTNET_factsheet_2007.pdf
- Daly, C., 2002: Variable influence of terrain on precipitation patterns: delineation and use of effective terrain height in PRISM. [Available at <http://www.ocs.orst.edu/pub/prism/docs/effectiveterrain-daly.pdf>]
- Daly, 2006: Guidelines for assessing the suitability of spatial climate data sets. *Int. J. Climatol.*, in press.
- Daly, and G.L. Johnson, 1999: PRISM spatial climate layers: their development and use. Short Course on Topics in Applied Climatology, *79th Annual Meeting*, Dallas, TX, Amer. Meteor. Soc., 49 pp. [Available at <http://www.ocs.orst.edu/prism/prisguid.pdf>].
- Daly, and D.B. Hannaway, 2005: *Visualizing China's future agriculture: climate, soils and suitability maps for improved decision-making*. 1st ed. Oregon State University, 296 pp.
- Daly, R. P. Neilson, and D. L. Phillips, 1994: A statistical-topographic model for mapping climatological precipitation over mountainous terrain. *J. Appl. Meteor.*, **33**, 140–158.

- Daly, G. H. Taylor, and W. Gibson, 1997: The PRISM approach to mapping precipitation and temperature. Preprints, *10th Conf. On Applied Climatology*, Reno, NV, Amer. Meteor. Soc., 10–12.
- Daly, E. H. Helmer, and M. Quinones, 2003: Mapping the climate of Puerto Rico, Vieques, and Culebra. *Int. J. Climatol.*, **23**, 1359–1381.
- Daly, W. P. Gibson, G.H. Taylor, G. L. Johnson, and P. A. Pasteris, 2002: A knowledge-based approach to the statistical mapping of climate. *Climate Res.*, **22**, 99–113.
- Daly, W.P. Gibson, M. Doggett, J. Smith, and G. Taylor, 2004: Up-to-date monthly climate maps for the conterminous United States. Preprints, *14th AMS Conf. on Applied Climatology and 84th AMS Annual Meeting*, Seattle, WA, Amer. Meteor. Soc., CD-ROM, P5.1.
- Daly, G.H. Taylor, W. P. Gibson, T.W. Parzybok, G. L. Johnson, and P. A. Pasteris, 2001: High-quality spatial climate data sets for the United States and beyond. *Trans. ASAE*, **43**, 1957–1962.
- Di Luzio M., G. L. Johnson, C. Daly, Jon K. Eischeid, J.G. Arnold. 2008. Constructing Retrospective Gridded Daily Precipitation and Temperature Datasets for the Conterminous United States. *Journal of Applied Meteorology and Climatology*. 47(2): 475–497.
- Eischeid, J.K., C.B. Baker, T.R. Karl, and H.F. Diaz, 1995: The quality control of long-term climatological data using objective data analysis. *J. Appl. Meteor.*, **34**, 2787-2795.
- Eischeid, P. A. Pasteris, H. F. Diaz, M. S. Plantico, and N. J. Lott, 2000: Creating a serially complete, national daily time series of temperature and precipitation for the Western United States. *J. Appl. Meteor.*, **39**, 1580-1591.
- Galarneau, E.; Bidleman, T. F.; Blanchard, P. Seasonality and interspecies differences in particle/gas partitioning of PAHs observed by the Integrated Atmospheric Deposition Network (IADN). *Atmos. Environ.* 2006, 40, 182-197.
- Gianessi, L.P., and Peskin, H.M., 1984, An overview of the RFF Environmental Data Inventory-- Methods and preliminary results: Resources for the Future, Washington, D.C., 111 p.
- Gibson, W.P., C. Daly, T. Kittel, D. Nychka, C. Johns, N. Rosenbloom, A. McNab, and G. Taylor, 2002: Development of a 103-year high-resolution climate data set for the conterminous United States. *Proc. 13th AMS Conf. On Applied Climatology*, Portland, OR, Amer. Meteor. Soc., 181-183.

- Hamlet, A. F., and D.P. Lettenmaier, 2005: Production of temporally consistent gridded precipitation and temperature fields for the continental United States. *J. Hydrometeor.*, **6**, 330-336.
- Hannaway, D.B., and Coauthors, 2005: Forage species suitability mapping for China using topographic, climatic and soils spatial data and quantitative plant tolerances. *Sci. Agric. Sin.*, **4**, 660-667.
- Holland, E. A., B. H. Braswell, J. M. Sulzman, and J.-F. Lamarque. 2005a. Nitrogen Deposition onto the United States and Western Europe. Data set. Available on-line [<http://www.daac.ornl.gov>] from Oak Ridge National Laboratory Distributed Active Archive Center, Oak Ridge, Tennessee, U.S.A. doi:10.3334/ORNLDAAC/730.
- Holland, E. A., B. H. Braswell, J.M. Sulzman, and J.-F, Lamarque. 2005b. Nitrogen Deposition onto the United States and Western Europe: Synthesis of Observations and Models. *Ecological Applications* 15(1): 38-57..
- Homer, C., J. Dewitz, J. Fry, M. Coan, N. Hossain, C. Larson, N. Herold, A. McKerrow, J.N. VanDriel and J. Wickham. 2007. Completion of the 2001 National Land-Cover Database for the Conterminous United States, *Photogrammetric Engineering and Remote Sensing*, Vol. 73, No. 4, pp 337-341.
- Homer, C. C. Huang, L. Yang, B. Wylie and M. Coan. 2004. **Development of a 2001 National Landcover Database for the United States. Photogrammetric Engineering and Remote Sensing**, Vol. 70, No. 7, July 2004, pp. 829-840.
- Johnson, G.L., C. Daly, C.L. Hanson, Y.Y. Lu, and G.H. Taylor. 2000: Spatial variability and interpolation of stochastic weather simulation model parameters. *J. Appl. Meteor.*, **39**, 778-796.
- Lamb, D. and Van Bowersox, 2000. The national atmospheric deposition program: an overview. *Atmospheric Environment* 34:1661-1663.
- Lehmann, Christopher M.B. and Van Bowersox. 2003. National Atmospheric Deposition Program Quality Management Plan. National Atmospheric Deposition Program Office at the Illinois State Water Survey. NADP QA Plan 2003-01. Champaign, IL
- Miller, D.A. and R.A. White, 1998: A Conterminous United States Multi-Layer Soil Characteristics Data Set for Regional Climate and Hydrology Modeling. *Earth Interactions*, **2**.

- NADP/NTN, 1995 and 2000. National Atmospheric Deposition Program / National Trends Network, <http://nadp.sws.uiuc.edu>.
- Plantico, M.S., L.A. Goss, C. Daly, and G. Taylor, 2000: A new U.S. climate atlas. *Proc. 12th Conf. on Applied Climatology*, Asheville, NC, Amer. Meteor. Soc., 247-248.
- Simpson, J.J., G.L. Hufford, C. Daly, J.S. Berg and M.D. Fleming, 2005: Comparing maps of mean monthly surface temperature and precipitation for Alaska and adjacent areas of Canada produced by two different methods. *Arctic*, **58**, 137-161.
- Thiessen, A.H., 1911: Precipitation averages for large areas. *Mon. Wea. Rev.*, **39**, 1082-1084.
- USDA-NRCS, 1998: PRISM Climate Mapping Project-Precipitation. Mean monthly and annual precipitation digital files for the continental U.S. CD-ROM. [Available from the USDA-NRCS National Cartography and Geospatial Center, Ft. Worth TX.]
- USGS, 1994: 1:250,000-scale Hydrologic Units of the United States. USGS Open-File Rep. 94-0236 [Available on line at <http://water.usgs.gov/GIS/metadata/usgswrd/XML/huc250k.xml>]
- Watson, D.F., and G.M. Philip, 1985: A refinement of Inverse Distance Weighted Interpolation. *Geo-Processing*, **2**, 315-327.
- Winter, T.C., 2001, The concept of hydrologic landscapes: *Journal of the American Water Resources Association*, v. 37, p. 335-349.
- Zhu, H., T. Luo, and C. Daly, 2003: Validation of simulated grid data sets of China's temperature and precipitation with high spatial resolution (In Chinese with English abstract). *Geogr. Res.*, **22**, 349-359.

Appendix 3-1: Wet Deposition - Annual average (AVER) estimated concentration (mg/L) of the ammonium (NH₄) and nitrate (NO₃) ion for the period 1960 for each 8-digit area within the Upper Mississippi Basin. In addition areal minimum (MIN), maximum (MAX), range (RANGE), and standard deviation (STD) are reported.

NH4						NO3				
HUC	MIN	MAX	RANGE	AVER	STD	MIN	MAX	RANGE	AVER	STD
7010101	0.37	0.49	0.12	0.41	0.03	1	1.14	0.15	1.06	0.04
7010102	0.38	0.48	0.11	0.43	0.03	1.01	1.15	0.14	1.09	0.03
7010103	0.37	0.46	0.1	0.4	0.03	1	1.17	0.17	1.06	0.05
7010104	0.44	0.52	0.07	0.5	0.02	1.12	1.2	0.08	1.18	0.01
7010105	0.44	0.51	0.07	0.48	0.02	1.1	1.18	0.08	1.16	0.02
7010106	0.46	0.52	0.06	0.5	0.01	1.12	1.18	0.06	1.17	0.02
7010107	0.49	0.52	0.02	0.51	0	1.16	1.18	0.03	1.18	0
7010108	0.51	0.53	0.02	0.52	0	1.18	1.2	0.02	1.18	0
7010201	0.51	0.53	0.02	0.52	0	1.18	1.23	0.05	1.2	0.01
7010202	0.52	0.55	0.03	0.53	0.01	1.18	1.25	0.06	1.21	0.02
7010203	0.52	0.55	0.03	0.54	0.01	1.21	1.29	0.07	1.26	0.02
7010204	0.53	0.59	0.06	0.55	0.01	1.2	1.29	0.09	1.25	0.02
7010205	0.55	0.66	0.11	0.59	0.03	1.25	1.29	0.04	1.28	0.01
7010206	0.53	0.55	0.03	0.54	0	1.28	1.29	0.01	1.29	0
7010207	0.49	0.55	0.06	0.52	0.02	1.19	1.29	0.1	1.24	0.04
7020001	0.59	0.67	0.09	0.62	0.02	1.2	1.29	0.09	1.25	0.02
7020002	0.52	0.62	0.1	0.56	0.03	1.18	1.26	0.08	1.21	0.02
7020003	0.63	0.68	0.05	0.66	0.01	1.26	1.3	0.04	1.29	0.01
7020004	0.57	0.68	0.11	0.65	0.02	1.24	1.3	0.06	1.28	0.01
7020005	0.52	0.64	0.12	0.57	0.03	1.18	1.28	0.09	1.23	0.02
7020006	0.67	0.68	0.01	0.67	0	1.29	1.3	0.01	1.3	0
7020007	0.57	0.67	0.1	0.64	0.02	1.29	1.3	0.01	1.3	0
7020008	0.65	0.68	0.03	0.67	0	1.3	1.3	0.01	1.3	0
7020009	0.57	0.67	0.1	0.62	0.03	1.3	1.34	0.04	1.32	0.01
7020010	0.62	0.67	0.05	0.66	0.01	1.3	1.31	0.01	1.3	0
7020011	0.56	0.62	0.07	0.59	0.02	1.3	1.34	0.04	1.31	0.01
7020012	0.54	0.65	0.11	0.58	0.03	1.28	1.3	0.02	1.29	0
7030001	0.44	0.5	0.06	0.47	0.01	1.16	1.23	0.07	1.19	0.01
7030002	0.44	0.48	0.04	0.47	0.01	1.18	1.2	0.02	1.19	0.01
7030003	0.42	0.5	0.08	0.47	0.02	1.11	1.22	0.11	1.19	0.03
7030004	0.48	0.53	0.05	0.5	0.01	1.2	1.27	0.07	1.23	0.01
7030005	0.48	0.54	0.06	0.52	0.02	1.19	1.29	0.1	1.25	0.03
7040001	0.51	0.55	0.04	0.52	0.01	1.26	1.32	0.07	1.29	0.01
7040002	0.52	0.59	0.07	0.55	0.01	1.29	1.34	0.05	1.31	0.01
7040003	0.49	0.53	0.03	0.51	0.01	1.31	1.4	0.09	1.35	0.02
7040004	0.51	0.54	0.04	0.53	0.01	1.31	1.37	0.06	1.33	0.01
7040005	0.5	0.51	0.02	0.5	0	1.34	1.39	0.05	1.37	0.01
7040006	0.51	0.52	0.01	0.52	0	1.39	1.41	0.02	1.4	0
7040007	0.47	0.52	0.04	0.5	0.01	1.31	1.4	0.1	1.37	0.02
7040008	0.52	0.55	0.03	0.53	0.01	1.35	1.43	0.08	1.4	0.02
7050001	0.39	0.48	0.09	0.46	0.02	1.15	1.27	0.12	1.21	0.02

NH4					
HUC	MIN	MAX	RANGE	AVER	STD
7050002	0.37	0.48	0.11	0.4	0.04
7050003	0.37	0.47	0.1	0.42	0.03
7050004	0.41	0.48	0.07	0.47	0.01
7050005	0.48	0.51	0.03	0.49	0.01
7050006	0.49	0.5	0.01	0.49	0
7050007	0.47	0.5	0.04	0.48	0.01
7060001	0.52	0.57	0.05	0.54	0.02
7060002	0.54	0.57	0.03	0.55	0.01
7060003	0.53	0.57	0.04	0.55	0.01
7060004	0.55	0.57	0.02	0.57	0.01
7060005	0.49	0.55	0.06	0.51	0.01
7060006	0.49	0.57	0.08	0.54	0.02
7070001	0.37	0.47	0.1	0.39	0.02
7070002	0.43	0.5	0.08	0.48	0.02
7070003	0.48	0.51	0.03	0.5	0
7070004	0.49	0.52	0.02	0.51	0
7070005	0.48	0.57	0.08	0.52	0.02
7070006	0.51	0.56	0.05	0.52	0.01
7080101	0.47	0.49	0.02	0.48	0.01
7080102	0.53	0.57	0.04	0.56	0.01
7080103	0.48	0.54	0.06	0.5	0.01
7080104	0.46	0.47	0.01	0.47	0
7080105	0.5	0.56	0.06	0.54	0.01
7080106	0.5	0.54	0.04	0.52	0.01
7080107	0.47	0.52	0.05	0.49	0.01
7080201	0.54	0.56	0.03	0.55	0
7080202	0.55	0.57	0.02	0.56	0
7080203	0.55	0.58	0.03	0.56	0.01
7080204	0.55	0.56	0.01	0.55	0
7080205	0.52	0.56	0.04	0.54	0.01
7080206	0.48	0.55	0.07	0.5	0.02
7080207	0.54	0.58	0.05	0.55	0.01
7080208	0.5	0.54	0.04	0.53	0.01
7080209	0.47	0.53	0.05	0.5	0.02
7090001	0.47	0.5	0.03	0.48	0.01
7090002	0.47	0.49	0.02	0.48	0
7090003	0.48	0.53	0.05	0.5	0.01
7090004	0.48	0.5	0.02	0.49	0
7090005	0.47	0.5	0.03	0.49	0.01
7090006	0.47	0.5	0.03	0.49	0.01
7090007	0.47	0.5	0.03	0.48	0.01
7100001	0.66	0.68	0.02	0.67	0
7100002	0.58	0.66	0.08	0.62	0.02
7100003	0.58	0.66	0.09	0.61	0.02
7100004	0.53	0.63	0.1	0.57	0.02
7100005	0.56	0.59	0.03	0.57	0.01

NO3				
MIN	MAX	RANGE	AVER	STD
1.11	1.25	0.14	1.16	0.05
1.12	1.26	0.14	1.19	0.04
1.2	1.32	0.12	1.27	0.02
1.24	1.33	0.09	1.29	0.02
1.29	1.36	0.07	1.33	0.01
1.18	1.29	0.12	1.22	0.03
1.4	1.46	0.06	1.43	0.02
1.39	1.46	0.07	1.43	0.02
1.44	1.46	0.02	1.45	0.01
1.41	1.46	0.05	1.45	0.01
1.44	1.51	0.06	1.46	0.01
1.42	1.46	0.04	1.45	0.01
1.11	1.33	0.22	1.19	0.05
1.26	1.45	0.19	1.38	0.04
1.36	1.45	0.09	1.41	0.01
1.4	1.45	0.05	1.41	0.01
1.4	1.48	0.08	1.43	0.02
1.4	1.45	0.05	1.41	0.01
1.33	1.49	0.16	1.38	0.05
1.39	1.46	0.07	1.44	0.01
1.37	1.45	0.07	1.41	0.02
1.33	1.39	0.06	1.34	0.01
1.37	1.39	0.02	1.39	0
1.37	1.4	0.02	1.39	0.01
1.33	1.38	0.05	1.36	0.01
1.33	1.44	0.11	1.39	0.03
1.33	1.44	0.1	1.39	0.03
1.34	1.41	0.07	1.36	0.02
1.37	1.43	0.06	1.4	0.01
1.4	1.45	0.05	1.43	0.01
1.35	1.44	0.09	1.39	0.02
1.35	1.41	0.06	1.39	0.01
1.39	1.43	0.03	1.41	0.01
1.33	1.4	0.07	1.38	0.02
1.46	1.57	0.11	1.54	0.03
1.47	1.56	0.09	1.51	0.02
1.44	1.56	0.12	1.49	0.03
1.47	1.54	0.08	1.51	0.02
1.34	1.57	0.23	1.49	0.05
1.52	1.57	0.06	1.54	0.02
1.35	1.52	0.16	1.45	0.05
1.3	1.31	0.01	1.3	0
1.31	1.37	0.06	1.33	0.02
1.3	1.37	0.06	1.34	0.02
1.34	1.39	0.05	1.37	0.01
1.35	1.38	0.04	1.37	0.01

NH4					
HUC	MIN	MAX	RANGE	AVER	STD
7100006	0.53	0.63	0.1	0.59	0.03
7100007	0.54	0.62	0.08	0.58	0.02
7100008	0.53	0.58	0.06	0.54	0.01
7100009	0.46	0.53	0.07	0.51	0.02
7110001	0.43	0.52	0.1	0.47	0.02
7110002	0.43	0.52	0.09	0.47	0.02
7110003	0.42	0.5	0.08	0.45	0.02
7110004	0.35	0.45	0.1	0.4	0.02
7110005	0.38	0.5	0.11	0.43	0.03
7110006	0.36	0.46	0.1	0.38	0.02
7110007	0.36	0.41	0.04	0.39	0.01
7110008	0.34	0.38	0.03	0.36	0.01
7110009	0.34	0.36	0.02	0.35	0.01
7120001	0.44	0.47	0.04	0.45	0.01
7120002	0.43	0.45	0.03	0.44	0.01
7120003	0.44	0.47	0.03	0.46	0.01
7120004	0.46	0.48	0.03	0.47	0
7120005	0.45	0.49	0.04	0.47	0.01
7120006	0.47	0.49	0.02	0.47	0
7120007	0.48	0.5	0.02	0.49	0.01
7130001	0.45	0.5	0.05	0.48	0.01
7130002	0.43	0.49	0.06	0.45	0.01
7130003	0.43	0.47	0.04	0.45	0.01
7130004	0.43	0.46	0.03	0.44	0.01
7130005	0.45	0.48	0.03	0.47	0
7130006	0.4	0.43	0.03	0.42	0.01
7130007	0.37	0.42	0.04	0.39	0.01
7130008	0.39	0.44	0.05	0.42	0.01
7130009	0.41	0.44	0.03	0.43	0
7130010	0.43	0.47	0.04	0.46	0.01
7130011	0.35	0.44	0.1	0.4	0.02
7130012	0.36	0.38	0.03	0.37	0.01
7140101	0.3	0.36	0.07	0.33	0.02
7140102	0.29	0.33	0.05	0.31	0.01
7140103	0.32	0.33	0.02	0.33	0
7140104	0.29	0.33	0.04	0.3	0.01
7140105	0.28	0.32	0.04	0.29	0.01
7140106	0.29	0.33	0.04	0.31	0.01
7140107	0.27	0.29	0.02	0.28	0
7140108	0.28	0.3	0.01	0.29	0
7140201	0.37	0.42	0.06	0.41	0.02
7140202	0.32	0.39	0.06	0.35	0.01
7140203	0.33	0.38	0.04	0.36	0.01
7140204	0.31	0.36	0.05	0.33	0.01

NO3				
MIN	MAX	RANGE	AVER	STD
1.34	1.39	0.05	1.37	0.01
1.38	1.4	0.02	1.39	0
1.38	1.39	0.01	1.38	0
1.33	1.38	0.05	1.37	0.02
1.29	1.38	0.09	1.33	0.02
1.29	1.37	0.09	1.33	0.02
1.27	1.35	0.08	1.3	0.02
1.19	1.31	0.12	1.25	0.03
1.21	1.35	0.14	1.27	0.04
1.15	1.3	0.15	1.19	0.03
1.17	1.25	0.08	1.22	0.02
1.16	1.22	0.06	1.18	0.01
1.17	1.25	0.08	1.21	0.02
1.52	1.66	0.13	1.61	0.03
1.47	1.62	0.15	1.53	0.03
1.57	1.65	0.08	1.6	0.02
1.55	1.59	0.04	1.57	0.01
1.51	1.56	0.05	1.53	0.01
1.53	1.57	0.04	1.57	0.01
1.52	1.56	0.05	1.53	0.01
1.41	1.52	0.11	1.48	0.03
1.47	1.53	0.06	1.5	0.01
1.33	1.42	0.09	1.37	0.02
1.38	1.48	0.1	1.45	0.02
1.33	1.46	0.13	1.36	0.03
1.37	1.47	0.1	1.44	0.03
1.3	1.43	0.13	1.35	0.03
1.32	1.41	0.09	1.36	0.02
1.38	1.46	0.08	1.43	0.02
1.32	1.34	0.02	1.33	0
1.2	1.35	0.15	1.29	0.03
1.22	1.31	0.09	1.27	0.02
1.1	1.27	0.18	1.17	0.04
1.03	1.18	0.15	1.09	0.04
1.09	1.15	0.06	1.12	0.01
1.06	1.16	0.1	1.1	0.02
1.08	1.16	0.08	1.11	0.02
1.1	1.21	0.11	1.14	0.02
1.04	1.09	0.05	1.06	0.01
1.08	1.12	0.03	1.11	0.01
1.3	1.46	0.16	1.41	0.05
1.18	1.36	0.18	1.25	0.04
1.2	1.32	0.12	1.26	0.03
1.12	1.26	0.14	1.19	0.03

Appendix 3-2: Dry Deposition- Annual average (AVER) nitrogen estimated flux (kg/ha/yr) of the ammonium (NH₄), nitrate (NO₃), and nitric acid (HNO₃) for the period 1960 for each 8-digit area within the Upper Mississippi Basin. Other areal statistics: minimum (MIN), maximum (MAX), range (RANGE), and standard deviation (STD).

HUC	NH ₄					NO ₃					HNO ₃				
	MIN	MAX	RANGE	AVER	STD	MIN	MAX	RANGE	AVER	STD	MIN	MAX	RANGE	AVER	STD
7010101	0.17	0.26	0.09	0.21	0.02	0.36	0.51	0.15	0.48	0.03	0.77	1.25	0.48	1.15	0.09
7010102	0.21	0.27	0.07	0.25	0.01	0.47	0.5	0.03	0.49	0.01	1.18	1.33	0.16	1.27	0.03
7010103	0.17	0.22	0.05	0.2	0.01	0.48	0.52	0.04	0.5	0.01	1.13	1.36	0.23	1.25	0.06
7010104	0.18	0.29	0.11	0.22	0.03	0.29	0.53	0.23	0.46	0.08	0.67	1.43	0.77	1.2	0.24
7010105	0.2	0.28	0.08	0.25	0.02	0.44	0.51	0.07	0.5	0.02	1.19	1.38	0.19	1.32	0.03
7010106	0.17	0.28	0.11	0.25	0.02	0.28	0.51	0.23	0.44	0.05	0.63	1.41	0.78	1.17	0.17
7010107	0.17	0.25	0.08	0.2	0.02	0.28	0.45	0.17	0.35	0.05	0.61	1.17	0.56	0.86	0.17
7010108	0.17	0.22	0.06	0.18	0.01	0.28	0.39	0.11	0.29	0.02	0.62	0.99	0.36	0.66	0.07
7010201	0.16	0.25	0.1	0.2	0.02	0.28	0.51	0.23	0.35	0.06	0.69	1.35	0.66	0.88	0.19
7010202	0.17	0.2	0.02	0.18	0.01	0.26	0.3	0.04	0.28	0.01	0.64	0.76	0.11	0.69	0.03
7010203	0.12	0.21	0.09	0.18	0.02	0.25	0.3	0.06	0.26	0.01	0.67	0.82	0.15	0.73	0.03
7010204	0.18	0.33	0.15	0.22	0.04	0.25	0.36	0.12	0.28	0.03	0.67	1.32	0.64	0.86	0.16
7010205	0.21	0.43	0.22	0.33	0.06	0.26	0.45	0.19	0.36	0.05	0.78	1.76	0.97	1.34	0.26
7010206	0.21	0.23	0.02	0.22	0	0.22	0.27	0.05	0.25	0.01	0.66	0.84	0.18	0.78	0.03
7010207	0.11	0.23	0.12	0.16	0.04	0.25	0.53	0.28	0.34	0.11	0.66	1.38	0.72	0.93	0.26
7020001	0.13	0.18	0.05	0.16	0.01	0.24	0.26	0.02	0.25	0.01	0.6	0.71	0.12	0.67	0.03
7020002	0.15	0.18	0.02	0.16	0.01	0.24	0.28	0.03	0.26	0.01	0.59	0.7	0.11	0.65	0.03
7020003	0.17	0.18	0.01	0.18	0	0.24	0.26	0.02	0.25	0	0.71	0.75	0.04	0.73	0.01
7020004	0.18	0.42	0.24	0.27	0.08	0.24	0.43	0.2	0.31	0.06	0.72	1.7	0.99	1.07	0.33
7020005	0.16	0.25	0.08	0.18	0.01	0.23	0.29	0.06	0.26	0.02	0.61	0.99	0.38	0.7	0.07
7020006	0.18	0.41	0.23	0.24	0.08	0.24	0.43	0.19	0.29	0.06	0.75	1.7	0.95	0.99	0.32
7020007	0.32	0.45	0.13	0.42	0.02	0.43	0.6	0.17	0.47	0.04	1.6	1.9	0.3	1.8	0.06
7020008	0.19	0.44	0.25	0.36	0.08	0.24	0.45	0.21	0.38	0.07	0.76	1.84	1.08	1.48	0.34
7020009	0.32	0.45	0.13	0.41	0.03	0.39	0.52	0.13	0.45	0.02	1.43	2.01	0.59	1.86	0.13
7020010	0.42	0.45	0.03	0.43	0.01	0.43	0.48	0.04	0.45	0.01	1.78	1.92	0.14	1.86	0.04
7020011	0.34	0.43	0.09	0.39	0.02	0.44	0.6	0.16	0.51	0.03	1.63	1.98	0.36	1.89	0.09
7020012	0.21	0.45	0.23	0.32	0.09	0.26	0.53	0.27	0.38	0.08	0.8	1.84	1.04	1.32	0.38
7030001	0.13	0.28	0.15	0.25	0.03	0.3	0.65	0.36	0.51	0.08	0.85	1.71	0.86	1.49	0.16
7030002	0.26	0.28	0.02	0.27	0	0.53	0.65	0.12	0.62	0.03	1.58	1.71	0.13	1.65	0.03
7030003	0.15	0.24	0.09	0.21	0.02	0.32	0.53	0.21	0.46	0.05	0.95	1.48	0.53	1.34	0.12
7030004	0.11	0.22	0.11	0.16	0.03	0.25	0.53	0.28	0.38	0.09	0.67	1.4	0.73	1.02	0.22
7030005	0.11	0.27	0.16	0.2	0.04	0.2	0.52	0.32	0.3	0.07	0.6	1.46	0.86	0.81	0.18

HUC	MIN	MAX	NH4			MIN	MAX	NO3			MIN	MAX	HNO3		
			RANGE	AVER	STD			RANGE	AVER	STD			RANGE	AVER	STD
7040001	0.22	0.27	0.05	0.23	0.01	0.27	0.49	0.22	0.32	0.05	0.81	1.2	0.38	0.88	0.05
7040002	0.23	0.38	0.15	0.27	0.04	0.27	0.61	0.35	0.35	0.09	0.85	1.89	1.04	1.15	0.3
7040003	0.25	0.38	0.13	0.33	0.04	0.36	0.79	0.43	0.66	0.13	0.94	2.11	1.17	1.72	0.35
7040004	0.23	0.3	0.07	0.25	0.01	0.27	0.57	0.3	0.34	0.05	0.88	1.44	0.56	0.98	0.1
7040005	0.36	0.38	0.02	0.37	0	0.72	0.81	0.09	0.79	0.02	1.92	2.18	0.25	2.11	0.05
7040006	0.38	0.48	0.1	0.44	0.02	0.69	0.91	0.23	0.86	0.05	1.87	2.47	0.6	2.31	0.13
7040007	0.36	0.43	0.07	0.39	0.02	0.77	1.04	0.27	0.87	0.06	2.02	2.41	0.39	2.21	0.08
7040008	0.25	0.44	0.19	0.28	0.04	0.32	0.81	0.49	0.41	0.11	0.97	2.2	1.23	1.16	0.27
7050001	0.27	0.4	0.12	0.3	0.03	0.56	0.75	0.2	0.67	0.04	1.68	1.93	0.25	1.78	0.06
7050002	0.29	0.44	0.15	0.39	0.05	0.52	0.74	0.22	0.59	0.06	1.78	2.03	0.26	1.92	0.07
7050003	0.3	0.44	0.13	0.4	0.04	0.55	0.7	0.15	0.6	0.05	1.83	2.05	0.22	1.96	0.06
7050004	0.31	0.43	0.12	0.36	0.03	0.66	0.89	0.23	0.75	0.05	1.85	2.11	0.26	1.98	0.07
7050005	0.23	0.37	0.14	0.33	0.04	0.36	0.87	0.51	0.69	0.12	0.84	2.06	1.22	1.77	0.35
7050006	0.36	0.37	0.02	0.36	0	0.77	0.82	0.05	0.78	0.01	2	2.11	0.12	2.05	0.03
7050007	0.23	0.35	0.11	0.3	0.03	0.39	0.75	0.36	0.63	0.09	0.89	1.93	1.04	1.61	0.25
7060001	0.28	0.48	0.2	0.37	0.07	0.37	0.9	0.54	0.61	0.19	1.09	2.47	1.38	1.7	0.48
7060002	0.26	0.35	0.1	0.28	0.02	0.33	0.57	0.24	0.38	0.05	1.01	1.6	0.59	1.12	0.13
7060003	0.28	0.4	0.12	0.32	0.03	0.37	0.66	0.29	0.44	0.07	1.03	1.83	0.81	1.3	0.18
7060004	0.26	0.31	0.05	0.28	0.01	0.34	0.41	0.06	0.37	0.01	1.03	1.26	0.24	1.11	0.05
7060005	0.28	0.35	0.07	0.32	0.01	0.37	0.43	0.07	0.41	0.02	0.98	1.47	0.48	1.26	0.1
7060006	0.3	0.48	0.18	0.34	0.04	0.39	0.57	0.18	0.43	0.04	1.19	2.13	0.94	1.41	0.21
7070001	0.4	0.46	0.06	0.44	0.01	0.55	0.86	0.31	0.63	0.09	2.02	2.22	0.19	2.1	0.05
7070002	0.39	0.42	0.03	0.4	0.01	0.82	1.02	0.2	0.97	0.04	2.11	2.39	0.28	2.26	0.06
7070003	0.39	0.58	0.19	0.47	0.05	0.88	1.06	0.18	1.02	0.03	2.2	2.69	0.49	2.48	0.09
7070004	0.51	0.58	0.07	0.56	0.02	0.93	1.06	0.12	1.02	0.03	2.44	2.72	0.28	2.61	0.06
7070005	0.33	0.59	0.27	0.5	0.06	0.47	1.07	0.6	0.88	0.15	1.39	2.77	1.38	2.31	0.34
7070006	0.38	0.53	0.15	0.48	0.03	0.61	0.98	0.36	0.89	0.09	1.75	2.59	0.83	2.42	0.19
7080101	0.33	0.63	0.3	0.52	0.11	0.36	0.71	0.35	0.58	0.13	1.35	2.99	1.65	2.36	0.63
7080102	0.26	0.48	0.23	0.33	0.06	0.33	0.7	0.37	0.44	0.1	1.02	2.44	1.42	1.42	0.4
7080103	0.31	0.61	0.3	0.46	0.09	0.39	0.71	0.32	0.54	0.09	1.26	2.88	1.62	2.04	0.46
7080104	0.37	0.65	0.28	0.6	0.07	0.38	0.71	0.33	0.65	0.07	1.55	3.14	1.58	2.86	0.37
7080105	0.29	0.53	0.23	0.43	0.07	0.33	0.58	0.25	0.49	0.08	1.22	2.47	1.25	2.05	0.42
7080106	0.29	0.48	0.19	0.34	0.05	0.33	0.54	0.21	0.38	0.06	1.2	2.31	1.12	1.44	0.31
7080107	0.3	0.61	0.31	0.47	0.09	0.34	0.67	0.33	0.52	0.11	1.22	2.94	1.71	2.11	0.51
7080201	0.25	0.41	0.16	0.29	0.04	0.33	0.49	0.17	0.37	0.04	1.01	1.99	0.98	1.23	0.24
7080202	0.25	0.41	0.16	0.3	0.05	0.33	0.49	0.17	0.37	0.05	1.02	1.98	0.96	1.28	0.29
7080203	0.25	0.37	0.12	0.28	0.03	0.32	0.45	0.13	0.35	0.03	1.02	1.75	0.74	1.17	0.19

HUC	MIN	MAX	NH4			MIN	MAX	NO3			MIN	MAX	HNO3		
			RANGE	AVER	STD			RANGE	AVER	STD			RANGE	AVER	STD
7080204	0.26	0.34	0.09	0.28	0.02	0.32	0.42	0.09	0.35	0.02	1.03	1.58	0.55	1.19	0.13
7080205	0.31	0.55	0.24	0.43	0.06	0.38	0.73	0.35	0.57	0.1	1.38	2.61	1.23	2.11	0.33
7080206	0.32	0.62	0.29	0.45	0.07	0.39	0.71	0.32	0.53	0.08	1.3	2.89	1.58	1.98	0.38
7080207	0.25	0.48	0.23	0.38	0.06	0.32	0.54	0.22	0.45	0.06	1.03	2.38	1.35	1.84	0.38
7080208	0.29	0.57	0.28	0.4	0.07	0.34	0.68	0.34	0.48	0.08	1.18	2.63	1.45	1.86	0.38
7080209	0.29	0.62	0.33	0.49	0.11	0.34	0.69	0.36	0.56	0.12	1.18	2.98	1.8	2.22	0.6
7090001	0.31	0.49	0.18	0.34	0.02	0.33	0.82	0.49	0.43	0.07	1.26	2.2	0.94	1.41	0.13
7090002	0.31	0.41	0.09	0.34	0.02	0.41	0.65	0.25	0.48	0.07	1.29	1.8	0.51	1.44	0.14
7090003	0.27	0.42	0.15	0.32	0.03	0.36	0.68	0.32	0.44	0.08	0.93	1.76	0.83	1.26	0.2
7090004	0.29	0.45	0.16	0.34	0.03	0.38	0.74	0.36	0.47	0.08	1.02	1.92	0.9	1.35	0.19
7090005	0.34	0.63	0.29	0.38	0.07	0.36	0.7	0.34	0.43	0.07	1.36	2.98	1.62	1.61	0.4
7090006	0.34	0.59	0.25	0.41	0.07	0.38	0.62	0.24	0.47	0.06	1.44	2.79	1.35	1.8	0.36
7090007	0.35	0.65	0.29	0.49	0.08	0.37	0.65	0.28	0.5	0.08	1.43	3.09	1.66	2.23	0.46
7100001	0.2	0.42	0.22	0.35	0.07	0.25	0.5	0.24	0.41	0.06	0.81	1.87	1.06	1.54	0.32
7100002	0.42	0.47	0.05	0.45	0.01	0.44	0.48	0.03	0.46	0.01	1.87	2.15	0.28	2.01	0.07
7100003	0.26	0.47	0.2	0.42	0.05	0.33	0.48	0.15	0.45	0.03	1.08	2.15	1.07	1.9	0.24
7100004	0.37	0.51	0.14	0.45	0.03	0.4	0.57	0.17	0.47	0.03	1.71	2.39	0.68	2.09	0.14
7100005	0.33	0.46	0.13	0.42	0.03	0.39	0.5	0.11	0.47	0.03	1.47	2.23	0.76	2.02	0.19
7100006	0.24	0.48	0.24	0.36	0.06	0.26	0.5	0.24	0.38	0.06	0.99	2.22	1.23	1.62	0.31
7100007	0.24	0.34	0.1	0.26	0.02	0.26	0.38	0.12	0.29	0.02	0.99	1.51	0.51	1.13	0.11
7100008	0.25	0.52	0.27	0.32	0.07	0.28	0.57	0.29	0.36	0.07	1.08	2.42	1.34	1.39	0.33
7100009	0.28	0.42	0.13	0.31	0.03	0.32	0.45	0.13	0.34	0.03	1.19	1.84	0.65	1.3	0.13
7110001	0.3	0.44	0.14	0.35	0.02	0.32	0.49	0.17	0.37	0.04	1.26	1.96	0.7	1.46	0.15
7110002	0.31	0.56	0.25	0.41	0.06	0.32	0.69	0.38	0.47	0.1	1.31	2.86	1.55	1.89	0.41
7110003	0.33	0.56	0.23	0.42	0.07	0.31	0.69	0.38	0.46	0.12	1.32	2.86	1.54	1.93	0.49
7110004	0.33	0.46	0.13	0.35	0.01	0.3	0.52	0.23	0.31	0.02	1.3	2.19	0.89	1.42	0.1
7110005	0.32	0.49	0.17	0.37	0.05	0.29	0.58	0.29	0.38	0.09	1.26	2.4	1.13	1.62	0.35
7110006	0.31	0.41	0.1	0.33	0.02	0.28	0.41	0.13	0.3	0.02	1.26	1.89	0.63	1.35	0.13
7110007	0.33	0.35	0.02	0.34	0	0.29	0.31	0.02	0.3	0	1.31	1.44	0.12	1.35	0.02
7110008	0.34	0.55	0.21	0.42	0.06	0.29	0.54	0.24	0.38	0.07	1.36	2.86	1.51	1.89	0.4
7110009	0.36	0.48	0.12	0.38	0.02	0.29	0.44	0.15	0.31	0.03	1.45	2.34	0.89	1.55	0.19
7120001	0.11	0.4	0.29	0.36	0.06	0.09	0.34	0.25	0.3	0.06	0.46	1.69	1.23	1.48	0.26
7120002	0.39	0.41	0.02	0.4	0	0.32	0.33	0.01	0.33	0	1.6	1.7	0.1	1.66	0.02
7120003	0.36	0.4	0.04	0.39	0.01	0.32	0.35	0.03	0.34	0	1.48	1.63	0.15	1.57	0.03
7120004	0.37	0.4	0.03	0.38	0.01	0.34	0.35	0.02	0.34	0	1.5	1.62	0.12	1.55	0.03
7120005	0.38	0.47	0.09	0.4	0.02	0.33	0.45	0.12	0.37	0.03	1.55	2.07	0.52	1.65	0.13
7120006	0.35	0.44	0.09	0.38	0.01	0.33	0.44	0.11	0.36	0.02	1.43	1.89	0.46	1.53	0.06

HUC	MIN	MAX	NH4			MIN	MAX	NO3			MIN	MAX	HNO3		
			RANGE	AVER	STD			RANGE	AVER	STD			RANGE	AVER	STD
7120007	0.37	0.65	0.28	0.5	0.07	0.34	0.67	0.33	0.5	0.08	1.5	3.12	1.62	2.26	0.41
7130001	0.36	0.56	0.19	0.41	0.05	0.35	0.56	0.21	0.41	0.05	1.48	2.58	1.1	1.76	0.26
7130002	0.37	0.4	0.03	0.38	0.01	0.33	0.37	0.05	0.35	0.01	1.52	1.62	0.1	1.59	0.02
7130003	0.37	0.65	0.28	0.48	0.08	0.34	0.61	0.27	0.45	0.07	1.51	3.2	1.69	2.16	0.47
7130004	0.37	0.41	0.05	0.38	0.01	0.33	0.38	0.05	0.35	0.01	1.52	1.79	0.27	1.58	0.04
7130005	0.47	0.66	0.19	0.61	0.04	0.46	0.69	0.24	0.6	0.05	2.07	3.2	1.13	2.91	0.26
7130006	0.39	0.68	0.29	0.48	0.1	0.32	0.59	0.27	0.41	0.09	1.63	3.41	1.78	2.13	0.63
7130007	0.43	0.68	0.24	0.55	0.06	0.36	0.59	0.22	0.47	0.06	1.85	3.35	1.49	2.55	0.39
7130008	0.37	0.67	0.3	0.54	0.06	0.34	0.58	0.24	0.49	0.05	1.54	3.31	1.77	2.55	0.34
7130009	0.38	0.62	0.24	0.43	0.06	0.34	0.54	0.2	0.38	0.05	1.56	3.03	1.47	1.87	0.35
7130010	0.34	0.61	0.27	0.45	0.08	0.34	0.62	0.29	0.46	0.09	1.41	2.94	1.53	2	0.46
7130011	0.34	0.51	0.17	0.38	0.04	0.3	0.46	0.16	0.34	0.04	1.39	2.37	0.99	1.58	0.24
7130012	0.36	0.52	0.16	0.4	0.04	0.3	0.44	0.14	0.34	0.04	1.45	2.38	0.93	1.65	0.23
7140101	0.37	0.66	0.29	0.52	0.11	0.3	0.58	0.28	0.44	0.11	1.49	3.66	2.17	2.63	0.86
7140102	0.43	0.62	0.19	0.53	0.04	0.36	0.58	0.22	0.45	0.07	2	3.48	1.48	3.15	0.28
7140103	0.53	0.61	0.08	0.59	0.02	0.48	0.59	0.11	0.55	0.03	2.78	3.39	0.61	3.27	0.11
7140104	0.51	0.65	0.14	0.58	0.04	0.38	0.58	0.2	0.49	0.06	2.81	3.63	0.82	3.4	0.14
7140105	0.33	0.69	0.36	0.57	0.1	0.17	0.57	0.4	0.43	0.12	1.46	3.8	2.34	2.96	0.69
7140106	0.34	0.52	0.18	0.39	0.04	0.19	0.4	0.21	0.26	0.04	1.49	2.65	1.16	1.69	0.24
7140107	0.49	0.68	0.19	0.65	0.03	0.29	0.56	0.27	0.48	0.05	2.32	3.71	1.39	3.47	0.27
7140108	0.33	0.43	0.1	0.35	0.02	0.18	0.25	0.07	0.19	0.02	1.47	2.01	0.54	1.57	0.13
7140201	0.4	0.46	0.06	0.41	0.01	0.32	0.39	0.07	0.33	0.01	1.61	2.01	0.39	1.68	0.08
7140202	0.38	0.43	0.05	0.39	0.01	0.28	0.36	0.08	0.31	0.01	1.56	1.85	0.28	1.62	0.03
7140203	0.38	0.46	0.08	0.39	0.01	0.29	0.39	0.1	0.32	0.02	1.55	2.03	0.48	1.6	0.08
7140204	0.38	0.59	0.22	0.43	0.06	0.28	0.51	0.23	0.34	0.06	1.53	3.19	1.66	1.92	0.48

Appendix 3-3. – Daily point source records for (Flow) water (m³/s), (TKN) total kjeldahl nitrogen (kg), (TOT-P) total phosphorus (kg) and (TSS) total suspended solids (kg) for each HUC in the Upper Mississippi Basin.

HUC	FLOW	TKN	TOT-P	TSS
7010101	5.48	207.45	60.79	548.87
7010102	0.04	102.09	35.45	120.53
7010103	1.15	781.03	121.41	1637.14
7010104	0.39	438.69	77.87	624.21
7010105	0.03	49.67	18.51	50.04
7010106	0.12	336.68	56.09	303.30
7010107	0.26	287.53	51.75	82.28
7010108	0.24	329.58	53.15	549.44
7010201	0.56	296.84	75.86	1698.10
7010202	0.36	558.35	67.97	708.93
7010203	19.64	609.52	138.35	1532.58
7010204	1.62	1950.99	255.21	1883.99
7010205	0.87	1325.59	279.88	1933.54
7010206	27.69	4764.18	3741.33	17846.60
7010207	0.33	677.30	158.83	667.51
7020001	1.36	1560.74	317.53	4248.48
7020002	0.09	1788.51	40.61	323.21
7020003	0.29	333.20	69.68	279.93
7020004	1.77	1531.64	277.84	1765.64
7020005	1.11	1364.83	287.76	3443.51
7020006	0.23	375.16	93.89	487.15
7020007	1.56	839.45	213.59	3837.46
7020008	1.17	1331.70	255.69	1463.47
7020009	0.69	736.92	256.64	896.81
7020010	0.17	299.35	72.60	423.59
7020011	0.45	710.86	136.13	674.88
7020012	15.69	3680.76	856.52	7114.97
7030001	0.26	296.88	95.84	922.49
7030002	0.00	0.00	0.00	0.00
7030003	0.20	263.34	66.38	471.40
7030004	0.04	63.37	9.32	72.81
7030005	11.96	2257.98	296.21	2645.89
7040001	17.82	2253.70	273.39	1651.57
7040002	2.07	1038.05	168.05	4910.39
7040003	15.17	1290.59	212.35	12792.81
7040004	1.57	1192.16	162.07	2613.51
7040005	0.26	1083.18	90.91	2561.37
7040006	1.72	1258.27	228.39	5299.01
7040007	0.54	1270.46	141.49	532.81
7040008	0.70	587.56	115.97	1038.42
7050001	0.94	1031.61	186.45	349.56
7050002	0.87	363.69	41.47	2190.09
7050003	0.02	31.05	8.64	46.33

HUC	FLOW	TKN	TOT-P	TSS
7050004	1.72	1668.43	300.12	1707.29
7050005	0.21	316.58	98.45	2879.86
7050006	0.12	562.43	171.52	913.48
7050007	1.81	2092.09	344.86	2021.52
7060001	16.54	1025.08	94.47	799.75
7060002	0.12	199.64	46.99	201.71
7060003	6.82	946.85	116.46	6248.36
7060004	0.55	955.79	151.57	660.02
7060005	3.62	2394.44	527.41	4018.84
7060006	0.29	484.82	95.90	877.06
7070001	1.62	550.66	74.67	6132.77
7070002	6.69	2132.93	249.47	24424.51
7070003	12.79	2276.03	507.81	17815.65
7070004	0.58	1279.52	237.09	2435.92
7070005	0.68	1319.99	106.61	812.43
7070006	0.16	863.83	88.53	548.91
7080101	30.20	24937.94	9479.19	23513.76
7080102	0.45	761.53	90.21	785.09
7080103	0.27	296.52	53.27	472.57
7080104	7.20	3999.53	1462.86	5528.43
7080105	0.70	931.01	265.73	1419.13
7080106	0.46	551.33	131.74	431.65
7080107	0.33	393.48	94.83	597.33
7080201	0.76	1270.25	205.55	1693.35
7080202	1.20	1309.52	230.44	4280.82
7080203	0.64	790.68	143.78	682.40
7080204	0.22	378.33	64.02	620.49
7080205	8.71	3278.66	955.94	3974.87
7080206	1.78	1884.90	327.70	3070.63
7080207	0.30	510.75	107.43	815.33
7080208	3.86	3518.77	475.49	1404.77
7080209	2.24	1190.90	312.83	5567.16
7090001	17.83	8212.37	1228.64	12521.05
7090002	0.22	1057.70	107.43	3345.37
7090003	0.44	1768.11	239.00	1621.82
7090004	0.38	895.78	109.58	736.55
7090005	2.92	4603.85	1111.14	4846.24
7090006	0.63	1354.11	370.21	1737.09
7090007	0.09	234.00	65.36	338.62
7100001	0.42	363.31	91.84	854.91
7100002	0.37	1008.36	134.77	1159.44
7100003	2.72	463.52	116.20	793.48
7100004	4.19	4727.00	1020.68	2260.36
7100005	0.17	193.66	34.39	517.24
7100006	0.50	955.07	163.41	1874.70
7100007	0.20	369.76	81.66	593.56
7100008	3.11	3492.08	726.56	5098.48

HUC	FLOW	TKN	TOT-P	TSS
7100009	0.93	2087.56	865.71	3083.93
7110001	0.26	22131.01	13010.54	46922.61
7110002	0.00	3598.52	815.81	3752.32
7110003	0.00	644.30	156.17	14206.43
7110004	0.11	71066.19	44079.81	71321.56
7110005	0.00	26306.14	15998.92	36259.90
7110006	0.00	24510.66	5063.98	36081.43
7110007	0.00	3405.66	2327.63	18287.97
7110008	0.00	64430.18	35176.72	46029.63
7110009	2.01	28367.70	16088.40	13672.31
7120001	4.32	2305.31	552.73	5635.87
7120002	0.41	512.18	93.09	744.42
7120003	15.62	18755.00	4938.24	20713.21
7120004	43.05	13964.95	8768.78	33489.87
7120005	0.62	1189.89	315.41	1452.43
7120006	3.36	7509.72	2265.66	10798.49
7120007	1.62	1925.46	466.85	1459.23
7130001	5.19	1674.74	450.28	4221.97
7130002	0.39	576.39	145.15	731.69
7130003	4.40	2412.31	736.16	4262.45
7130004	0.18	1033.24	188.61	1015.41
7130005	2.02	931.68	240.27	8525.03
7130006	1.62	1799.57	411.39	1936.38
7130007	0.66	884.99	193.61	1587.19
7130008	1.02	1152.29	238.26	1465.09
7130009	1.33	1619.78	455.96	3675.07
7130010	0.14	401.07	116.49	466.86
7130011	0.84	1413.16	196.12	2170.32
7130012	0.16	405.90	92.47	768.68
7140101	2.91	114703.46	68201.93	167752.90
7140102	0.05	50240.23	21749.56	150380.67
7140103	0.19	41790.18	12068.72	67685.59
7140104	0.00	18732.77	9629.88	54231.47
7140105	0.15	26580.39	19786.10	68680.20
7140106	0.81	2587.25	1128.60	3415.43
7140107	0.00	10965.00	5328.95	29158.25
7140108	0.00	183.90	85.23	319.11
7140201	0.25	375.63	99.94	717.46
7140202	0.25	918.85	266.15	1350.86
7140203	0.42	569.93	152.92	1151.14
7140204	3.20	3751.64	933.20	1859.44

CHAPTER 4

UN-CULTIVATED MANAGEMENT SYSTEMS

4.1 PASTURE

Pasture is separated into two categories; both are grazed and receive non-recoverable manure. Non-recoverable manure is defined as manure on pastureland from grazing animals. One category also receives recoverable manure (manure that is available for land application) from confined animal feeding operations (CAFOs).

4.1.1 PASTURE – NO RECOVERABLE MANURE APPLICATION

For modeling purposes, pasture is considered to be planted with a grass typical of the region modeled. In southern states a warm-season grass was simulated and in northern states a cool-season forage variety was simulated. These areas are continuously grazed, but not overgrazed. A minimum of 1200 kg/ha of dry biomass is present during the growing season.

The amount of non-recoverable manure application was based on cattle production estimates derived from US Agricultural Census (Kellogg et al 2000). Non-recoverable manure associated with grazing cattle was applied in four equal portions at 3 month intervals. Commercial nitrogen and phosphorus fertilizer was also applied in the spring of each year at a rate equal to $\frac{1}{4}$ the total non-recoverable manure nutrient application.

4.1.2 PASTURE - WITH RECOVERABLE MANURE APPLICATION

Pasture areas with recoverable manure application are managed identically to other pastures with the addition of a single manure application each spring. This application is scheduled to occur just after the start of the growing season. The amount and nutrient content of this recoverable manure application are derived from US Agricultural Census (Kellogg et al 2000). Recoverable manure is calculated by multiplying the tons of manure excreted per animal unit (AU) by the number of AU by the recoverability factor by the nutrients per ton of manure after losses (Kellogg et al 2000). Manure mass and nutrient content losses are due to losses during collection, transfer, storage and treatment.

4.2 HAY

Hay is also separated into two categories; legume hay and other hay

4.2.1 LEGUME HAY

4.2.1.1 NO RECOVERABLE MANURE APPLICATION

Legume hay is simulated as alfalfa in a four year rotation. During the first year, the seedbed is prepared with a chisel, 2 disking operations, and one pass with a cultipacker. Legume hay is the only cultivated land use simulated in CEAP using SWAT. Alfalfa is planted and given a 50 lb/acre application of commercial phosphate fertilizer. The crop is hayed one the first year, and three times during each of the second, third and fourth years. Phosphate is applied at a rate of 13/lb/acre each spring of years 2 through 4.

4.2.2.2 WITH RECOVERABLE MANURE APPLICATION

This category is managed similar to non-manured legume hay with a few exceptions. A manure application is scheduled each spring at rates derived from Kellogg et al 2000. Phosphate applications during years 2 through 4 are suspended because of the spring manure applications.

4.2.3 OTHER HAY

Other hay represents all hay other than legume hay. Other hay is also separated into two categories with one category receiving recoverable manure from confined animal feeding operations.

4.2.3.1 NO RECOVERABLE MANURE APPLICATION

The areas are planted with a grass typical of the region modeled. In southern states this is a warm season grass and in northern states a cool season forage variety was simulated. An automated fertilizer application is used to apply 28-0-0 at rates which prevent excessive plant stress due to nutrient deficiencies. Hay is harvested 3 times each year.

4.2.3.2 WITH RECOVERABLE MANURE APPLICATION

This land use is managed like hay with no recoverable manure application with the substitution of a manure application (derived from Kellogg et al 2000) for the commercial fertilizer application.

4.3 SIMULATION OF URBAN AREAS

Large watersheds such as Upper Mississippi river basin contain areas of urban land use. Estimates of quantity and quality of runoff from urban areas are required for comprehensive management analysis. Urban areas contain impervious surfaces such as constructed buildings, parking lots, paved streets etc. that increases the volume and velocity of runoff in response to rainfall and pervious areas, such as grass or bare soil.

For modeling water quality of urban areas, the model uses the parameters defined in the urban database. The parameters are urban land type, maximum amount of solids allowed to buildup on impervious areas (kg/curb km), number of days for amount of solids on impervious area to build up from 0 kg/curb km to $\frac{1}{2}$ sed_{max}, wash-off coefficient, curb length density, concentration of total nitrogen in suspended solid load (mg N/kg), concentration of total phosphorus in suspended solid load (mg P/kg) and concentration of nitrate in suspended solid load (mg N/kg) (Neitsch et. al, 2002 and 2005). Pervious surfaces within the urban HRU are modeled as grass. The parameters for modeling grass are taken from plant growth database.

4.3.1 IMPERVIOUS AREAS

Urban areas differ from rural areas in the fraction of total area that is impervious. Construction of buildings, parking lots and paved roads increases the impervious cover in a watershed and reduces infiltration. With development, the spatial flow pattern of water is altered

and the hydraulic efficiency of flow is increased through artificial channels, curbing, and storm drainage and collection systems.

The impervious areas in HUMUS-SWAT are broadly categorized into two groups: (1) those hydraulically connected to drainage systems (e.g. paved roads draining to storm drains); and (2) those that are not hydraulically connected (e.g. a house roof draining to pervious yard). The response to rainfall as runoff is modeled differently for these two types of impervious areas. For directly connected impervious areas, a curve number of 98 is always used. For disconnected impervious areas a composite curve number (depending on the proportion of pervious and impervious areas) is estimated and used for surface runoff calculations (Eq. 1 and 2).

$$CN_c = \frac{CN_p \times (1 - imp_{tot} + \frac{imp_{dcon}}{2}) + 98 \times (\frac{imp_{dcon}}{2})}{1 - imp_{con}} \quad \text{if } imp_{tot} \leq 0.30 \quad (1)$$

$$CN_c = \frac{CN_p \times (1 - imp_{tot}) + 98 \times imp_{dcon}}{1 - imp_{con}} \quad \text{if } imp_{tot} \geq 0.30 \quad (2)$$

Where:

CN_c is the composite moisture condition II curve number;

CN_p is the pervious moisture condition II curve number;

imp_{tot} is the fraction of the HRU area that is impervious (both directly connected and disconnected);

imp_{con} is the fraction of the HRU area that is impervious and hydraulically connected to the drainage system; and

imp_{dcon} is the fraction of the HRU area that is impervious but not hydraulically connected to the drainage system.

The proportion of impervious areas and the connectedness of the impervious areas are defined for each urban land use type. The user is allowed to vary these values if needed. The possible types of urban land use are residential (high, medium and medium-low and low densities), commercial, industrial, transportation and institutional. Table 4-1 lists typical values for impervious and directly connected impervious fractions in different urban land types.

Table 4-1: Range and average impervious fractions for different urban land types.

Urban Land Type	Average total impervious	Range total impervious	Average directly connected impervious	Range directly connected impervious
Residential-High Density (> 8 unit/acre or unit/2.5 ha)	.60	.44 - .82	.44	.32 - .60
Residential-Medium Density (1-4 unit/acre or unit/2.5 ha)	.38	.23 - .46	.30	.18 - .36
Residential-Med/Low Density (> 0.5-1 unit/acre or unit/2.5 ha)	.20	.14 - .26	.17	.12 - .22
Residential-Low Density (< 0.5 unit/acre or unit/2.5 ha)	.12	.07 - .18	.10	.06 - .14
Commercial	.67	.48 - .99	.62	.44 - .92
Industrial	.84	.63 - .99	.79	.59 - .93
Transportation	.98	.88 - 1.00	.95	.85 - 1.00
Institutional	.51	.33 - .84	.47	.30 - .77

HUMUS-SWAT uses a medium density classification for modeling purposes. The total impervious area is 24% of the total urban area and 18% of the impervious area is considered directly connected.

For simulating water quality in impervious urban areas, HUMUS-SWAT uses a buildup and wash off mechanism. The concept behind the buildup-wash off algorithm is that over a period of time, dust, dirt and other constituents are built up on street surfaces during dry periods (preceding a storm). During a storm event the materials built up are washed off in response to rainfall. Build up is a function of time, traffic flow, dry fallout and street sweeping. The build up/wash off algorithm calculates the build up and wash off of solids. The solids are assumed to possess a constant concentration of organic and mineral nitrogen and phosphorus where the concentrations are a function of the urban land type.

Build up of solids is simulated on dry days with a Michaelis-Menton equation:

$$SED = \frac{SED_{mx} \cdot td}{(t_{half} + td)} \quad 6:3.4.1$$

Where:

SED is the solid build up (kg/curb km) td days after the last occurrence of $SED = 0$ kg/curb km,

SED_{mx} is the maximum accumulation of solids possible for the urban land type (kg/curb km), and

t_{half} is the length of time needed for solid build up to increase from 0 kg/curb km to $\frac{1}{2}$ SED_{mx} (days).

A dry day is defined as a day with surface runoff less than 0.1 mm. As can be seen from the plot, the Michaelis-Menton function will initially rise steeply and then approach the asymptote slowly.

4.3.2 SEDIMENT LOAD FROM CONSTRUCTION SITES

Construction and development (C&D) activities typically involve excavating and clearing the existing vegetation. During the construction period, the affected land is usually stripped, and the soil compacted, leading to increased stormwater runoff and high rates of soil erosion. In addition, there is high potential for hazardous pollutants from C&D areas to migrate to nearby streams and rivers. The most obvious and important pollution from C&D is sediment. One study points out that construction areas can transport as much as 80 million tons of sediment into receiving waters each year (Goldman et al., 1986). On a unit area basis, construction sites, can transport sediment at 20 to 1,000 times the rate of other land uses (Schueler, 1997). Given the estimates, sediment from C&D activities is not something to ignore in large-scale watershed level modeling studies although the area of C&D activities are small.

The data on sediment load from C&D activities are very limited. To account for sediment load from C&D activities in CEAP-HUMUS, the necessary information is taken from a published EPA report ((USEPA, 2008) based on a national-scale study. To assess the pollutant loading from C&D and for regulatory purposes, the EPA developed a series of model construction sites throughout the country. Because of the large variation in soil types and rainfall patterns nationwide, EPA selected high-growth urban areas that could be used to produce representative point estimates. Using the greatest rate of development, EPA identified major metropolitan areas within each of the 10 EPA Regions to serve as indicators. The indicator cities selected for the 10 EPA Regions (with their state code in braces) are Manchester (NH), Albany (NY), Washington (DC), Atlanta (GA), Chicago (IL), Dallas (TX), Kansas City (MO), Denver (CO), Las Vegas (NV), Boise City (ID), and Seattle (WA). The indicator city may cross state boundaries and includes surrounding suburban areas (e.g. Seattle). Two indicator cities were

selected for EPA Region 10, in part to assess expected variability in rainfall between damp coastal areas (e.g., Seattle) and the arid inland western flank of the Rocky Mountains (e.g., Boise, Idaho) (USEPA, 2008).

EPA used Revised Universal Soil Loss Equation (RUSLE) (USDA, 2000) to estimate annual sediment load from C&D activities.

$$\text{Per Acre Yield of Eroded Soil Tons} = R \times K \times LS \times C \times P \quad (4)$$

Where:

Land Condition Parameters;

C = Cover Management Factor

P = Support Factor/Soil Management Factor

Soil Erodibility Factor

K = Soil Erodibility, tons/acre

Site Location Factor;

R = Rainfall – Runoff Erosivity Factor

Site Geometry

LS = Length Slope Factor.

The parameter estimates used for the RUSLE are shown in table (Table 4-2) and the estimated soil erosion rates for various model construction projects are shown in Table (Table 4-3)

Table 4-2. Parameter estimates used in RUSLE for construction sites		
RUSLE term	Source of information	Processing for model project erosion estimation
C	SEDCAD4 documentation*	Set to 1 for all regions. Represents denuded soil
P	SEDCAD4 documentation*	Set to 0.9 for all regions. Represents rough and irregularly tracked soils
K	STATSGO	Spatially averaged value determined from soil data for each indicator city
R	RUSLE database**	Value reported each city/adjacent county
LS	Length factor estimated on the basis of model project geometry Regional slope ranges obtained from STATSGO	Length and regional slope value are combined to yield LS value. Assumption: high ratio of rill-inter-rill erosion

* SEDCAD 4 Documentation (Warner et al. 2006)

** RUSLE 2 ARS Version Jan 19 2005, Program Database

Construction and Development activity	City	Low End (t/ha/year)	Average (t/ha/year)	High End (t/ha/year)
Small, medium and large transportation model construction projects	Chicago	71.1	93.8	117.2
	Kansas City	181.2	224.7	269.4
	average	126.1	159.3	193.3
Medium and large residential model construction projects	Chicago	109.1	172.9	242.0
	Kansas City	22.3	35.4	50.1
	Average	65.7	104.1	146.0
Large and medium non-residential model construction projects	Chicago	118.6	190.2	268.3
	Kansas City	25.3	40.4	40.4
	Average	71.9	115.3	154.3
Small non-residential and small residential model construction projects	Chicago	94.5	146.5	201.7
	Kansas City	18.0	28.1	39.3
	Average	56.2	87.3	120.5

4.3.2.1 Representation of sediment produced from construction areas within SWAT

For modeling purposes, constructions areas are considered to comprise 3% of urban areas. Typically each HUC has a single construction site HRU. However, the construction HRUs are not distinguished by the category such as transportation, residential or non-residential. All the construction HRUs use the same soil and HRU properties as we cannot accommodate all the possible combination of soils, land cover, slope and construction type in a large-scale modeling study.

To determine runoff, soil erosion and sediment yield produced from construction areas, the parameters in soil input file, and HRU input file in HUMUS-SWAT were modified to produce high surface runoff and high sediment yield. CN was adjusted to simulate fallow conditions and the soil erodibility factor (K), sediment concentration in lateral flow, and the proportion of sand silt and clay were adjusted to realistically model C& D areas. Kansas city and Chicago were the only two indicator cities of Upper Mississippi river basin in the EPA study. Therefore, the model parameters were so adjusted to simulate the average sediment load in various construction categories.

4.3.4 PERVIOUS AREAS:

For the pervious portion of the urban HRU, all processes of management are simulated exactly the same and any non-urban HRU assuming a grass surface mowed to 4 in. continuously (1200 kg/ha of dry material), except for construction areas, where the pervious area is modeled as bare soil. The grass is considered irrigated as needed based on plant stress demand. Grass areas are modeled as receiving a fertilizer application of 40 lbs N/acre/year.

4.4 MODELING FOREST AREAS

In HUMUS-SWAT forest can be modeled under 3 different categories: deciduous; evergreen; and mixed. Trees/shrubs of these three forest types differ in height, rooting depth, biomass, metabolism and adaptation. This creates differences in uptake and transport of water, and nutrients from the soil. The NLCD 2001 Land Cover Class Definitions of the three forest types are as follows:

Deciduous Forest - Areas dominated by trees generally greater than 5 meters tall, and greater than 20% of total vegetation cover. More than 75 percent of the tree species shed foliage simultaneously in response to seasonal change.

Evergreen Forest - Areas dominated by trees generally greater than 5 meters tall, and greater than 20% of total vegetation cover. More than 75 percent of the tree species maintain their leaves all year. Canopy is never without green foliage.

Mixed Forest - Areas dominated by trees generally greater than 5 meters tall, and greater than 20% of total vegetation cover. Neither deciduous nor evergreen species are greater than 75 percent of total tree cover.

4.4.1 MODELING FOREST IN HUMUS-SWAT

During dormancy most of the trees shed their leaves. This is modeled by a minimum leaf area index (LAI) parameter. The user has the option of varying this parameter depending on region. The growth of trees /shrubs in forest is governed by the accumulated heat units and the

parameters defined in the plant database (more details available in modeling of plant growth section). The important plant growth parameters vary for different types of forest. The growth parameters include leaf area development, plant height, base temperature and nutrient uptake. The differences in plant growth parameters bring differences in biomass, and leaf area index and therefore differences in the uptake and transport of water and nutrients from the soil.

4.4.2 MODELING FORESTLAND EROSION RATES AT WATERSHED SCALE

Similar to cultivated and other land cover categories, the RUSLE factors were defined. However, to accommodate the forestland rotation cycles, climate and cultural operations utilized for tree production, the factors were allowed to vary from year to year as per the guidelines given in Tables 4-4 and 4-5. Forestland is assumed to have no protective cover during first year following harvest.

Table 4-4: C factors-Harvest Cycle/Forest Management Effects

	Year				
	1	2-4	5-8	8-20	> 20
Disk, raked, rough surface > 6 inches	0.17	0.05	0.012	0.003	0.001

Table 4-5: P factors-Harvest Cycle/Forestland Conservation Practice Effects

	Year				
	1	2-4	5-8	8-20	> 20
Some contour effects	0.80	0.90	1.0	1.0	1.0

4.5 WETLANDS

Wetlands in SWAT are modeled under two categories: forested wetlands, and non-forested wetlands. The model allows growth of vegetation in wetlands. Similar to cultivated crops, and trees, growth of wetlands is modeled by accumulated heat units and the parameters governing plant growth. In reality, a wetland can have many different types of plants. However, to avoid complexities a single set of plant growth parameters is adopted for modeling forested wetlands. The important differences between the two wetland categories is simulated by the model with differences in plant growth, ET patterns and hence differences in base flow and water yield.

For modeling of flow and pollutants, a wetland is treated as an impoundment. The fraction of the subbasin (8-digit watershed for HUMUS) that drains into wetlands is input to the model. Wetlands can release water, receive precipitation and inflow, evaporate and seep water. In terms of water balance wetlands are similar to ponds. Evaporation and seepage from wetlands are modeled as a function of surface area. Wetland surface area is computed daily based on normal and maximum water levels. Inflow to the wetland is based on flow from upland and the fraction of subbasin area drained by the wetland. Outflow is released from wetland whenever the water volume exceeds normal storage volume of wetland.

SWAT uses a simple mass balance model to simulate the transport of sediment into and out of wetlands. For modeling sediment in wetland, the model assumes uniform depth and complete mixing. This means as soon as sediment enters wetland it is instantaneously distributed throughout the volume. Sediment is allowed to settle in wetland as a function of amount of sediment in the inflow, inflow volume, water stored in wetland and amount of sediment in wetland.

Nutrient transformations in wetlands are modeled in SWAT by empirical equations. Similar to sediments, the model assumes complete mixing in the system for modeling nutrients. Complete mixing assumption distributes the nutrients throughout the wetland volume ignoring water stratification and intensification of phytoplankton. The only form of a nutrient transformation in wetland is settling for which SWAT uses an empirical equation. Nutrient settling is a function of settling velocity of the particular nutrient, surface area, and initial concentration of nutrient in wetland. The model does not consider nutrient transformation within

different pools (e.g. $\text{NO}_3 \leftrightarrow \text{NO}_2 \leftrightarrow \text{NH}_4$). A number of inflow and impoundment properties affect the settling rate of nutrients. e.g. form of nutrients (dissolved or sediment bound), potential for sediment re-suspension etc. They are not considered in the model.

4.6 BARREN LAND

Barren lands include deserts, dry salt flats, beaches, sand dunes, exposed rock, strip mines, quarries, and gravel pits. In reality, barren land has thin soil, sand, or rocks. Vegetation is very rare. Therefore, they typically produce more runoff and have a high potential to transport sediments. In the model, plants do not grow in barren lands. In the model set up of study area, the soils that come under barren lands have relatively less water holding capacity when compared to other land cover categories. In addition, barren land will have high curve number (CN) values. High CN values combined with low water holding capacities increases runoff and potentially sediment yield from barren land.

4.7 REFERENCES:

- Goldman, S.J., K. Jackson, and T.A. Bursztynsky. 1986. Erosion and Sediment Control Handbook. McGraw-Hill, New York.
- Neitsch, S.L., J. G. Arnold, J.R. Kiniry, R. Srinivasan, and J.R. Williams. 2002 Soil and Water Assessment Tool (Version 2000). User's Manual. Grassland, Soil and Water Research Laboratory, USDA-ARS, Temple, TX 76502 and Blackland Research Center, Temple, TX 76502.
- Neitsch, S.L., J. G. Arnold, J.R. Kiniry, and J.R. Williams. 2005 Soil and Water Assessment Tool (Version 2005). Theoretical Documentation. Grassland, Soil and Water Research Laboratory, USDA-ARS, Temple, TX 76502 and Blackland Research Center, Temple, TX 76502.
- Schueler, T. 1997. Impact of Suspended and Deposited Sediment. Article 14 in The Practice of Watershed Protection, eds. T.R. Schueler and H.K. Holland, pp. 64-65. Center for Watershed Protection. Ellicott City, MD.

United States Department of Agriculture (U.S. Department of Agriculture). 2000. Predicting Soil Erosion by Water: A Guide to Conservation Planning With the Revised Universal Soil Loss Equation (RUSLE). Agriculture Handbook Number 703. U.S. Department of Agriculture, Agricultural Research Service. Washington, DC.

United States Environmental Protection Agency (USEPA), 2008. Development document for proposed effluent guidelines and standards for the construction & development category, USEPA, Office of Water, 1200 Pennsylvania Avenue NW, Washington D.C.20460. Warner, R., P. Schwab, and D. Marshall. 2006. SEDCAD 4.0 for Windows, Design Manual and User's Guide 2006. Civil Software Design, LLC, Lexington, KY.

CHAPTER 5

APEX INTEGRATION

The APEX model is an integrated dynamic tool that is capable of simulating extensive land management strategies, such as different nutrient management practices, tillage operations, and alternative cropping systems on field, farm, or small watershed scales. It can be configured to simulate filter strip impacts on pollutant losses from upslope fields, intensive rotational grazing scenarios depicting movement of cows between paddocks, impacts of vegetated grassed waterways in combination with filter strip, and land application of manure, removal from livestock feedlots or waste storage

ponds (Gassman et al., 2010). APEX operates on a daily time step. Detailed theoretical description of APEX can be found in Williams and Izaurralde (2006).

The APEX model was selected for the CEAP field-level cropland modeling due to its flexibility and features including (1) field units within APEX have spatial relationship and can be routed at the field scale, which provides for physically based simulation of conservation practices like filter strips, terraces, and waterways; (2) APEX crop growth component enables simulation of mixed stands with plant competition for light, water and nutrients; (3) APEX simulates detailed management practices related to farm animal productions, rotational grazing, and wind erosion; (4) APEX enables dynamic soil layers associated with soil erosion and the removal of eroded material, and it provides eight options (including RUSLE 2) for estimating water erosion; (5) APEX simulates tillage with the functions of mixing nutrients and crop residues, converting standing residue to flat residue, changing bulk density and subsequent settling after tillage, speeding mineralization; (6) APEX features an improved soil carbon cycling routine that follows the Century model (Parton et al., 1987, 1993, 1994; Vitousek et al., 1994); and (7) APEX has manure management with automatic application from stockpile or lagoon, and manure erosion from feedlots and application fields.

5.1 STATISTICAL SAMPLING AND MODELING APPROACH

In the CEAP cropland national assessment, a subset of the 2001, 2002, and 2003 Annual National Resources Inventory (NRI) sample points was selected for CEAP cropland survey to determine conservation practices currently in use. Because the samples were drawn statistically, an acreage weight is derived for each sample point (Goebel, 2009) so that individual results can be aggregated to represent the landscape condition. The NRI-CEAP samples are statistically representative of cultivated cropland and formerly cultivated land currently in long-term conserving cover and capture the diversity of soils, climate, field characteristics, farming practices, and conservation systems throughout the agricultural land in the United States.

The NRI-CEAP points served as "representative fields" to be simulated using APEX. A total of 5534 representative cultivated fields (3703 NRI-CEAP cropland points and 1831 CRP

points) were setup to run using APEX. The statistical acreage weights associated with each representative field range from 2.4 hectares to 554 thousand hectares. The statistical sample weight associated with each sample point was used to aggregate the edge-of-field APEX modeling results for national reporting of onsite benefits. APEX also provides 8-digit watershed output to SWAT by using delivery ratios computed within APEX considering the 8-digit watershed channel lengths and slopes. APEX outputs to SWAT from each NRI-CEAP point were area weighted and added for each 8-digit watershed as below:

$$SWAT_{in} = \frac{\sum_{i=1}^n (APEX_{out_i} \times AWeight_i)}{\sum_{i=1}^n AWeight_i} \quad (1)$$

Where:

$SWAT_{in}$ is the aggregated APEX-watershed-output-to-SWAT for one 8-digit watershed (e.g., water yield in mm or sediment yield in Mg ha⁻¹);

$APEX_{out_i}$ is the corresponding APEX-watershed-output-to-SWAT for one NRI-CEAP point i in the 8-digit watershed;

$AWeight_i$ is the acreage weight of the point i in ha; and

n is the total number of NRI-CEAP points simulated for this 8-digit watershed.

In concept, this is similar to handling SWAT HRUs, where individual HRUs are simulated independently, area weighted and added for each subbasin. The aggregated results, representing the outputs from cultivated cropland areas, were passed to SWAT. SWAT reads in the aggregated APEX output for each 8-digit and adds it to the reach at the 8-digit outlet. They were then combined with SWAT outputs for uncultivated land at the 8-digit watershed outlets for further routing downstream in SWAT for estimating the offsite effects at each major river basin outlet. In SWAT, the major river basin is treated as a watershed and each United States Geological Survey (USGS) delineated 8-digit watershed as a subbasin.

5.2 MODELING CONSERVATION PRACTICES

APEX requires weather, soil, site, and field management information. The available data and sources for APEX modeling are summarized in Table 5-1. In this study, conservation practices are classified into cultural practices and structural practices. Cultural practices are those that a farmer or land manager implements, usually based on annual decisions, by changing the way cropland is managed to achieve production or conservation goals. Reducing tillage intensity through practices such as conservation tillage, improving vegetative cover over the soil surface through practices such as cover crops, conservation crop rotations, and applying mulch are examples of cultural practices. Managing nutrient applications through a nutrient management plan and pest problems using integrated pest management are other cultural techniques. APEX management capabilities include processes built for simulating these practices as physically and realistically as possible. For example, tillage simulation is designed for mixing nutrients and crop residues, changing surface roughness and bulk density, and subsequent settling. Crop growth simulates the growth of plants which vary from vegetables, field crops (cover crops, crop rotations), annual & perennial grasses, brush, trees and mixed stands. And during the plant growth cycle, the crop management factor (USLE C factor) is updated daily to reflect change in plant cover.

Structural practices are considered permanent practices that require more than annual management decisions. Usually these practices are considered permanent because implementation usually requires engineering design, surveying, and usually contracting with a vendor. Planting of perennial grasses, trees, or herbaceous cover to achieve desired conservation effect are also considered as structural practices. Practices like contour farming and strip cropping tend to “support” cultural management practices. Structural practices such as terraces and diversions work by intercepting and diverting surface runoff to stable outlets. Other structural practices, including field borders, buffer strips, and riparian buffers, filter surface runoff and allow contaminated water to infiltrate into the soil. To capture combined effects and eliminate duplicate functions, practices were assigned into one of the following functional categories: managed in-field flow interceptor, engineered in-field flow interceptor, riparian buffer, and wind erosion control (Table 5-2). APEX provides considerable flexibility for simulating conservation practice effects. The model allows one to simulate effects using

empirically based techniques, theoretical techniques, or a combination of both. In this study, managed and engineered flow interceptor effects were simulated via changes in the conservation practice factor (P factor), slope, slope length, or curve number. Riparian areas were simulated as areas of grasses or trees separate from the cropland area which the water runoff from the cropland had to cross prior to reaching the “edge of field”. Effects from wind erosion control were simulated by changing the unsheltered distance in the field length and width. Field border effects were simulated by reducing the P factor by 5 percent. Grade stabilization structures and grass waterways were simulated by channelizing water flow through part of the cropped field and comparing effects to those from an unstable channel.

Table 5-1. Available data and sources

Data Type	Source	Date	Description
Landscape	NRI	1997 or 2003	NRI point attribute data, including links to soil attribute data, slope and slope length, use indicators, conservation practices, land-use history
Crop management	NRI-CEAP cropland survey	2003 - 2006	Crop rotation, including cover crops, fallow, no-till crops and CRP vegetative cover; Tillage, planting, and harvesting operations; Fertilizer and manure management; Pesticide management
Structural conservation practices	NRI CEAP surveyed farmers NRCS field office Farm Service Administration (C)	1997 or 2003 NRI 2003 – 2006 CEAP :	See Table 2, structural conservation practices code
Soils	NASIS (USDA-NRCS 2007) Pre-NASIS Soils_5 database NSSL NCSS laboratories	-	Layer depth, bulk density, organic carbon content, silt Content, coarse fragment content, soil albedo, soil hydrologic group, soil water content at wilting point, soil water content at field capacity, organic N, P concentration, initial soluble concentrations, saturated conductivity, lateral hydraulic conductivity
Weather	Eischeid et al. (2000) Daly et al. (1997 and 2002) Di Luzio et al. (2008)	1960 - 2006	Daily precipitation and maximum and minimum temperature
8-digit watershed channel /slope	watershed/HUMUS/SWAT database	-	8-digit watershed channel length and slope for each 8-digit watershed in the United States, used for estimating the times of concentration in APEX for the purpose of calculating the sediment delivery ratio from the simulation site to the 8-digit outlet

5.2.1 CURVE NUMBER

The daily runoff volume is calculated using a modification of the NRCS curve number method (Mockus, 1969; USDA-NRCS, 2004). In the Curve Number method of runoff estimation, the combination of a hydrologic soil group and a land cover class indicate the potential for surface runoff. Changes in land use, conservation practices, or hydrologic conditions change the quantity of surface water runoff, thus affect the transport of waterborne soil, soil-bound nutrients, and soluble nutrients. This affect is simulated in APEX by changing the curve number. We parameterized the runoff potential of the land cover using a land use number (LUN) (Table 5-2). The LUN classifies an area by land use type (i.e. row crops, small grains, fallow, pasture, grass, trees, road), conservation practice (i.e. none, contour farming, strip cropping, terraces), and the indirect effects of cropland management decisions on surface hydrology (poor or good hydrologic condition). Table 2 gives the LUN used in this study for conservation practices such as contour farming, strip cropping, contour buffer strips, terraces, vegetative barrier and filter strips.

5.2.2 CONSERVATION PRACTICE EFFECTS (P FACTOR)

Conservation practices including contours, strip cropping, contour buffer strips, and terraces can be simulated by adjusting the RUSLE conservation support practice factor (P factor), slope length, and the curve number. The P factor is an empirically derived factor that is multiplied into the RUSLE derived erosion estimate to account for effects from conservation support practices. The factor varies from 1.0 (to simulate straight row, up-downhill farming) to 0.15 (e.g., combination of contour buffer strips and grass terraces) to represent multiple practices on a gentle slope based on literature values. Bracmort et al. (2006) simulated the effects of parallel terraces by modifying P factor (0.2-0.3), slope length, and the curve number. Yin et al. (2009) simulated the effects of mixed wood-grass with horizontal terraces or woodland with ditches by adjusting P factor (0.21-0.29) and the curve number. Secchi et al. (2007) used the P factor based to represent contouring and terraces. Tuppad et al. (2010) also represented terraces and contour farming by conservation support practice P factor (0.1-0.5) and curve number.

5.2.3 CHANNEL FLOW TECHNIQUE

Channel flow techniques are employed for conservation practices designed to create a stable channel where the prior condition is an unstable or degrading channel or gully. The basic concept is to parameterize the model so that very little channel degradation occurs when practices are in place. Two situations: 1) easily eroded channel material and 2) high velocity water flow through the channel, are assumed as the main drivers of channel degradation. Practice techniques target the two drivers. Unstable narrow channels consisting of easily eroded earth in pre-BMP condition are converted into stable channels by changing the channel dimensions (depth, top width, and bottom width), Manning's roughness coefficient and the channel C factor (Bracmort et al., 2006; Secchi et al., 2007). Flow in steep, high-velocity channels in pre-BMP condition can be slowed by reducing the channel gradient (Table 2).

5.2.4 RIPARIAN SIMULATION TECHNIQUE

Riparian simulation techniques entail spreading and slowing water flow from an upland cropped area across buffer strips consisting of grasses, shrubs, and/or trees. Simulating riparian buffers makes use of the model feature which allows areas to be subdivided into fields, soil types, or landscape positions. Flow is spread across the buffer strip using a special flood flow subroutine which is triggered by setting a filter flag, designating the fraction of flow spreading across the filter, and setting the floodplain dimensions. Figure 5-1 illustrates the field configuration and various subareas associated with a riparian buffer system.

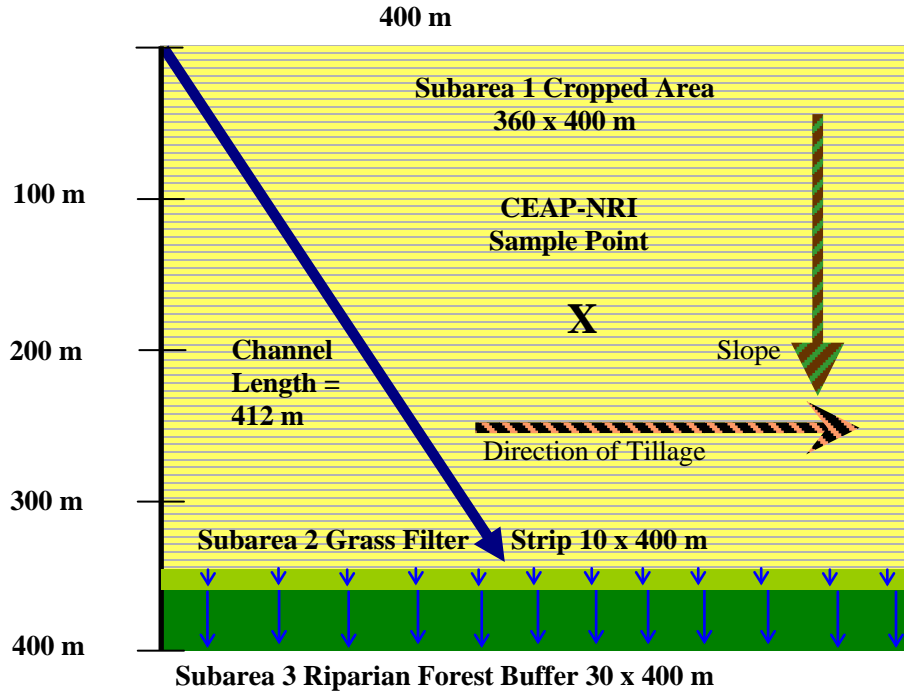


Figure 5-1. Field configuration used to represent a riparian buffer (shown w/ tillage across the slope).

5.2.5 WIND EROSION ESTIMATES AND UNSHELTERED DISTANCE

Wind erosion is estimated in APEX using the Wind Erosion Continuous Simulation (WECS) model. WECS incorporates the daily distribution of wind speeds as the force driving wind erosion (Williams, 1995). The wind erosion estimated in APEX represents the amount of eroded material leaving the field. In wind erosion science, a field is defined as the unsheltered distance along the prevailing wind erosion direction for the field or area being evaluated. WECS does not account for any material deposited in fence rows, barrow ditches or other barriers on the downwind side of the field. Estimated wind erosion can be adjusted based on soil properties, surface roughness, cover, and unsheltered distance across the field in the wind direction. For structural conservation practices, only the unsheltered distance factors (field length and field width) are adjusted when accounting for the wind erosion control practices (Table 5-2).

Table 5-2. Structural conservation practices simulated in CEAP cropland national assessment

Structural conservation practices Simulated by modifying APEX parameters [‡]			Field configuration
<i>Managed in-field flow interceptor</i> P factor: (vary w/ overland slope)			
Contour farming	0.6 - 0.9	LUN: +2	Within field (1 subarea)
Strip cropping	0.5 - 0.9	LUN: +4	
Contour buffer strips	0.25 - 0.45	LUN: +4	
<i>Engineered flow interceptors</i> P factor: (vary w/ overland slope)			
Terraces	0.45 - 0.75	LUN: +2	
Grass terraces	0.25 - 0.45	LUN: +4	Within field (1 subarea)
Vegetative barrier	0.45 - 0.75	LUN: +2	
Diversions		SPLG=0.5*NRI	
<i>Riparian buffers</i>			
Filter strips	Simulated as a grass filter	LUN=26	2-3 subareas: an upland subarea
Riparian herbaceous or forest buffer	Simulated as a grass filter and a buffer	LUN=26 & LUN=29	grass filter strip, a forest buffer (fi
	P factor = 0.6; RCHC=0.001; RCHN=0.2	Grass filter: FFPQ=0.95; RCHS=.25 Forest buffer: FFPQ=0.85; RCHS=.1	
<i>Wind erosion control</i> Unsheltered field length*width [†] Unsheltered distance with strip crop			
Hedgerows	0.06 km*0.06 km	0.03 km	Within field (1 subarea)
Cross wind practices	0.04 km*0.04 km	0.03 km	
Windbreak/shelterbelt	0.03 km*0.03 km	0.02 km	
Herbaceous wind barrier	0.04 km*0.04 km	0.03 km	
Field borders P factor: 0.95			Within field (1 subarea)
Grass waterway RCHC=0.001 RCHN=0.25 RCHS=0.52*NRI			2 subareas: an upland subarea & downstream subarea with a routing channel
Grade stabilization structures RCHS=0.1*NRI			2 subareas: an upland subarea & downstream subarea with a routing channel

[‡] parameter changes for combinations between different groups or within group are not listed here, see Potter et al. (2009) for more detail.

[†] without practices the field was assumed to be 0.4 km*0.4 km.

FFPQ: Fraction floodplain flow, e.g., FFPQ=0.95 means that 95% is overland flow in the floodplain and 5% channel flow.

NRI: National Resources Inventory reported value

LUN: Land use number for looking up curve number

RCHC: Channel USLE C factor of routing reach

RCHN: Channel Mannings N of routing reach

RCHS: Channel slope of routing reach (m/m)

SPLG: Average upland slope length (m)

5.3 REFERENCES

- Bracmort, K. S., M. Arabi, J. R. Frankenberger, B. A. Engel, and J. G. Arnold. 2006. Modeling long-term water quality impact of structural BMPs. *Trans. ASABE* 49(2): 367-374.
- Daly, W. P. Gibson, G.H. Taylor, G. L. Johnson, and P. A. Pasteris, 2002: A knowledge-based approach to the statistical mapping of climate. *Climate Res.*, 22, 99–113.
- Di Luzio M., G. L. Johnson, C. Daly, Jon K. Eischeid, J.G. Arnold. 2008. Constructing retrospective gridded daily precipitation and temperature datasets for the conterminous United States. *Journal of Applied Meteorology and Climatology* 47(2): 475–497.
- Eischeid, J.K., Pasteris, P.A., Diaz, H.F., Plantico, M.S., Lott, N.J., 2000. Creating a serially complete, national daily time series of temperature and precipitation for the Western United States. *Journal of Applied Meteorology* 39, 1580–1591.
38(2):423- 438.
- Gassman, P.W., J.R. Williams, X. Wang, A. Saleh, E. Osei, L. Hauck, C. Izaurralde, and J. Flowers. 2010. The Agricultural Policy Environmental Extender (APEX) Model: An emerging tool for landscape and watershed environmental analyses. *Trans. ASABE* 53(3): 711-740.
- Goebel, J.J. 2009. **NRI-CEAP Cropland Survey Design and Statistical Documentation.** Available at: <http://www.nrcs.usda.gov/technical/NRI/ceap/umrbdocumentation/>. Accessed 11 May 2010.
- Mockus, V. 1969. Hydrologic soil-cover complexes. In: *SCS National Engineering Handbook, Section 4, Hydrology*. U.S. Department of Agriculture, Soil Conservation Service, Washington, D.C., pp. 10.1-10.24.
- Parton, W. J., D. S. Schimel, C. V. Cole, and D. S. Ojima. 1987. Analysis of factors controlling soil organic matter levels in Great Plains grasslands. *Soil Sci. Soc. Amer. J.* 51: 1173-1179.
- Parton, W. J., J. M. O. Scurlock, D. S. Ojima, T. G. Gilmanov, R. J. Scholes, D. S. Schimel, T. Kirchner, J-C. Menaut, T. Seastedt, E. Garcia Moya, A. Kamnalrut, and J. I. Kinyamario. 1993. Observations and modelling of biomass and soil organic matter dynamics for the grassland biome worldwide. *Global Biogeochem.l Cycl.* 7: 785-1661 809.

- Parton, W.J., Ojima, D.S., Cole, C.V. and Schimel, D.S., 1994. A general model for soil organic matter dynamics: Sensitivity to litter chemistry, texture and management. In: Quantitative Modeling of Soil Forming Processes, SSSA Spec. Public. No. 39, Madison, WI, pp. 147-167.
- Secchi, S., P.W. Gassman, M. Jha, L. Kurkalova, H.H. Feng, T. Campbell, and C.L. Kling. 2007. The cost of cleaner water: Assessing agricultural pollution reduction at the watershed scale. *Journal of Soil and Water Conservation* 62(1): 10-21.
- Tuppad, P. R. Srinivasan, N. Kannan, C.G. Rossi, and J.G. Arnold. 2010. Simulation of agricultural management alternatives for watershed protection. *Water Resources Management*. *Water Resources Management*, DOI 10.1007/s11269-010-9598-8 (Published online 10 February, 2010).
- U.S. Department of Agriculture, National Resources Conservation Service. 2004. Chapter 10: Estimation of direct runoff from storm rainfall. In: *NRCS National Engineering Handbook, Part 630, Hydrology*, USDA NRCS, Washington, D.C., pp. 10.1-10.22. Available at: www.wsi.nrcs.usda.gov/products/w2Q/H&H/tech_refs/eng_Hbk/chap.html. Accessed 1 February 2010.
- U.S. Department of Agriculture-Natural Resources Conservation Service. 2007. Soil data MART. Washinton, DC. Available at: <http://soildatanart.nrcs.usda.gov/>
- Vitousek, P.M., Turner, D.R., Parton, W.J. and Sanford, R.L., 1994. Litter decomposition on the Mauna Loa environmental matrix, Hawaii: Patterns, mechanisms, and models. *Ecology* 75, 418-429.
- Williams, J. R. 1995. The EPIC Model. In V.P. Singh, *Computer Models of Watershed Hydrology*. 909-1000. 1744 Highlands Ranch, CO: Water Resources Publications.
- Williams, J. R. and R. C. Izaurralde. 2006. The APEX model. In *Watershed Models*, 437-482. Singh, V.P. and D.K. Frevert, eds. Boca Raton, FL: CRC Press, Taylor & Francis.
- Yin, L., X. Wang, J. Pan, P.W. Gassman. 2009. Evaluation of APEX for Daily Runoff and Sediment Yield from Three Plots in the Middle and Upland Huaihe River Watershed, China. *Transactions of the American Society of Agricultural Engineers* 52(6): 1833-1845.

CHAPTER 6

WATERSHED DELIVERY RATIOS

6.1 DEVELOPMENT OF DELIVERY RATIOS

The APEX modeling setup for CEAP utilized information from the NRI-CEAP Cropland Survey. The survey was conducted at a subset of NRI sample points which provide statistical samples representing the diversity of soils and other conditions on the landscape. Since each APEX simulation represents a fraction of the cultivated areas within an 8-digit watershed, the actual locations are not known and are assumed to be randomly distributed. Faced with this limitation, the development of SDR in this study depends on efficiency of the algorithm with modest input parameter requirement. The SDR can be estimated as:

$$SDR = \frac{Y_B}{\sum Y_S} \quad (1)$$

Where:

Y_B is the sediment yield at the basin outlet

Y_S is the sediment yield at the outlet of the APEX sites.

Sediment yield can be estimated using a variation of MUSLE called MUST (Williams 1995):

$$Y = 2.5 \times (Q \times q_p)^a \times K \times C \times P \times LS \quad (2)$$

Where:

Q is the runoff volume (mm)

q_p is the peak runoff rate (mm h⁻¹)

K , C , P , and LS are the linear USLE factors

a is runoff and peak runoff rate exponent set as 0.5 in the original MUST equation (Williams 1995)

The a can be smaller than 0.5 in developing the delivery ratio. Y_B can be calculated with Eq 2 by area-weighting the linear USLE factors and Q , and estimating q_p at the basin outlet. LS can be estimated for each of the APEX sites using appropriate values of the linear USLE factors, Q , and q_p . The delivery ratio can be estimated by substituting these values into Eq 1. Since the linear USLE factors and Q cancel, the delivery ratio for each APEX site can be estimated with the equation:

$$SDR_s = \left(\frac{q_{pB}}{q_{pS}} \right)^a \quad (3)$$

Where:

SDR_s is the delivery ratio for the APEX site s

q_{pB} is the peak runoff rate at the basin outlet (mm h^{-1}),

q_{pS} is the peak runoff rate at the outlet of the APEX site s (mm h^{-1}).

Since the APEX simulation results are passed to SWAT at the basin outlet, q_{pB} is not known when APEX is running. However, the peak runoff rate is a function of runoff volume and watershed time of concentration:

$$q_p = f\left(\frac{Q}{t_c}\right) \quad (4)$$

Substituting the inverse of t_c for q_p (Q cancels) in Eq. 3 yields:

$$SDR_s = \left(\frac{t_{cS}}{t_{cB}}\right)^\alpha \quad (5)$$

Where:

t_{cS} is the time of concentration of the APEX site

t_{cB} is the time of concentration of the basin.

The times of concentration can be estimated with the Kirpich equation in the metric form:

$$t_c = 0.0663 \times \frac{L^{0.77}}{S^{0.385}} \quad (6)$$

Where:

L is the watershed length along the main stem from the outlet to the most distant point
(km)

S is the main stem slope (m m^{-1})

Substituting t_{cS} and t_{cB} calculated from Eq 6 in Eq 5 yields:

$$SDR_s = \left[\left(\frac{L_S}{L_B}\right)^{0.77} \times \left(\frac{S_B}{S_S}\right)^{0.385} \right]^\alpha \quad (7)$$

Where:

L_B and S_B are the 8-digit watershed basin channel length and basin channel slope ($m\ m^{-1}$), respectively;

L_S and S_S are the APEX watershed length (km) and slope ($m\ m^{-1}$), respectively.

Sediment transported nutrients and pesticides are simulated using an enrichment ratio approach:

$$YNP_B = YNP_S \times DR \times ERTO \quad (8)$$

Where:

YNP is the nutrient or pesticide load

$ERTO$ is the enrichment ratio (concentration of nutrient/pesticide in outflow from APEX sites divided by that at the basin outlet).

The enrichment ratio is calculated by considering sediment concentration in the equation:

$$ERTO = b_1 \times Y_{SC}^{b_2} \quad (9)$$

Where:

Y_{SC} is the sediment concentration of the outflow from the APEX sites

b_1 and b_2 are parameters that can be determined by considering two points in Eq. 9.

For the enrichment ratio to approach 1.0, the sediment concentration must be extremely high. Conversely, for the enrichment ratio to approach 1/SDR, the sediment concentration must be low. The simultaneous solution of Eq 9 at the boundaries assuming that sediment concentrations range from 5×10^{-4} to $0.1\ mg\ m^{-3}$ gives:

$$b_2 = \log(SDR)/2.301 \quad (10)$$

$$b_1 = 1/0.1^{b_2} \quad (11)$$

Thus, the delivery ratios and enrichment ratios are used to transport sediment, nutrients, and pesticides from SPEX sites to the basin outlet for input to SWAT.

6.2 DELIVERY RATIO FOR UN-CULTIVATED LAND

Traditionally, SDR is the ratio of sediment load delivered at the watershed outlet (sediment yield) to erosion on the landscape. Erosion is typically determined using the USLE equation which accounts for erosion (soil loss) from a standard 72.4 foot plot from sheet and rill erosion. Sediment yield is the amount of sediment that is transported in the channel at the watershed out-let. Processes occurring from the landscape to the watershed outlet (sediment yield) include additional erosion or degradation in gullies and channels and deposition in buffers, wetlands, channels, and flood plains.

SDR can be affected by a number of factors including hydro-logical inputs (rainfall-runoff factors), landscape and watershed characteristics (e.g., land-use/land-cover, nearness to the main stream, channel density, drainage area, slope, length), soil properties (sediment source, texture) and their interactions. Numerous SDR relationships have been developed based on combinations of these factors (Ouyang and Bartholic, 1997) and mostly their empirical.

For CEAP, both APEX and SWAT compute SDR as a function of the ratio of time of concentration of the field or HRU to the time of concentration of the HUC. As previously described, SDR's are typically defined as the ratio of erosion (soil loss) to sediment yield. In the SWAT analysis for uncultivated land-uses, SDR is defined as sediment load delivered from each HRU to the sediment delivered to the channel at the outlet of the 8-digit HUC. Sediment loads from each HRU are estimated for each runoff event using the Modified Universal Soil Loss (MUSLE) equation. The sediment load from MUSLE is multiplied by the SDR to obtain sediment delivered to the 8-digit watershed outlet.

There are, on average, 40 to 50 HRUs representing uncultivated land use areas such as pasture, range shrub, range grass, urban, mixed forest, deciduous forest, evergreen forest, horticultural lands, and wetlands within each 8-digit watershed (HUC). Each HRU represents a portion of the 8-digit watershed area and does not represent a contiguous land area. Hence, the delivery ratio procedure was developed for CEAP national assessment to estimate the sediment delivered at the 8-digit watershed outlets from the HRUs.

SWAT simulates the sediment yield from the uncultivated land HRUs using the Modified Universal Soil Loss Equation developed by Williams et al. (1975a and 1975b; 1995).

$$sed = 11.8 \times (Q_{surf} \times q_{peak} \times area_{hru})^{0.56} \times K_{USLE} \times C_{USLE} \times LS_{USLE} \times CFRG \quad (12)$$

Where:

sed is the sediment load on a given day (metric tons)

Q_{surf} is the surface runoff volume (mm H₂O/ha)

q_{peak} is the peak runoff rate (m³/s)

$area_{hru}$ is the area of the HRU (ha)

K_{USLE} is the USLE soil erodibility factor

C_{USLE} is the USLE cover and management factor

P_{USLE} is the USLE support practice factor

LS_{USLE} is the USLE topographic factor

$CFRG$ is the coarse fragment factor (Neitsch et al., 2005).

The area of each HRU for various land-use classes vary from a few hundred acres to several thousands of acres within each 8-digit watershed.

6.2.1 DESCRIPTION OF THE DELIVERY RATIO PROCEDURE USED IN SWAT

After estimating the sediment load for each HRU, a delivery ratio is applied to determine the amount of sediment that reaches the HUC outlet from each HRU. In SWAT, sediment delivery ratio is estimated as a function of the time of concentration of HRU to the time of concentration of the HUC/8-digit watershed. Time of concentration is related to watershed characteristics such as slope, slope length, landscape characteristics and drainage area.

$$SDR = (t_{c,hru} / t_{c,sub})^{dr_{exp}} \quad (13)$$

Where:

$t_{c,hru}$ is the time of concentration of HRU in hours

$t_{c,sub}$ is the time of concentration of the subbasin (8-digit HUC) in hours, typically more than 24 hours for most of the 8-digit watersheds. Time of concentration of HRU and time of 8-digit HUC also varies across the 8-digit watersheds.

dr_exp is the delivery ratio exponent parameter represents the rainfall-peak runoff rate and similar to the rainfall-runoff rate (a) in APEX modeling. For the CEAP national assessment, the delivery ratio exponent (dr_exp) was set to 0.5 within SWAT for calibrating the observed and simulated sediment loads at Grafton, IL.

[Note: The time of concentration is calculated by summing the overland flow time (the time it takes for flow from the most re-mote point in the subbasin to reach the channel) and the channel flow time (the time it takes for flow in the upstream channels to reach the outlet)]

6.2.2 COMPUTATION OF TIME OF CONCENTRATION OF SUBBASIN/HUC

Total time of concentration is the sum of overland and channel flow times.

$$t_{c,sub} = t_{ov} + t_{ch,sub} \quad (14)$$

Where:

$t_{c,sub}$ is the time of concentration for a subbasin (hr)

t_{ov} is the time of concentration for overland flow (hr)

t_{ch} is the time of concentration for channel flow (hr).

6.2.2.1 COMPUTATION OF TIME OF CONCENTRATION OF OVERLAND FLOW:

Tributary channel characteristics related to HRU such as average slope length (m), HRU slope steepness ($m\ m^{-1}$) and Manning's "n" values representing roughness coefficient for overland flow are used in computing overland flow time of concentration.

$$t_{ov} = \frac{L_{slp}^{0.6} \times n^{0.6}}{18 \times slp^{0.3}} \quad (15)$$

Where:

L_{slp} is the average subbasin slope length (m)

slp is the average slope of HRU in the subbasin (m/m)

n is Manning's roughness coefficient for the overland flow representing characteristics of the land surface with residue cover or tillage operations. Manning 'n' ranges from 0.01 to 0.600.

6.2.2.2 COMPUTATION OF TIME OF CONCENTRATION OF CHANNEL FLOW:

The time of concentration for channel flow is computed as

$$t_{ch,sub} = \frac{0.62 \times L \times n^{0.75}}{Sub_area^{0.125} \times slp_{ch}^{0.375}} \quad (16)$$

Where:

t_{ch} is the time of concentration for channel flow (hr)

L is the channel length from the most distant point to the sub-basin/HUC outlet (km) or the longest tributary channel length

n is Manning's roughness coefficient for the channel representing the characteristics of the channel (ranges from 0.025 through 0.100)

Sub_area is the subbasin/HUC area (km²)

slp_{ch} is the average slope of the longest tributary channel (m/m).

As per the above equations (14, 15 and 16), time of concentration is estimated for the HUC.

6.3 COMPUTATION OF TIME OF CONCENTRATION OF THE HRU

The time of concentration of HRU is estimated using the following equations:

$$t_{c,hru} = t_{ov} + t_{ch,hru} \quad (17)$$

$$t_{ch,hru} = \frac{0.62 \times L \times hru_prop \times n^{0.75}}{hru_area^{0.125} \times slp_{ch}^{0.375}} \quad (18)$$

Where:

hru_prop is the proportion of the tributary channel length in HRU. It is estimated by multiplying the longest tributary channel length by the ratio of *hru_area* to subbasin area

hru_area is the area of HRU.

Equations 15 and 18 are used in computing time of concentration for HRU as in shown in equation 17. Thus, equations 14 and 17 are used in equation 12 to compute the sediment delivery ratio.

Sediment delivered from the uncultivated land HRUs at the JUC outlet is estimated and added with the sediment load from the cultivated land and point sources and routed through each HUC main channel.

6.4 REFERENCES

- Arnold, J.G., R. Srinivasan, R.S. Muttiah, and P.M. Allen. 1999. Continental scale simulation of the hydrologic balance. *J. Amer. Water Res. Assoc.* 35(5):1037-1052.
- Neitsch, S.L., J. G. Arnold, J.R. Kiniry, and J.R. Williams. 2005 Soil and Water Assessment Tool (Version 2005). Theoretical Documentation. Grassland, Soil and Water Research Laboratory, USDA-ARS, Temple, TX 76502 and Blackland Research Center, Temple, TX 76502.
- Ouyang, D. and J. Bartholic. 1997. Predicting sediment delivery ratio in Saginaw Bay Watershed. *In* The 22nd National Association of Environmental Professionals Conference Proceedings. May 19-23, 1997, Orlando, FL. pp 659-671.
- Santhi, C., Kannan, N., Di Luzio, M., Potter, S.R., Arnold, J.G., Atwood, J.D., and Kellogg, R.L. 2005. An approach for estimating water quality benefits of conservation practices at the national level. *In* American Society of Agricultural and Biological Engineers (ASABE), Annual International Meeting, Tampa, Florida, USA, July 17-20, 2005 (Paper Number: 052043).
- Williams, J.R. 1975a. Sediment yield prediction with universal equation using runoff energy factor. U. S. Dept. Agric. Agric. Res. Serv, ARS-S-40.

Williams, J.R. 1975b. Sediment routing for agricultural watersheds. *Water Resour. Bull.* 11(5), 965-974.

Williams, J.R. 1995. The EPIC model. *In* *Computer Models of Watershed Hydrology*, 909-1000. V.P. Singh, ed. Highlands Ranch, Colo.: Water Resources Publications.

CHAPTER 7

CALIBRATION AND VALIDATION

The SWAT-HUMUS modeling setup quantifies the offsite environmental benefits obtained from the conservation practices implemented on cropland in the United States. To perform this task, reasonably accurate estimates of water runoff and material transfer via both surface and subsurface pathways are required. In addition to matching predicted and observed runoff, it is essential to partition simulated runoff correctly into different hydrological pathways such as surface runoff and subsurface flow, or base flow. This requires a robust procedure to calibrate runoff/water yield as well as partition runoff into surface runoff and subsurface flow.

At the 8-digit watershed level, two simulation models, APEX for cultivated areas and SWAT for other land-uses, were run independently. Since the APEX simulation results are passed to HUMUS/SWAT at the 8-digit watershed outlet, the average flow from both cultivated and un-cultivated land (simulated by SWAT) for the 8-digit watershed is not known when APEX is running. Therefore, the water yield calibrations of APEX for the cultivated portion of the watershed and SWAT for the un-cultivated portion are both required so that the water yields from cultivated area would be reasonable when HUMUS/SWAT stream flow is compared to observed stream flow. The cultivated area estimates are made via a sampling and modeling approach; simulated water yields are aggregated to the 8-digit watershed level using the statistical sampling weights derived from the National Resource Inventory (NRI) data. Therefore, the calibration procedure is different for cultivated land and other land-uses. The Upper Mississippi River Basin will be used to describe and illustrate the CEAP validation procedure.

7.1 FLOW CALIBRATION AND VALIDATION PROCEDURE

The APEX and HUMUS/SWAT system was run with weather data from 1960 through 2006 (47 years) to represent long-term weather conditions in the Upper Mississippi River Basin (UMRB) (Figure 7-1). For the purpose of the CEAP national assessment, the APEX model and SWAT model were calibrated with 30 years of data (1961-90) and validated with 16 years of data (1991-2006) before scenario trials. Average annual runoff from each 8-digit watershed was used for spatial calibration. The Upper Mississippi River Basin is used as an example basin to illustrate the calibration and validation procedure. Monthly and annual average stream flow at selected gauging stations along the Mississippi river were used for temporal calibration and validation. Model outputs from the current conditions scenario were used for calibration and validation. Calibration of average annual runoff helps ensure local water balance at the 8-digit watershed level. The temporal calibration and validation (annual and monthly) is performed to ensure annual and seasonal variability.

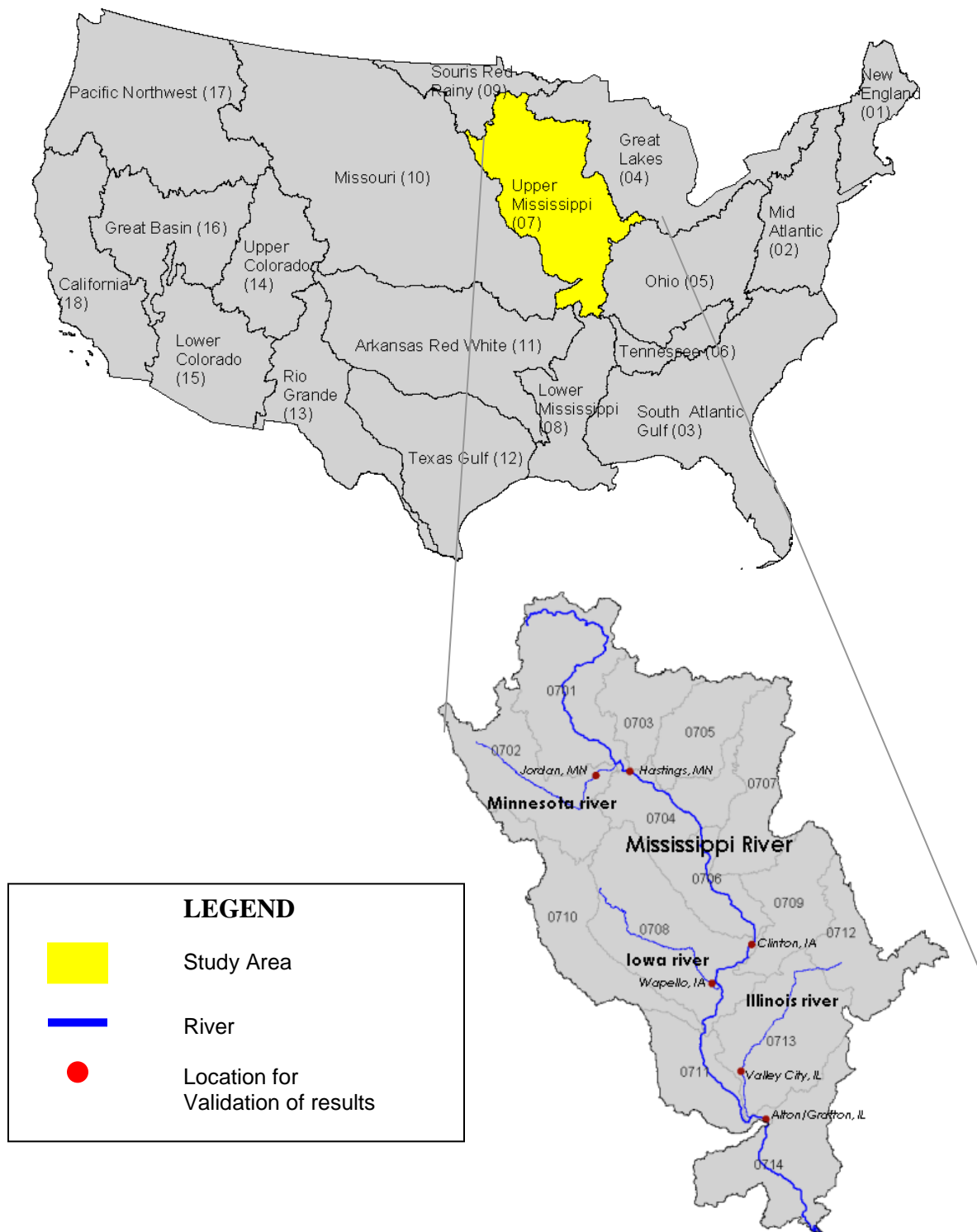


Figure 7-1. Location of the Upper Mississippi River Basin and sampling locations

7.2 CALIBRATION OF AVERAGE ANNUAL RUNOFF AT 8-DIGIT WATERSHEDS

At the 8-digit watershed level the two models were run independently, the simulated average annual water yield by each model were calibrated separately against the observed runoff estimated from the USGS runoff contours (Gebert et al., 1987). The results from APEX represent the average annual values from only the cultivated areas at each 8-digit watershed; the results from SWAT represent the average annual values from all other land-uses. The observed runoff was the average annual value from all land-uses.

The criteria for APEX calibration was established based on the percentage of cultivated land at each 8-digit watershed (Table 7-1). The criteria for SWAT calibration was set to the simulated average annual water yields within 20 percent of the observed values. This ensures good agreement on contribution of annual runoff spatially across 8-digit watersheds.

Table 7-1. Criteria for APEX water yield calibration at the 8-digit watershed level

% (Cultivated+CRP) Area	% difference between APEX and USGS annual average water yields
<10	within 50
10-20	within 45
20-30	within 40
30-40	within 35
40-50	within 30
50-60	within 25
60 & above	within 20

7.2.1 CALIBRATION OF APEX

Figure 7-2 shows the calibration procedure, which demonstrates how the average annual water yield calibration is carried for 8-digit watersheds. Four parameters were used for APEX water yield calibration (Table 7-2). The soil water depletion coefficient adjusts surface runoff and subsurface flow in accordance with soil water depletion (Kannan et al., 2006). The Hargreaves PET equation exponent is a coefficient used to adjust evapotranspiration (ET) estimated by the Hargreaves method (Hargreaves and Samani 1985) and water yield. The

return flow ratio is the ratio of return flow to channel and the total percolation flow. The tile drainage saturated hydraulic conductivity coefficient controls the upper limit of tile drain flow. The adjustable ranges of these parameters (Table 7-2) were based on the APEX user manual (Williams et al., 2003), literature reported ranges (Wang et al., 2006), and expert knowledge from the model developer, Jimmy Williams.

Table 7-2. Parameters used in the APEX calibration procedure, their range, and their effect on different components of runoff

Parameter	Changes			Range Used	
	Surface Runoff	Sub-Surface Runoff	Water Yield	Minimum	Maximum
Depletion Coefficient	x	x	x	0.5	1.5
Hargreaves PET Equation Exponent	x	x	x	0.5	0.6
Return Flow Ratio	x		x	0.05	0.95
Tile Drainage Saturated Hydraulic Conductivity Coefficient		Tile Drain Flow	x	0.8	3

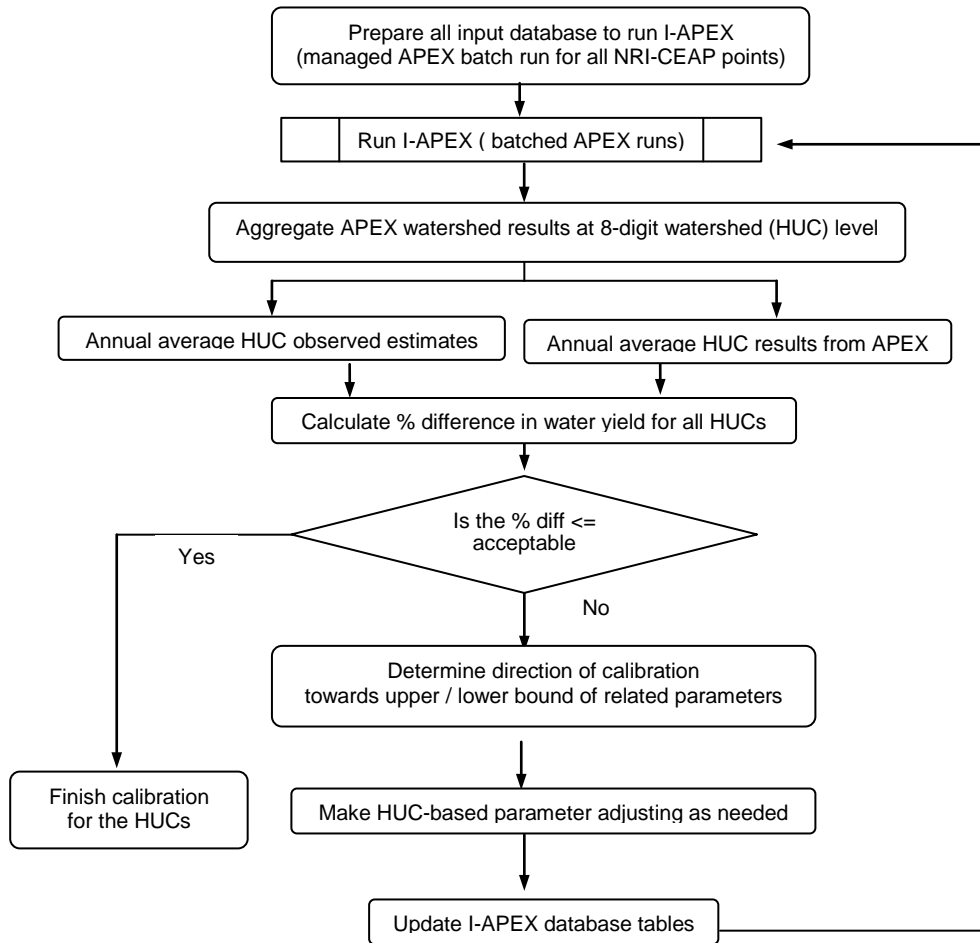


Figure 7-2. APEX calibration procedure for water yield from cultivated land aggregated at the 8-digit watershed level

7.2.2 CALIBRATION OF SWAT

An automated calibration procedure (Kannan et al., 2008) uses nine parameters to calibrate average annual water yield or total runoff, surface runoff, and subsurface flow, respectively. If necessary, the procedure uses a linear interpolation method to obtain a better value of a model parameter. The calibration process is carried out in three major steps: (1) adjustment of water yield, (2) surface runoff, and (3) subsurface runoff.

Figures 7-2b and 7-2c show the automated calibration procedure, which demonstrates in detail how the average water yield calibration is carried out for the 8-digit watersheds.

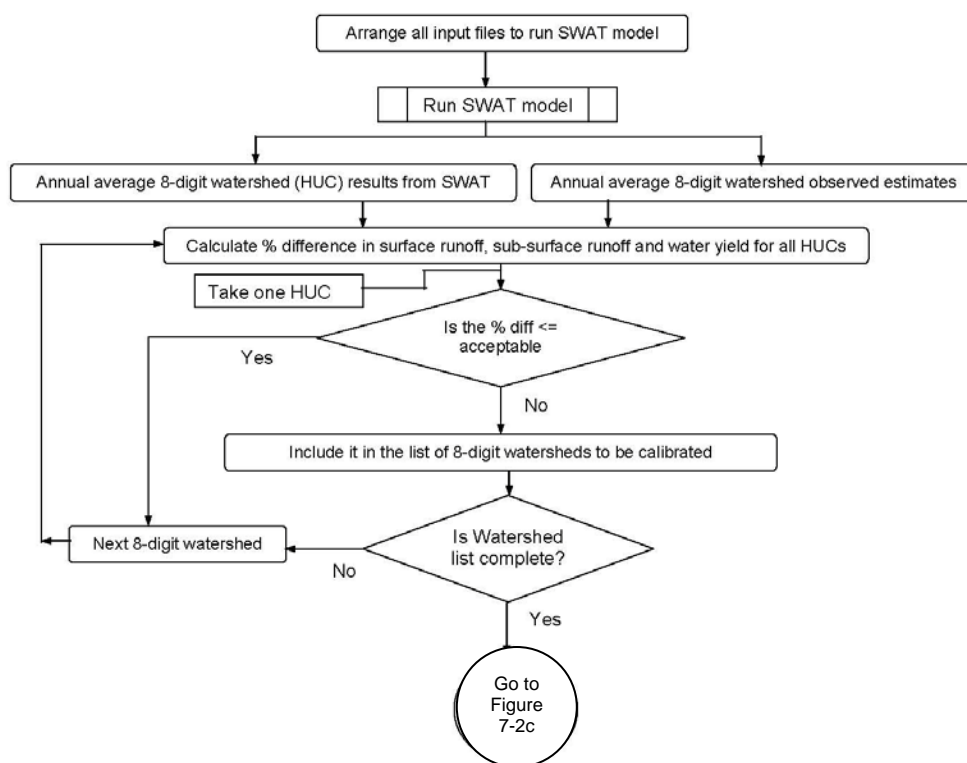


Figure 7-3 Automated calibration procedure-Determination of 8-digit watersheds to be calibrated

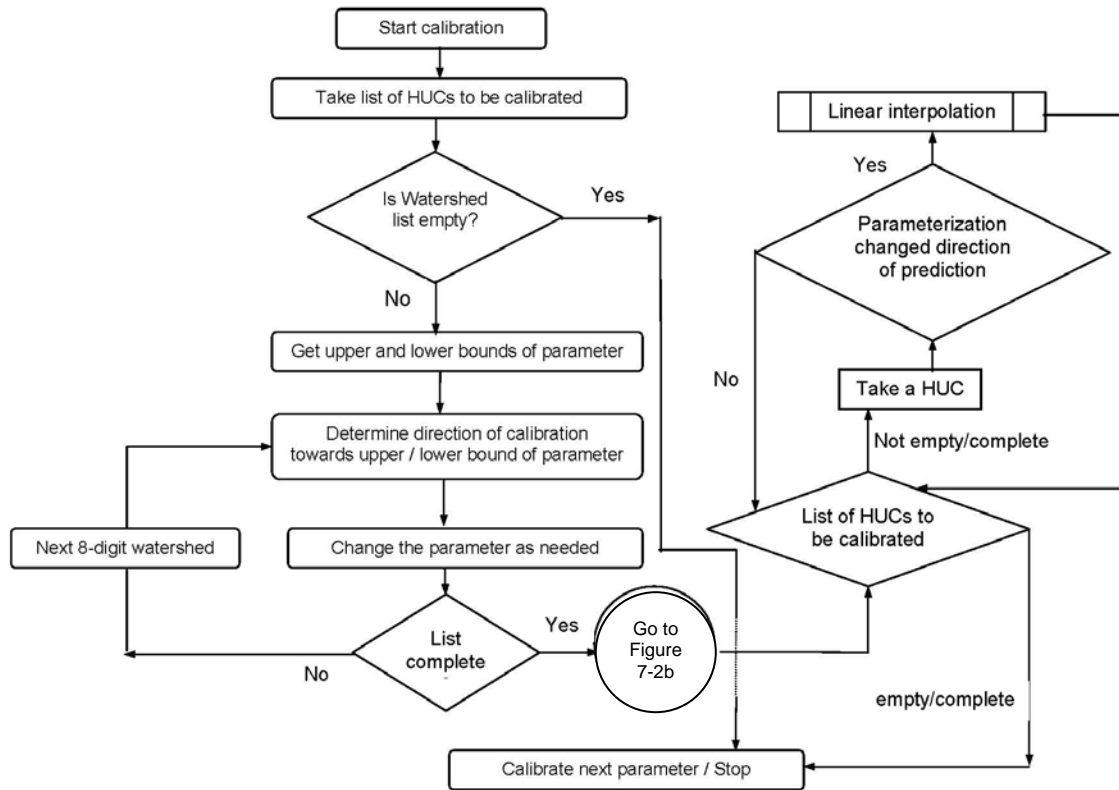


Figure 7-4. Adjustment and interpolation of parameters

7.3 OBSERVED/ESTIMATED DATA USED FOR SPATIAL CALIBRATION

7.3.1 OBSERVED/TARGETED WATER YIELD

The target values for calibration are based on runoff contours for the nation prepared by Gebert et al.(1987). The source of information for the runoff contours was stream flow recorded from 5951 USGS gauging stations during 1951-1980 with an area of not more than an 8-digit watershed. Stations with major reservoirs in the watershed were omitted from the analysis. Annual average water yield for each HUC is obtained by overlaying interpolated runoff contours representing average annual runoff with the HUC map.

7.3.2 OBSERVED/TARGETED SUBSURFACE FLOW

Arnold et al. (2000) developed a digital filter technique to partition the stream flow between surface runoff and base flow. In this technique, the base flow ratio is the ratio of subsurface flow to total flow. To estimate subsurface flow, the ratio is multiplied by the observed water yield. Santhi et al. (2008) have estimated the base flow (subsurface flow) ratio for all the 8-digit watersheds in the United States using the digital filter technique. Therefore, to obtain subsurface flow for an 8-digit watershed in a river basin, the base flow ratio should be multiplied with the corresponding water yield for the 8-digit watershed. The difference between water yield and subsurface flow is considered surface runoff. The data obtained this way are used as observations/target values to calibrate runoff/water yield, subsurface flow, and surface runoff.

7.3.3 ANNUAL AND MONTHLY FLOW CALIBRATION AND VALIDATION AT STREAM GAGES

Five USGS stream gages were selected in the UMRB for annual and monthly flow calibration and validation (all gauges shown in Fig 1, except Hastings, MN that had very limited flow data). Calibration was performed for the period 1961 to 1990 to ensure that there was a reasonable agreement between predicted and observed flow at annual and monthly time steps. The model was validated for annual and monthly flows in the same stream gages for the period 1991 to 2006 without changing the calibrated input parameters.

7.3.4 EVALUATION CRITERIA FOR ANNUAL AND MONTHLY FLOW CALIBRATION

Statistical measures such as mean, standard deviation, coefficient of determination (R^2), and Nash-Sutcliffe prediction efficiency (NSE) (Nash and Sutcliffe 1970) were used to evaluate the annual and monthly simulated flows against the measured flows at the gages. If the R^2 and NSE values were less than or very close to zero, the model prediction is considered “unacceptable or poor.” If the values are 1.0, then the model prediction is “perfect.” Values greater than 0.6 for R^2 and greater than 0.5 for NSE were considered “acceptable” (Santhi et al., 2001; Moriasi et al., 2007).

7.4 DEMONSTRATION OF THE SWAT AUTOMATED FLOW CALIBRATION PROCEDURES

The automated calibration procedure spatially calibrates the following HUMUS-SWAT model parameters so that the simulated average annual water yield, sub-surface flow and surface runoff match the corresponding target values for each USGS 8-digit watershed (Kannan et al., 2008) in the river basin. The calibration goals are to keep the differences between simulated and target values within 10 percent for surface runoff, 10 percent for subsurface flow, and 20 percent for water yield.

- HARG_PETCO, a coefficient used to adjust potential evapotranspiration (PET) estimated by the Hargreaves method (Hargreaves and Samani 1985; Hargreaves and Allen 2003) and calibrate the runoff/water yield in each 8-digit watershed. In the Hargreaves method, PET is related to temperature and terrestrial radiation. This coefficient is related to radiation and can be varied to account for the differences in PET in different parts of the river basin depending on weather conditions (Hargreaves and Allen 2003).
- Soil water depletion coefficient (CN_COEF), a coefficient used in the curve number method to adjust the antecedent moisture conditions on surface runoff generation.
- Curve Number (CN), used to adjust surface runoff and relates to soil, land-use, and hydrologic condition at the HRU level.

- Groundwater re-evaporation coefficient (GWREVAP) controls the upward movement of water from shallow aquifer to root zone due to water deficiencies in proportion to potential evapotranspiration. This parameter can be varied depending on the land-use/crop. The revap process is significant in areas where deep-rooted plants are growing and affects the groundwater and the water balance.
- GWQMN—Minimum threshold depth of water in the shallow aquifer to be maintained for groundwater flow to occur to the main channel.
- Soil available water-holding capacity (AWC), which varies by soil at HRU level.
- Soil evaporation compensation factor (ESCO), which controls the depth distribution of water in soil layers to meet soil evaporative demand. This parameter varies by soil at the HRU level.
- Plant evaporation compensation factor (EPCO), which allows water from lower soil layers to meet the potential water uptake in upper soil layers and varies by soil at the HRU level.

The above input parameters were adjusted within literature reported ranges for the SWAT model (Neitsch et al., 2002; Santhi et al., 2001), and expert knowledge from the SWAT model developer Jeff Arnold.

Table 7-3 demonstrates the auto-calibration procedure using the 8-digit watershed 07020008 of the UMRB for the un-cultivated area.

The table shows that the difference between predicted and target water yield at the beginning is within the acceptable range (4.2 percent existing vs. 20 percent target). Therefore, HARG_PETCO was not parameterized to adjust the water yield. However, the percent difference between predicted and observed annual average surface runoff is beyond the threshold (-54 percent existing vs. 10 percent threshold), indicating underestimation of surface runoff. Therefore, the depletion coefficient is adjusted to bring predicted surface runoff to within 10 percent of the target value. In doing so, the underestimation (before depletion coefficient parameterization) has changed to overestimation (after depletion coefficient parameterization). Hence, a linear interpolation was performed to identify the suitable value for depletion coefficient that keeps the predicted surface runoff within 10 percent of target value. After the adjustment of depletion coefficient, the percent difference between predictions and observations of annual average surface runoff is 1.9 (within the target/benchmark) eliminating the need for further adjustment of surface runoff using CN.

Table 7-3. Demonstration of auto-calibration procedure for HUMUS-SWAT using an 8-digit watershed (7020008) in the Upper Mississippi River Basin

Parameter	Adjustment / Interpolation	% Difference between predictions and observations			Surface runoff (mm)	Subsurface runoff (mm)	Water yield (mm)
		Surface runoff	Subsurface flow	Water yield			
No calibration	None	-54	68.4	4.2	20.39	67.52	87.92
harg_petco	None	-54	68.4	4.2	20.39	67.52	87.92
depletion coefficient	Adjusted	17.5	8.2	13.1	52.03	43.38	95.41
depletion coefficient	Interpolated	1.9	20.6	10.8	45.13	48.37	93.51
curve number	None	1.9	20.6		45.13	48.37	93.51
GWREVP	Adjusted	1.9	19.6	10.8	45.13	47.95	93.08
GWQMN	Adjusted	1.9	-79.9		45.13	8.05	53.18
GWQMN	Interpolated	1.9	13.3	10.3	45.13		90.55
AWC	Adjusted	1.9	13.3	-37	45.13	45.42	90.55
Slope length	Adjusted	1.9	13.2	7.3	45.13		90.53
EPCO	Adjusted	1.9	13.3	7.3	45.13	45.42	90.56
ESCO	Adjusted	1.1	-58.4	7.3	44.78	45.39	61.48
ESCO	Interpolated	1.8	-7.4	7.3	45.1	45.43	82.24
Observed/Estimated	Not applicable			-27.2	44.3	16.7	84.4
				-2.6		37.14	
						40.1	

Although the predicted water yield is still within 20 percent of observation (after adjustment of depletion coefficient), the subsurface flow is not within the target value of 10 percent. Therefore, subsurface flow was adjusted using appropriate parameters. After the parameterization of GWREVP, GWQMN, slope length, EPCO, and ESCO, respectively, the predicted annual average subsurface flow for HUC 07020008 is brought within 10 percent of target. In Table 7-3, the predicted values for surface runoff, subsurface flow, and water yield and the percent difference between predictions and target are shown at every step of calibration for better understanding of the automated calibration procedure.

The performance of the automated calibration procedure is analyzed considering the entire UMRB (cultivated and un-cultivated area). Figure 7-4 showing percentage difference between predictions and target values of annual average water yield for entire UMRB implies that the quality of calibrated (predicted) annual average water yield is very good. Means and standard deviations of predicted and target annual average water yields of all the HUCs in the river basin, also support the conclusion (Table 7-4). Performance evaluation of the model after

calibration using Nash and Sutcliffe prediction efficiency and R^2 are given in Figure 7-5, which shows that the prediction efficiency is acceptable after calibration. In addition, the number of HUCs outside the calibration targets decreased appreciably after calibration (Figure 7-6).

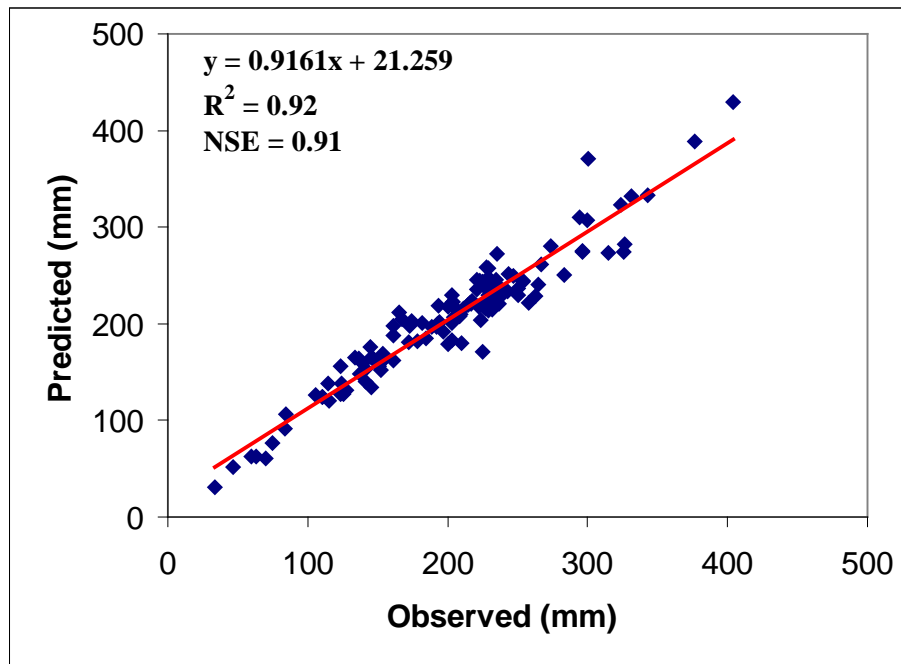


Figure 7-5 Average annual water yield of all 8-digit watersheds in the Upper Mississippi River Basin from cultivated and un-cultivated area (combined water yield from APEX and SWAT)

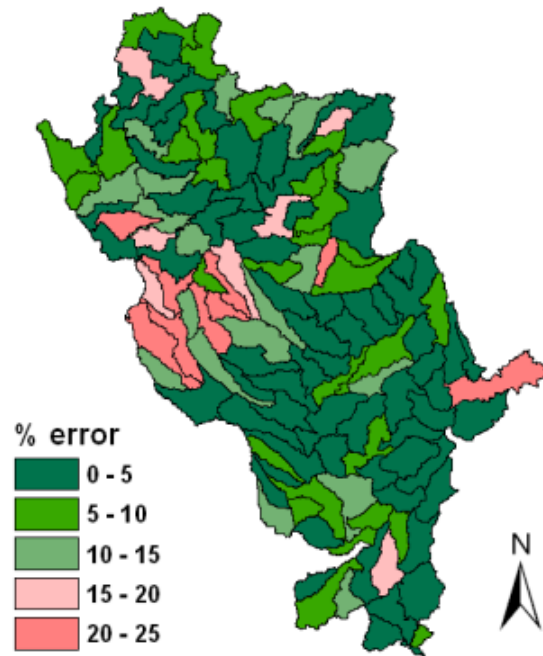


Figure 7-4 Percentage difference between predictions and observations of annual average flow in the UMRB (combined water yield from APEX and SWAT after calibration)

7.4.1 CALIBRATION RESULTS OF THE AVERAGE ANNUAL RUNOFF AT 8-DIGIT WATERSHEDS

7.4.1.1 AVERAGE ANNUAL WATER YIELD FROM CULTIVATED AND UN-CULTIVATED LAND

The average annual simulated and targeted runoff of the 8-digit watersheds in the Upper Mississippi River Basin is shown in Figure 7-4. Targeted and simulated runoff patterns concur with the precipitation patterns of this basin. The regression relationship between targeted and simulated runoff at 8-digit watersheds (R^2 is 0.91), the means and standard deviations of annual runoff (of all the 8-digit watersheds in the river basin) indicate that the model prediction is satisfactory (Figure 7-6 and Table 7-4).

Table 7-4. Basin-average statistics for predicted and target annual water yield for all 8-digit water-sheds in the UMRB—Combined water yield results from APEX and SWAT after calibration (1961–90)

Calibration	Statistic (mm)	Value
Predictions (After calibration)	Mean	207.4
	Standard deviation	63.5
Observations	Mean	203.1
	Standard deviation	66.4

7.4.1.2 ANNUAL AND MONTHLY FLOW CALIBRATION AND VALIDATION AT STREAM GAGES

Flow calibration and validation results at annual and monthly time step are shown in Figures 7-5 to 7-8 and Tables 7-5 to 7-8 for the stream gages located in Minnesota river (Jordan, MN), Iowa river (Wapello, IA), Illinois river (Valley City, IL) and Mississippi river (Clinton, IA and Alton/Grafton, IL). Because the Missouri River joins the Mississippi River above Thebes, IL, results for the gage at Thebes will be reported in a future report on the Missouri River Basin.

Observed and simulated flows at annual and monthly time steps matched very well for the calibration period (Figures 7-5 and 7-6). Means and standard deviations of predictions and observations are in close agreement (Table 7-5). In addition, the coefficient of determination is greater than 0.6 (R^2) and NSE is greater than 0.5 (Tables 7-6) for all the gauges during the calibration period. In summary, the model performance evaluation measures suggest an overall good agreement between observed and simulated flows at the annual and monthly time step, throughout the river basin.

Annual and monthly flow results for the above listed gauging stations for validation period are shown in (Figure 7-7, and 7-8 and tables 7-7 and 7-8). Except for the Minnesota River (Jordan, MN) at an annual time step and the Mississippi river (Clinton, IA) at an annual time step, all the other gauges show acceptable predictions from model. For the gauges at Jordan, MN and Clinton, IA the NSE values were low because of under-estimation. In addition, for the same gauging stations, we have acceptable performance in monthly time steps. In summary, HUMUS-SWAT is able to capture the annual and monthly flow patterns very well in the Upper Mississippi river basin.

7.4.2 CALIBRATION/VALIDATION OF SEDIMENT, NUTRIENT, AND PESTICIDE CONCENTRATION AT THE USGS GAUGING STATIONS

Sediment and nutrient (various forms of nitrogen and phosphorus) calibration was a challenging task. Similar to flow, water quality data were not available at the 8-digit watershed (spatial) scale. As well, continuous data from the gauging stations selected for validation is not available for sediments, nutrients, and pesticides. Therefore, the regular split sample procedure for calibration and validation was not done because of limited availability of data. Instead, the entire set of available water quality loads were used to validate the quality of model predictions for each water quality parameter (e.g. ammonia nitrogen validation).

Limited water quality data available from USGS under their regular monitoring program and a special program, NASQAN, were used for validation of predicted results from the UMRB. Grab samples of monitored data of suspended sediment, and atrazine were available from USGS for selected gauging stations. Typically there were 10-20 samples per year available for a few years. These grab sample concentrations, along with observed daily flow (because instantaneous flow is not available for all the corresponding water quality grab samples) is input to a load estimator program (Runkel et al., 2004) to estimate annual average loads of suspended sediment and atrazine. Uncertainty limits were estimated by the program whenever there were adequate grab samples.

The NASQAN data set provides monthly and annual average nutrient loads with uncertainty limits wherever possible. For this dataset, nutrient fluxes are estimated using an adjusted maximum likelihood estimate, a type of regression-model method and a composite method using various components of nutrient observations (nitrate nitrogen, ammonia nitrogen, orthophosphate etc.) monitored from 1960 through 2005 (Aulenbach et al., 2007). Nutrient flux estimates are provided for six water-quality constituents: dissolved nitrite plus nitrate, total organic nitrogen plus ammonia nitrogen (total Kjeldahl nitrogen), dissolved ammonia, total phosphorous, dissolved orthophosphate, and dissolved silica. For this study reported annual loads (of water years) from NASQAN were not used. Instead, the annual loads for calendar years were aggregated from monthly loads.

Simulated annual average pollutant loads corresponding to the years of available observed/estimated calibration target loads were used to validate the water quality predictions

from model. Wherever possible, uncertainty limits of observations/estimated targets for calibration were presented to make reasonable judgments on model predictive capability. For all the gauging stations selected for validation, the predicted pollutant loads were compared against the observed/estimated targets using graphs with error bars. To limit the content of this appendix, graphs for only three (out of six) stations were presented. However, comparison of annual predicted and target means were presented for all the water quality parameters in tables.

In the UMRB, a major portion of the river basin is cultivated. Therefore, water quality validation relies heavily on APEX's results. For cultivated land, after making sure that the fertilizer/manure rates and nutrient dynamics are reasonable, limited parameter adjustment is performed based on over or under-estimation of predicted results when compared to observed data. Delivery ratios were used for transport of sediment, nutrient and pesticide from edge-of-field to the 8-digit watershed outlet. Water quality calibration/validation for HUMUS-SWAT is described in the following sections.

7.4.2.1 SEDIMENT CALIBRATION IN HUMUS-SWAT

For calibration of sediment yield simulated for un-cultivated land-use, soil erosion and sediment routing parameters within SWAT were adjusted. The soil erodibility factor (K) was adjusted within reasonable uncertainty ranges when there was under/over-prediction of sediment. The delivery ratio that accounts for losses occurring from the fields to the 8-digit watershed outlet was also adjusted. (See Appendix G for details.)

The in-stream sediment-related parameters such as SPCON and SPEXP within SWAT were adjusted for the channel and flood plain deposition and degradation to be realistic. SWAT uses the modified Bagnold stream power equation for channel sediment routing (Arnold et al., 1995; Neitsch et al., 2002). In this equation, the maximum amount of sediment that can be transported by water from a reach segment is related to the peak channel velocity estimated for each 8-digit channel reach using a linear parameter (SPCON) and exponential parameter (SPEXP). SPCON is the linear parameter used for calculating the maximum amount of sediment that can be re-entrained during channel sediment routing. It is a user defined coefficient and varies between 0.0001 and 0.03. For the CEAP national assessment for UMRB this was set to 0.03. SPEXP is an exponent parameter used for calculating the maximum

amount of sediment that can be re-entrained during channel sediment routing. It can vary between 1.0 and 2.0. For UMRB, this parameter was set at 1.0. These two parameters were calibrated to match the observed sediment load at selected gauging stations for validation. In addition, the sediment routing process was modified considering the cumulative drainage area and an exponential coefficient at main reach along the Upper Mississippi river to account for channel losses to be realistic for the CEAP National Assessment (Barry et al., 2005).

Predicted sediment results were validated in 5 different gauging stations (Fig 7-1) in UMRB as outlined in Table 7-9. To limit the contents of this section, detailed results are shown only for three locations. However, the means are shown for all stations (Table 7-9). Figure 7-9 shows a detailed comparison of predicted and target sediment loads in Mississippi river at Clinton, IA, Illinois river at Valley City, IL and Mississippi river at Alton/Grafton, IL. In general, there are under and over-estimations (Table 7-9, Figure 7-12) of annual sediment load in different locations. For gauges in Valley City, IL and Grafton/Alton, IL there is close match between predictions and target values of sediment load (Figure 7-9). In other places the predicted loads are within an order of magnitude from the target values. Uncertainty limits were not available to make any further judgment on the quality of predicted results. However, considering the quality of predicted sediment loads in all the places of validation, we could say the model results are adequate for making scenario trials.

7.5 NUTRIENT CALIBRATION

Whenever there is over or under-estimation of nutrients, the first item checked is the rate of application of fertilizer/manure for the crops and pasture/hay. The second item checked is the nutrient dynamics and partitioning of applied nutrients (i.e. transformation between different pools of N and P such as mineral, organic, soluble, sediment bound etc.). If the above two are reasonable and still there is a mismatch between predictions and target values, then parameterization is attempted.

7.5.1 NITROGEN CALIBRATION IN HUMUS-SWAT

For un-cultivated land, once the rates and nutrient dynamics are reasonable, upland parameters (basin level) such as the nitrogen uptake distribution parameter (UBN) and nitrogen percolation coefficient (NPERCO) were adjusted to match the predicted nutrient load with that of target. UBN changes the plant uptake of applied nitrogen and NPERCO changes the proportion of soluble N available for surface runoff and leaching. If results are still unacceptable, the in-stream nutrient sensitive parameters were adjusted (e.g. for nitrogen it is hydrolysis rate constant (BC3) of nitrogen (N to NH_4)).

7.5.2 PHOSPHORUS CALIBRATION IN HUMUS-SWAT

The basin level parameters adjusted are phosphorus uptake distribution parameter (UBP), phosphorus percolation coefficient (PPERCO) and phosphorus soil partitioning coefficient (PHOSKD). In the model they affect plant uptake of applied phosphorus, proportion of soluble P available for surface runoff and leaching and partitioning of phosphorus between soluble and sediment bound phases. The in-stream phosphorus parameters used in calibration are: (1) Mineralization rate (BC4) of organic phosphorus (organic P to Soluble P); and (2) Benthic source rate (RS2) for soluble P in the reach.

Predicted nutrient results were validated in six gauging stations (Figure 7-1) in UMRB as outlined in Table 7-10, and Table 7-11. To limit the contents of this section, detailed results are shown for three locations only. However, the predicted and target means are shown for all the six stations (Table 7-10 and Table 7-11). Figures 7-10 through 7-14 show a detailed comparison of predicted and target nutrient loads (various constituents of N and P) in Mississippi river at Clinton, IA, Illinois River at Valley City, IL and Mississippi river at Alton/Grafton, IL. Error bars or the upper and lower confidence levels of target values are also presented. In general, the predicted nutrient loads from HUMUS-SWAT are in good agreement with the target values and within the uncertainty limits of target values for a majority of the nutrient constituent-location combination suggesting the suitability of the model for making scenario trials.

7.5.3 PESTICIDE CALIBRATION IN HUMUS-SWAT

Similar to sediment, only limited grab sample data was available for calibration of pesticides. It is very likely that many different pesticides were applied to crop and non-crop areas in the river basin. However, for this UMRB study, only the fate and transport of atrazine is considered. The only source of atrazine load is cultivated land; point sources and uncultivated land had no atrazine contributions. Therefore, the overall quality of predicted atrazine results depend on APEX results for cultivated land. After incorporating APEX output, if there is a disagreement between predictions and target values, in-stream pesticide parameters such as pesticide reaction coefficient in reach (CHPST_REA) (function of pesticide aquatic half-life), and the pesticide water/sediment partitioning coefficient were attempted to improve the model predictions.

Predicted atrazine results were validated in four gauging stations in UMRB as outlined in Table 7-12, Figure 7-15. To limit the contents of this appendix, detailed results are shown for three locations only. However, the predicted and target annual means are shown for all the four stations (Table 7-12). Figure 7-15 show a detailed comparison of predicted and target atrazine loads in Mississippi river at Clinton, IA, Illinois river at Valley City, IL and Mississippi river at Alton/Grafton, IL. In general, the pattern/trend of predicted atrazine loads from HUMUS-SWAT is in good agreement with the target values for all the gauges selected for validation. However, atrazine loads are under-estimated in Illinois river at Valley City and Mississippi river at Grafton/Alton, IL. The under-estimation can be attributed to uncertainties in observations, procedure used to obtain annual loads from daily grab samples, model input in particular the management operations, inadequate accounting some of the possible sources etc. Within the limited time given for calibration, it was only possible to check the rates, proportion of constituents (soluble vs. sorbed) etc. Further investigation into the above mentioned items could have improved our estimates. The same reasons could be attributed to the few mismatches in sediment and nutrient loads.

In this study, two models, APEX and SWAT were used for modeling cultivated and uncultivated land respectively. Therefore, the calibration/validation process involves many back and forth efforts. First the APEX model is calibrated, and then SWAT. After verifying the in-stream flow and pollutant loads feedback was given to APEX or HUMUS-SWAT team

depending on the possible source of problems in cultivated/un-cultivated land. After identifying the source of problems, the necessary remedial measures were attempted.

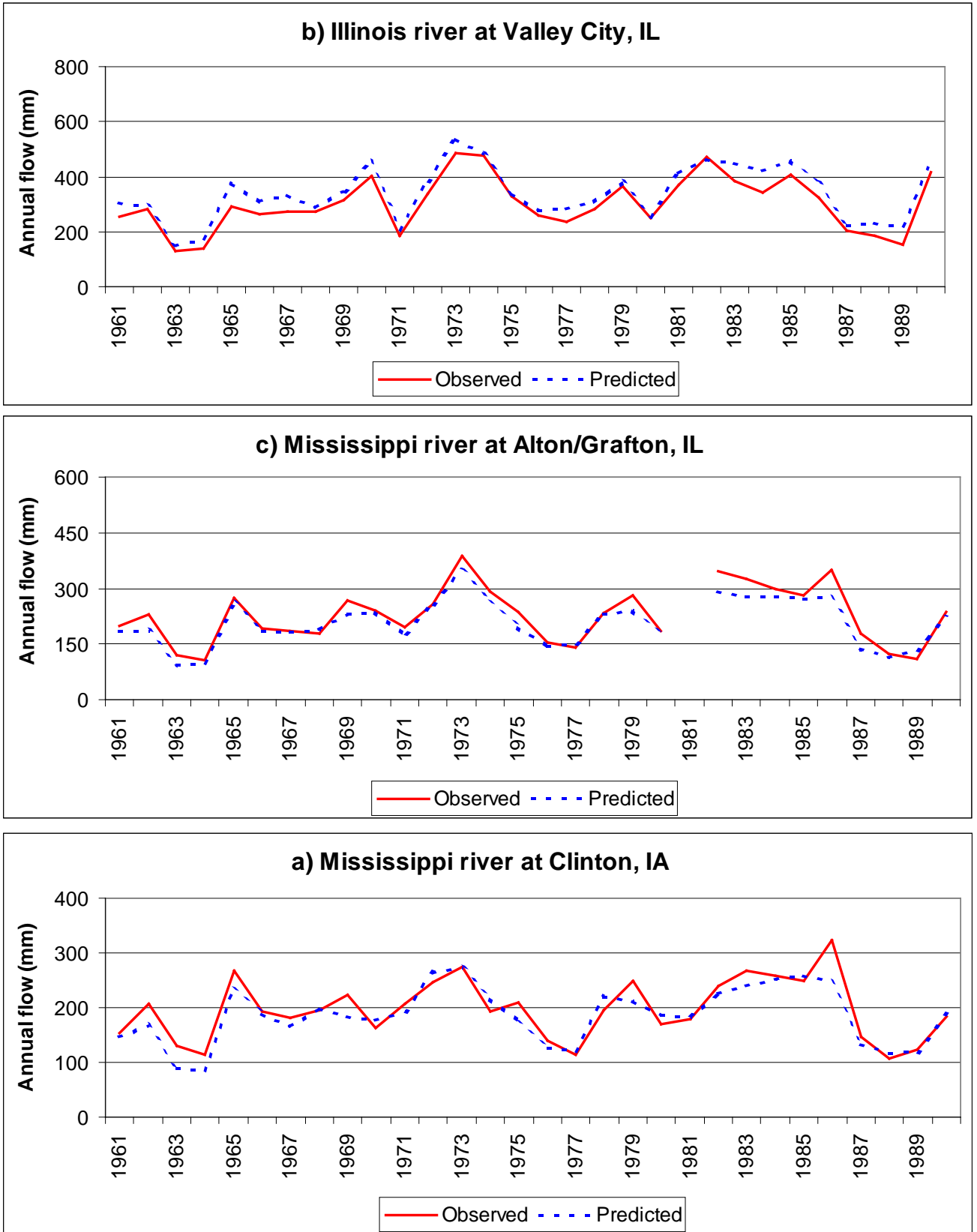


Figure 7-5 Average annual stream flow for the Upper Mississippi river basin-Calibration period.

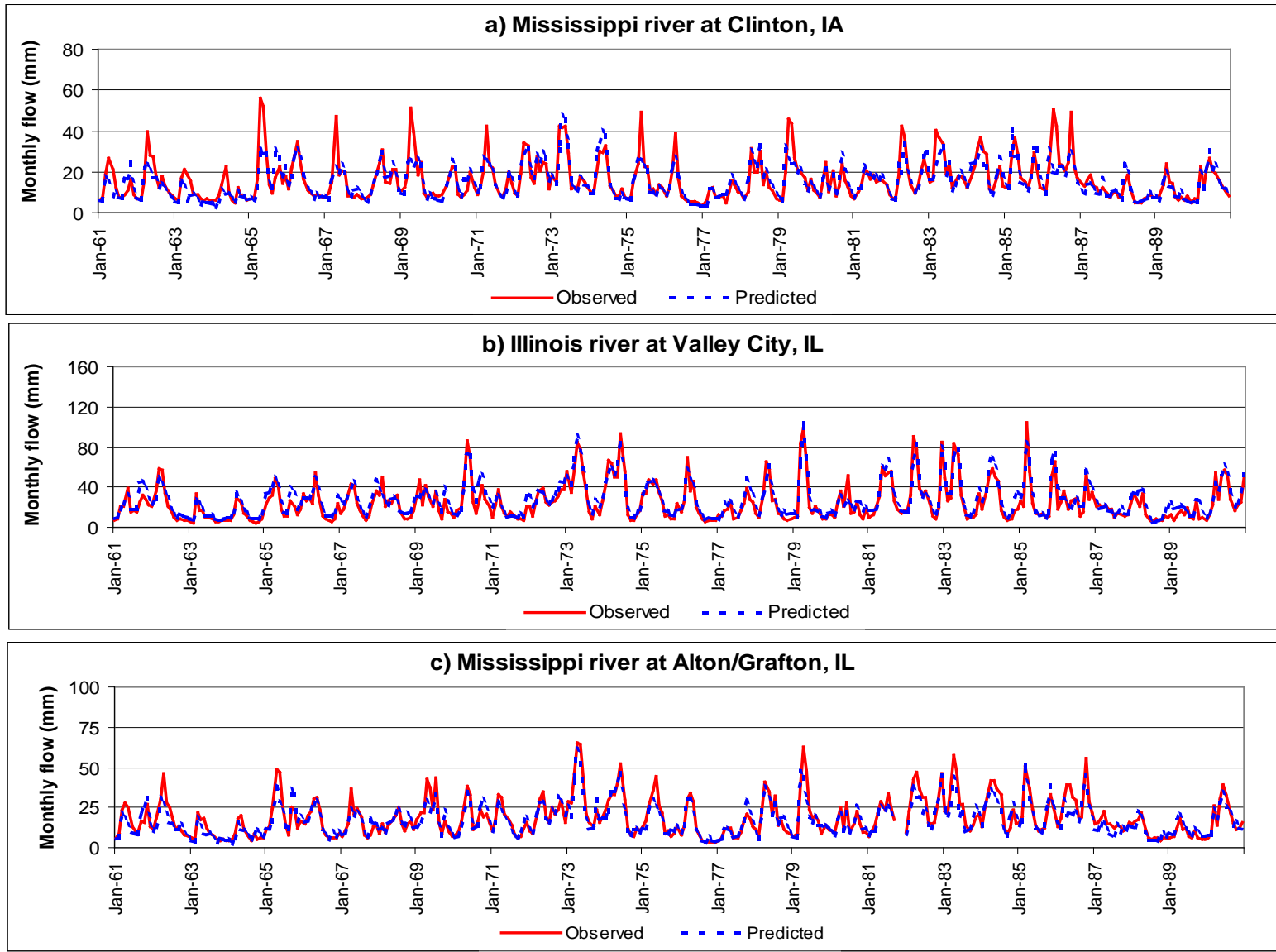


Figure 7-6 Average monthly stream flow for the Upper Mississippi river basin-Calibration period.

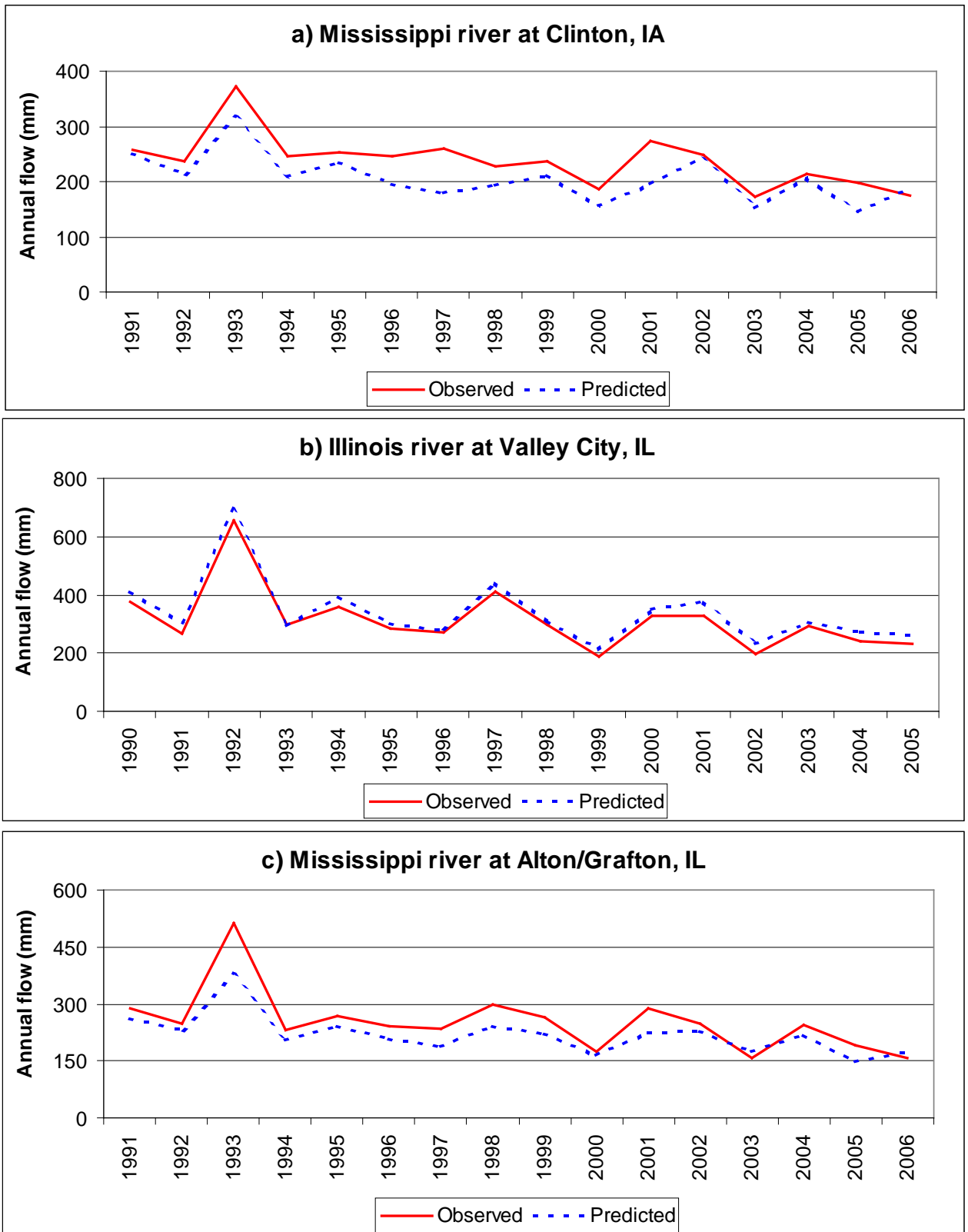


Figure 7-7 Average annual stream flow for the Upper Mississippi river basin-Validation period.

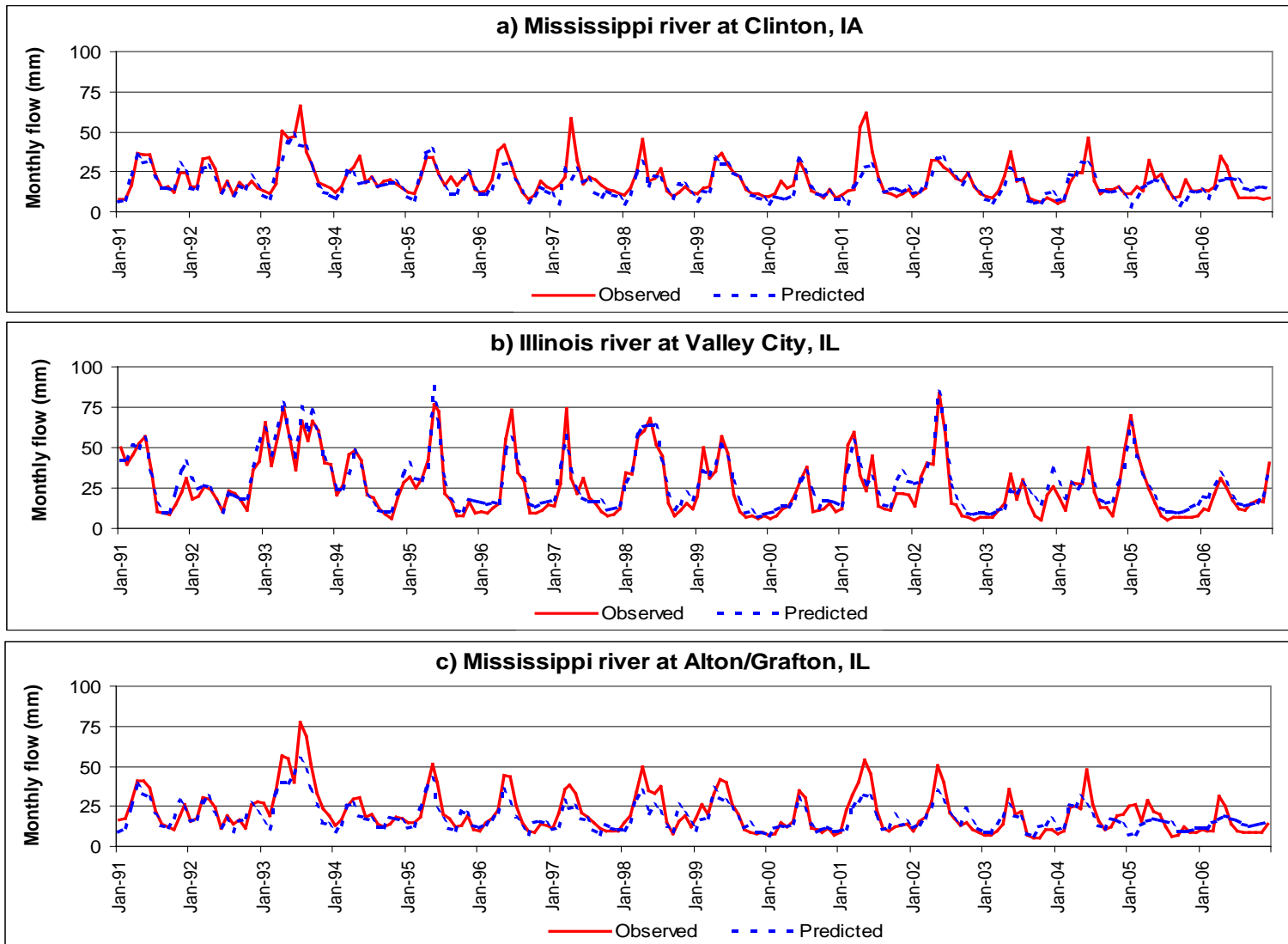


Figure 7-8 Average monthly stream flow for the Upper Mississippi river basin-Validation period.

Table 7-5. Mean and standard deviation of the predicted and observed annual and monthly stream flow at selected gauging stations for the calibration period

	Jordan, MN	Clinton, IA	Wapello, IA	Valley City, IL	Alton/Grafton, IL
Gauge details					
River	Minnesota river	Mississippi river	Iowa river	Illinois river	Mississippi river
River reach-HUC	7020012	7080101	7080209	7130011	7110009
Drainage area (Km ²)	41,957.80	221,704.00	32,374.90	69,264.10	444,183.00
Data availability (period)	1961-1986, 1989-1990	1961-1990	1961-1990	1961-1990	1961-1990
Mean flow (mm)					
Annual-Predictions	87.8	185.9	193	339	207.6
Annual-Observations	92.5	196.8	233.3	302.8	227.6
Monthly-Predictions	7.1	15.5	16.1	28.3	17.3
Monthly-Observations	8.7	16.2	19.5	25.3	18.7
Standard deviation (mm)					
Annual-Predictions	41.2	52.5	82.4	100.2	63.6
Annual-Observations	55.3	55	108.7	97.9	75.5
Monthly-Predictions	8.7	8.5	16	17.8	10
Monthly-Observations	10.5	9.9	16.6	18.7	11.9

Table 7-6. Coefficient of determination and efficiency of the predicted and observed annual and monthly stream flow at selected gauging stations for the calibration period

	Jordan, MN	Clinton, IA	Wapello, IA	Valley City, IL	Alton/Grafton, IL
Gauge Details					
River River reach-HUC	Minnesota river 7020012	Mississippi river 7080101	Iowa river 7080209	Illinois river 7130011	Mississippi river 7110009
Drainage area (Km ²)	41,957.80	221,704.00	32,374.90	69,264.10	444,183.00
Data availability (period)	1961-1986, 1989- 1990	1961-1990	1961-1990	1961-1990	1961-1990
R²					
Annual	0.82	0.83	0.92	0.94	0.93
Monthly	0.66	0.68	0.66	0.89	0.84
Nash and Sutcliffe Efficiency					
Annual	0.79	0.79	0.74	0.8	0.85
Monthly	0.65	0.67	0.59	0.86	0.82

Table 7-7. Mean and standard deviation of the predicted and observed annual and monthly stream flow at selected gauging stations for the validation period (1991-2006)

	Jordan, MN	Clinton, IA	Wapello, IA	Valley City, IL	Alton/Grafton, IL
Gauge Details					
River	Minnesota river	Mississippi river	Iowa river	Illinois river	Mississippi river
River reach-HUC	7020012	7080101	7080209	7130011	7110009
Drainage area (Km ²)	41,957.80	221,704.00	32,374.90	69,264.10	444,183.00
Data availability (period)	1991-2006	1991-2006	1991-2006	1991-2006	1991-2006
Mean flow (mm)					
Annual-Predictions	96.8	205.6	203.1	339.4	218.8
Annual-Observations	150.7	237.6	287.9	314	253.3
Monthly-Predictions	8.1	17.1	16.9	28.3	18.2
Monthly-Observations	13.1	19.5	24	26.2	20.8
Standard deviation (mm)					
Annual-Predictions	46.8	42.3	110.1	113.9	52.8
Annual-Observations	70.2	47.6	163.9	109.6	82.6
Monthly-Predictions	9.4	8.6	18.3	17.1	8.8
Monthly-Observations	15.3	11	24.1	18.6	12.9

Table 7-8. Coefficient of determination and efficiency of the predicted and observed annual and monthly stream flow at selected gauging stations for the validation period (1991-2006)

	Jordan, MN	Clinton, IA	Wapello, IA	Valley City, IL	Alton/Grafton, IL
Gauge Details					
River	Minnesota river	Mississippi river	Iowa river	Illinois river	Mississippi river
River reach-HUC	7020012	7080101	7080209	7130011	7110009
Drainage area (Km ²)	41,957.80	221,704.00	32,374.90	69,264.10	444,183.00
Data availability (period)	1991-2006	1991-2006	1991-2006	1991-2006	1991-2006
R²					
Annual	0.87	0.7	0.97	0.99	0.92
Monthly	0.69	0.66	0.79	0.91	0.78
Nash and Sutcliffe Efficiency					
Annual	0.17	0.21	0.62	0.93	0.63
Monthly	0.54	0.61	0.69	0.89	0.7

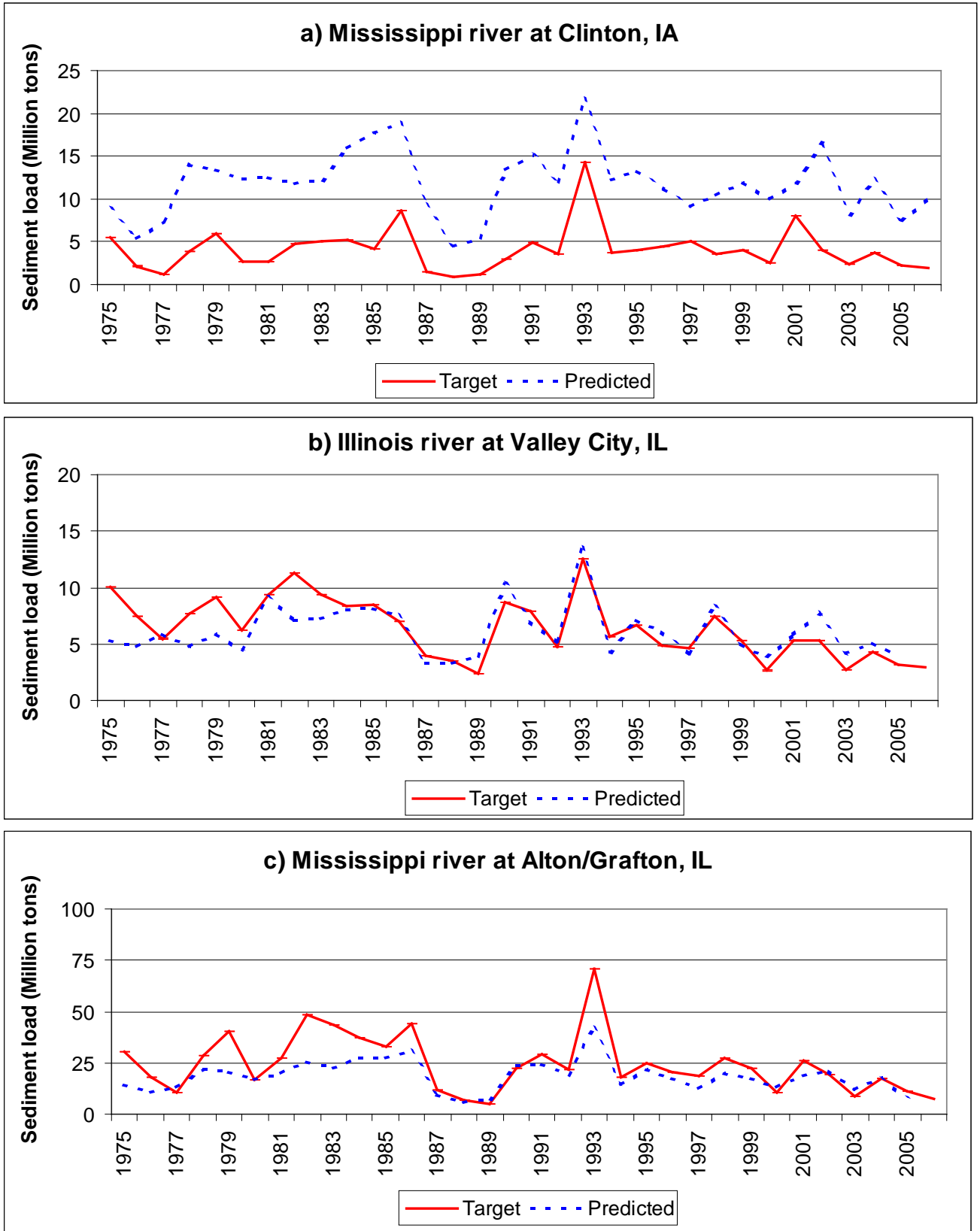


Figure 7-9 Average annual sediment load for the Upper Mississippi river basin

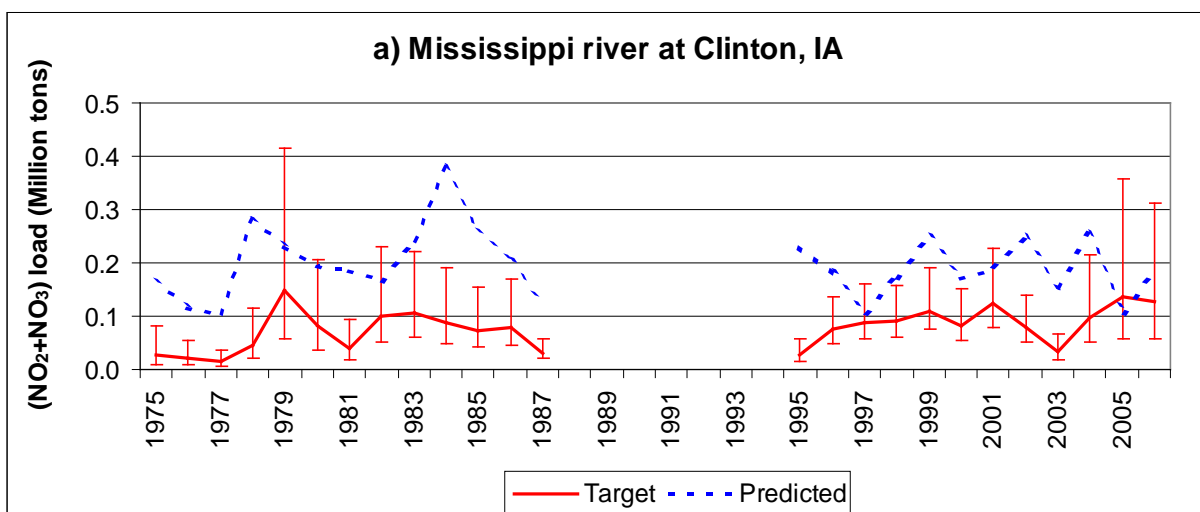
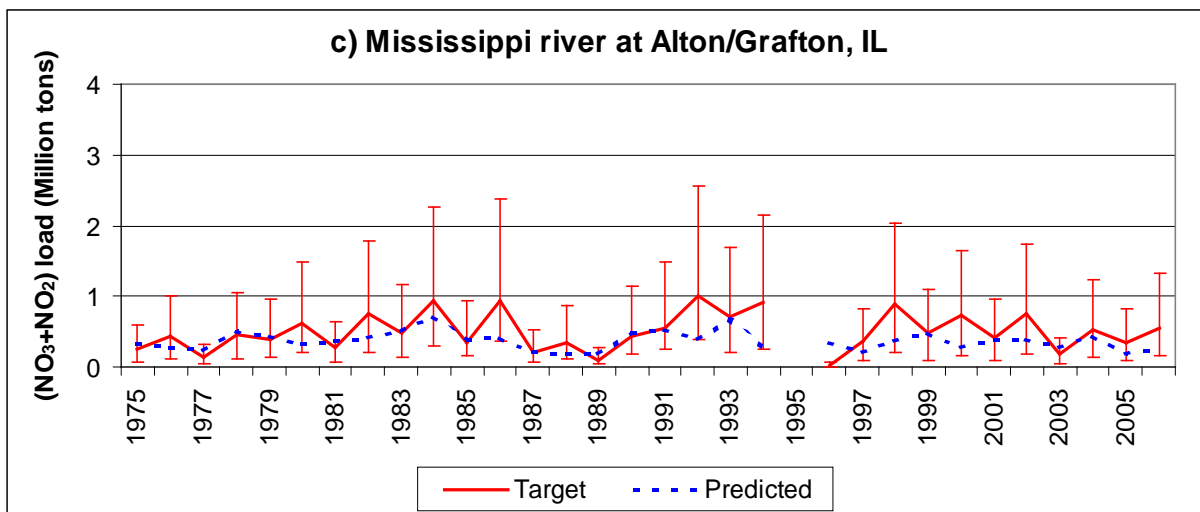
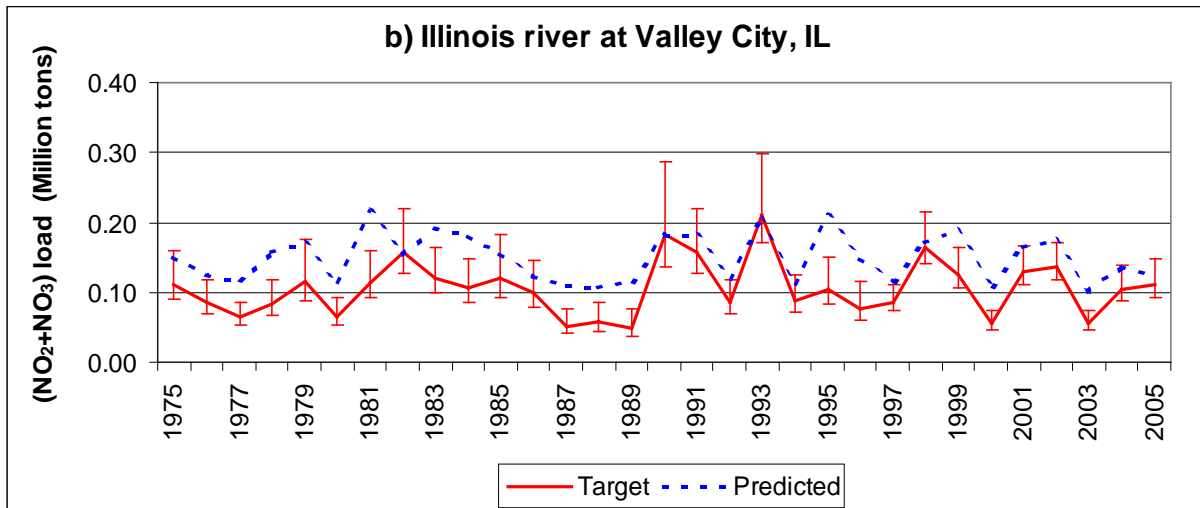


Figure 7-10 Average annual nitrite and nitrate Nitrogen (NO₂+NO₃) load for the Upper Mississippi river basin

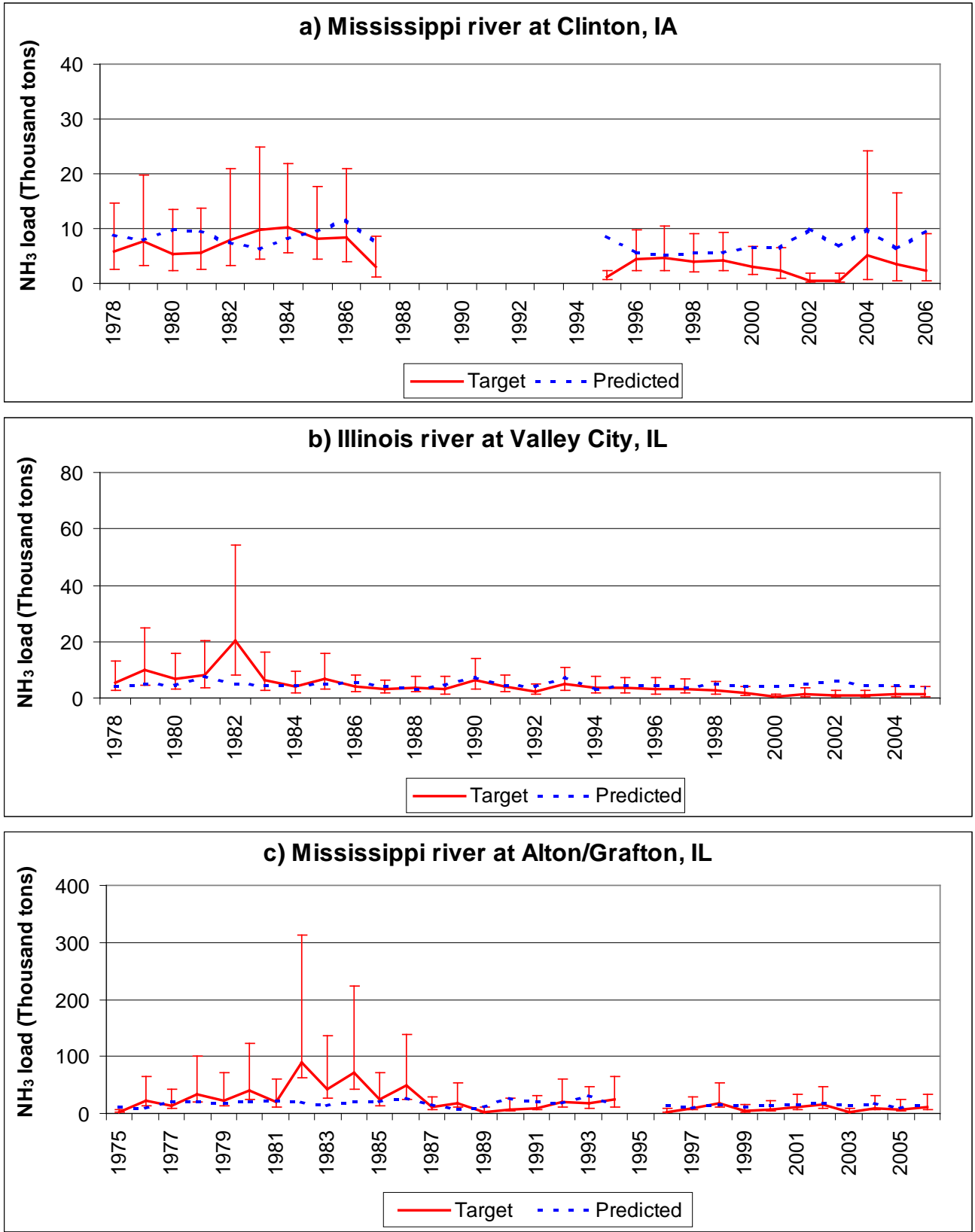


Figure 7-11 Average annual ammonia Nitrogen (NH₃) load for the Upper Mississippi river basin.

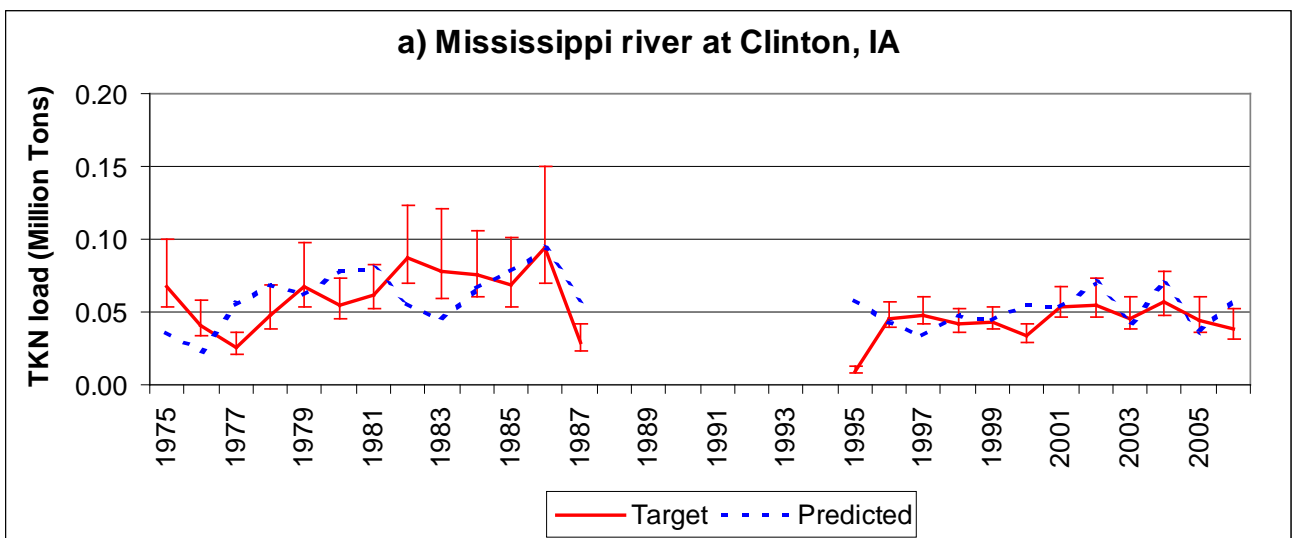
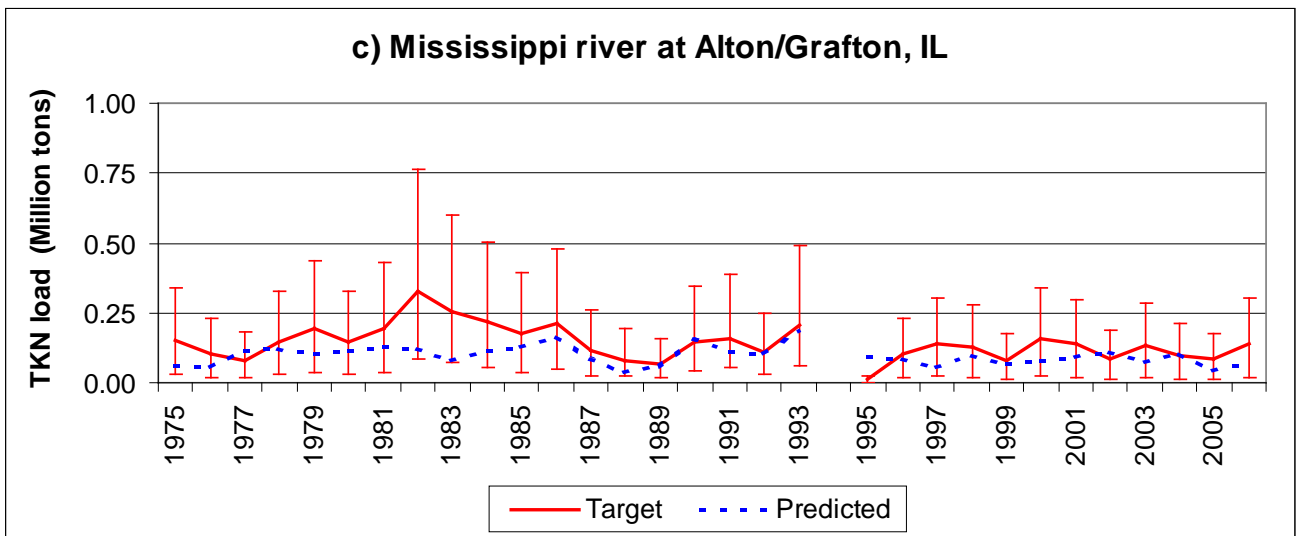
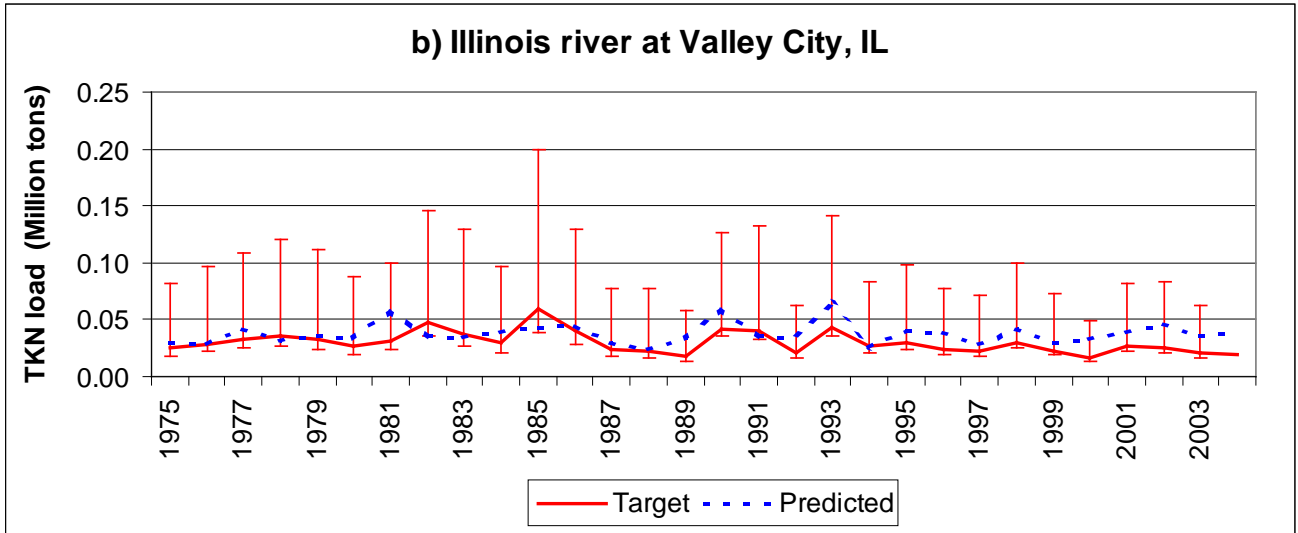


Figure 7-12. Average annual total Kjeldahl Nitrogen (TKN) load for the Upper Mississippi river basin.

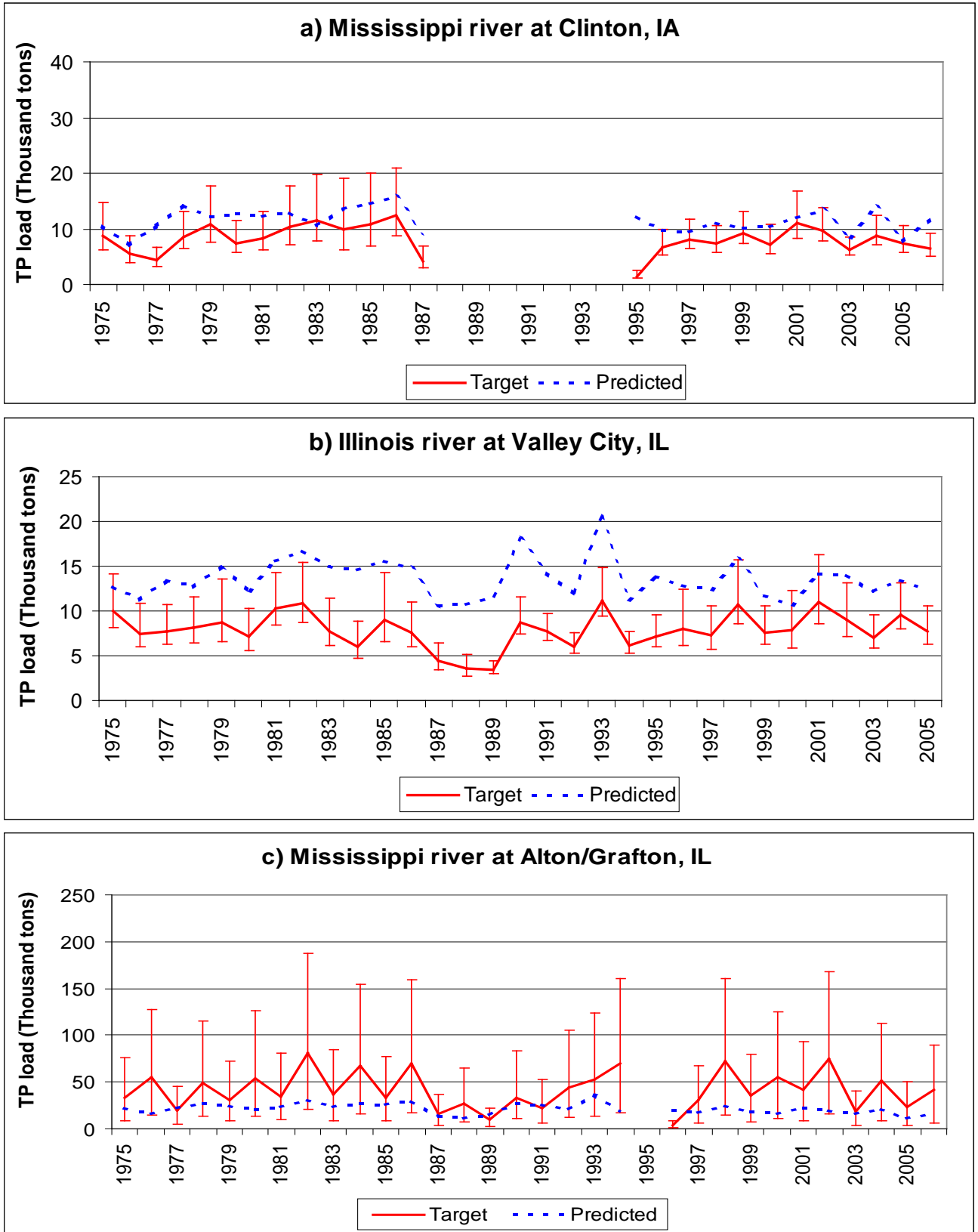


Figure 7-13. Average annual total Phosphorus (TP) load for the Upper Mississippi river basin

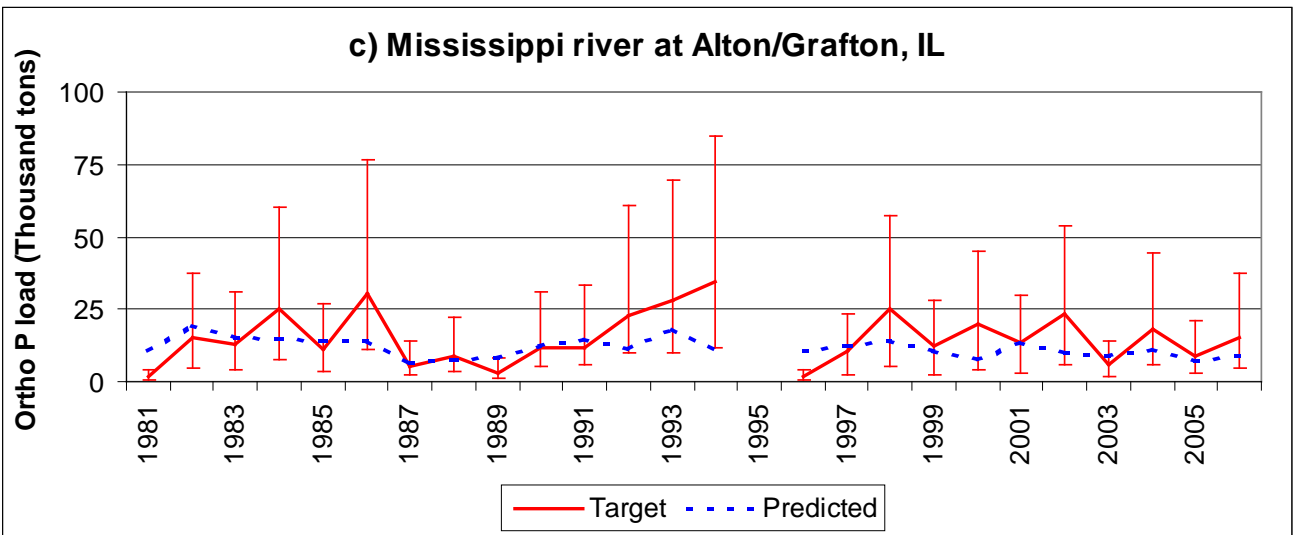
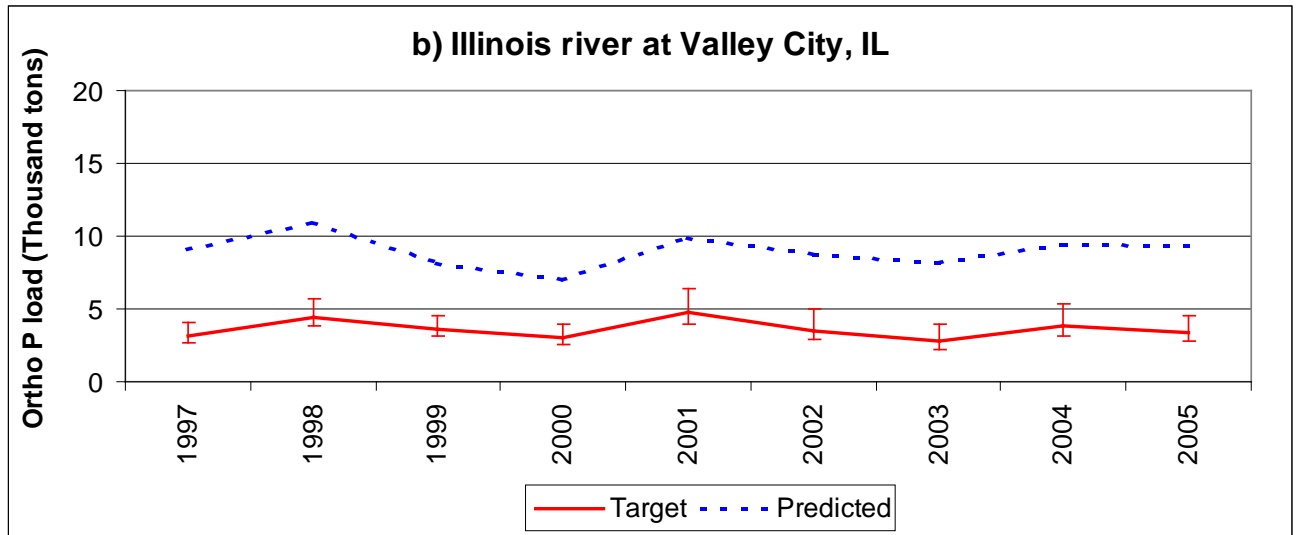
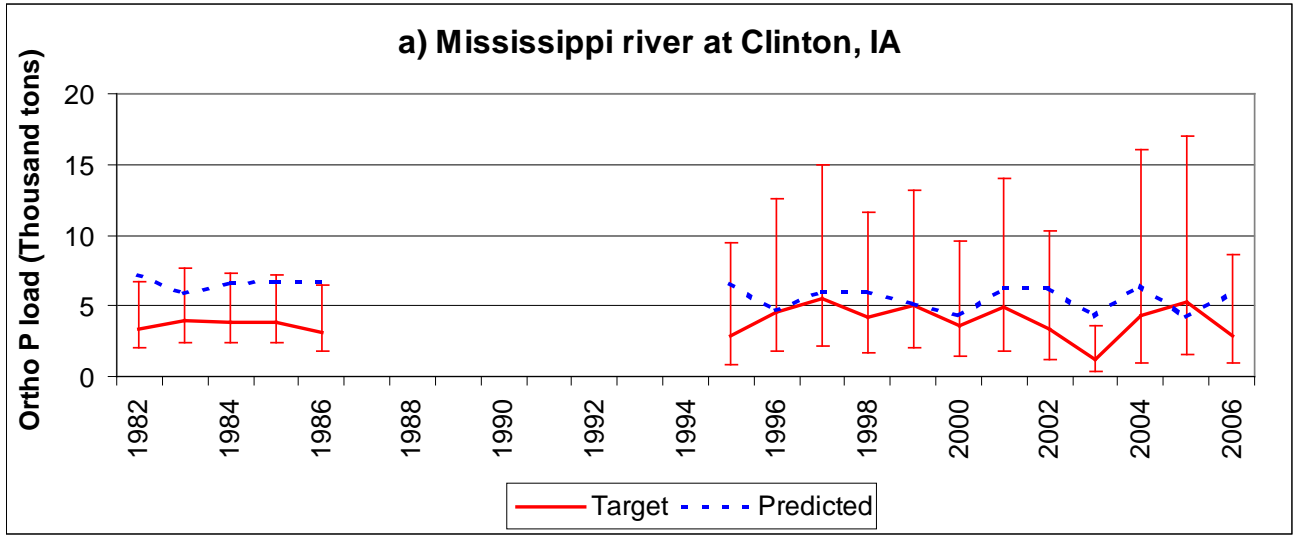


Figure 7-14. Average annual Ortho Phosphate (ortho-P) load for the Upper Mississippi river basin

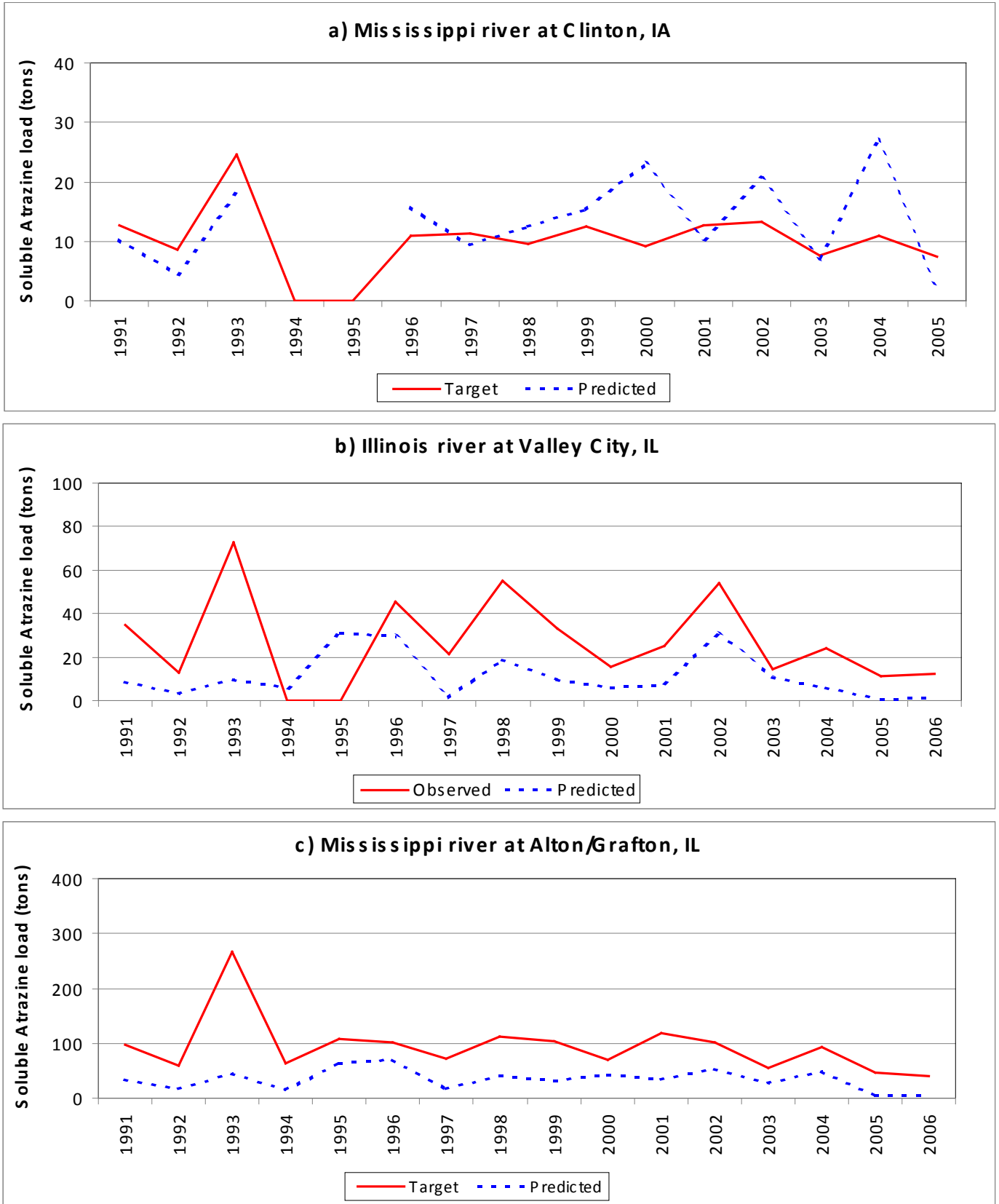


Figure 7-15. Average annual soluble Atrazine load for the Upper Mississippi river basin

Table 7-9. Average annual Suspended Sediment load at selected gauging stations

River-Gauging station-Location	Reach (HUC)	Predicted (tons)	Observed (tons)
Minnesota river at Jordan, MN	07020012	770,013	1,265,214
Mississippi river at Clinton, IA	07080101	11,725,219	4,088,298
Iowa river at Wapello, IA	07080209	1,449,519	3,632,896
Illinois river at Valley City, IL	07130011	6,068,781	6,398,700
Mississippi river at Grafton/Alton, IL	07110009	18,253,219	24,314,751

Table 7-10a. Average annual Nitrate and Nitrite Nitrogen load at selected gauging stations

River-Gauging station-Location	Reach (HUC)	Predicted (tons)	Observed (tons)
Minnesota river at Jordan, MN	07020012	41,123	64,200
Mississippi river at Hastings, MN	07010206	53,204	43,969
Mississippi river at Clinton, IA	07080101	196,060	76,982
Iowa river at Wapello, IA	07080209	40,183	65,402
Illinois river at Valley City, IL	07130011	148,838	105,404
Mississippi river at Grafton/Alton, IL	07110009	366,170	502,821

Table 7-10b Average annual Total Kjeldahl Nitrogen load at selected gauging stations

River-Gauging station-Location	Reach (HUC)	Predicted (tons)	Observed (tons)
Minnesota river at Jordan, MN	07020012	6,013	7,223
Mississippi river at Hastings, MN	07010206	10,420	17,873
Mississippi river at Clinton, IA	07080101	56,276	52,453
Iowa river at Wapello, IA	07080209	12,736	15,214
Illinois river at Valley City, IL	07130011	37,584	23,302
Mississippi river at Grafton/Alton, IL	07110009	97,471	141,509

Table 7-10c Average annual Ammonia Nitrogen load at selected gauging stations

River-Gauging station-Location	Reach (HUC)	Predicted (tons)	Observed (tons)
Minnesota river at Jordan, MN	07020012	820	747
Mississippi river at Hastings, MN	07010206	1,132	1,728
Mississippi river at Clinton, IA	07080101	7,831	4,896
Iowa river at Wapello, IA	07080209	1,453	1,360
Illinois river at Valley City, IL	07130011	4,797	4,419
Mississippi river at Grafton/Alton, IL	07110009	16,681	20,587

Table 7-11a Average annual Total Phosphorus load at selected gauging stations

River-Gauging station-Location	Reach (HUC)	Predicted (tons)	Observed (tons)
Minnesota river at Jordan, MN	07020012	1,420	1,321
Mississippi river at Hastings, MN	07010206	2,902	3,188
Mississippi river at Clinton, IA	07080101	11,425	8,077
Iowa river at Wapello, IA	07080209	2,867	2,979
Illinois river at Valley City, IL	07130011	13,597	7,889
Mississippi river at Grafton/Alton, IL	07110009	21,351	41,493

Table 7-11b Average annual Ortho Phosphate load at selected gauging stations

River-Gauging station-Location	Reach (HUC)	Predicted (tons)	Observed (tons)
Minnesota river at Jordan, MN	07020012	825	613
Mississippi river at Hastings, MN	07010206	1,655	1,368
Mississippi river at Clinton, IA	07080101	5,840	3,874
Iowa river at Wapello, IA	07080209	1,525	1,510
Illinois river at Valley City, IL	07130011	8,964	3,593
Mississippi river at Grafton/Alton, IL	07110009	11,698	15,123

Table 7-12 Average annual Atrazine load at selected gauging stations

River-Gauging station-Location	Reach (HUC)	Predicted (tons)	Observed (tons)
Mississippi river at Clinton, IA	07080101	13.5	10.1
Iowa river at Wapello, IA	07080209	6.7	10.2
Illinois river at Valley City, IL	07130011	11.3	27.0
Mississippi river at Grafton/Alton, IL	07110009	34.1	94.3

7.6 REFERENCES

- Arnold, J.G., J.R. Williams, and D.A. Maidment., 1995. Continuous-time water and sediment-routing model for large basins *Journal of Hydraulic Engineering-ASCE*. 121(2); 171-183
- Arnold, J.G, R.S. Muttiah, R. Srinivasan, and P.M. Allen, 2000. Regional estimation of base flow and groundwater recharge in the Upper Mississippi River Basin. *Journal of Hydrology* 227:21-40.
- Aulenbach, B.T., Buxton, H.T., Battaglin, W.T., and Coupe R.H., 2007, Stream flow and nutrient fluxes of the Mississippi-Atchafalaya River Basin and subbasins for the period of record through 2005: U.S. Geological Survey Open-File Report 2007-1080
- Barry, J. J., Buffington, J. M. and J. G. King, 2005. A general power equation for predicting bed load transport rates in gravel bed rivers. *Water Resources Research*, 41. W07016, DOI: 1029/2005WR04172.
- Gebert, W.A., D.J. Graczyk, and W.R. Krug. 1987. Annual average runoff in the United States, 1951–1980: US Geological Survey Hydrologic Investigations Atlas HA-710, 1 sheet, scale 1:7,500,000.
- Hargreaves, G.H., and Samani. Z.A. 1985. Reference crop evapotranspiration from temperature. *Applied Engineering in Agriculture* 1(2), 96-99
- Hargreaves G.H., and Allen, R.G. 2003. History and evaluation of Hargreaves evapotranspiration equation. *Journal of Irrigation and Drainage Engineering*, 129(1), 53-63.
- Kannan N., C. Santhi, J. R. Williams and J. G. Arnold. 2008. Development of a continuous soil moisture accounting procedure for curve number methodology and its behavior with different evapotranspiration methods. *Hydrological Processes*, 22, 2114-2121 DOI: 10.1002/hyp.6811
- Kannan. N., C. Santhi , and J.G. Arnold, 2008. Development of an automated procedure for estimation of the spatial variation of runoff in large river basins. *Journal of Hydrology* 359:1–15. (doi:10.1016/j.jhydrol.2008.06.001)
- Moriasi, D.N., J.G. Arnold, M.W. Van Liew, R.L. Bingner, R.D. Harmel, and T.L. Veith. 2007. Model Evaluation Guidelines for Systematic Quantification of Accuracy in Watershed Simulations. *Transactions of the American Society of Agricultural and Biological Engineers* 50(3):885-900.

- Nash, J.E., and J.V. Sutcliffe. 1970. River flow forecasting through conceptual models. Part 1: A discussion of principles. *Journal of Hydrology* 10(3): 282-290.
- Neitsch, S.L., J.G. Arnold, J.R. Kiniry, J.R. Williams, and K.W. King. 2002. Soil and Water Assessment Tool (Version 2000) Theoretical Documentation: GSWRL Report 02-01, BRC Report 02-05, Publ. Texas Water Resources Institute, TR-191. College Station, TX, 458pp.
- Runkel, R.L., Crawford, C.G., and Cohn, T.A., 2004, Load Estimator (LOADEST): A FORTRAN Program for Estimating Constituent Loads in Streams and Rivers: U.S. Geological Survey Techniques and Methods Book 4, Chapter A5, 69 p.
- Santhi, C., Arnold, J. G., Williams, J. R., Dugas, W. A., Srinivasan, R., Hauck, L. M., 2001. Validation of the SWAT model on a large river basin with point and nonpoint sources. *Journal of the American Water Resources Association* 37(5), 1169-1188.
- Santhi, C., N. Kannan, J.G. Arnold, and M. Di Luzio. 2008a. Spatial calibration and temporal validation of flow for regional scale hydrologic modeling. *Journal of the American Water Resources Association (JAWRA)* 44(4):829-846. (doi: 10.1111 / j.1752-1688.2008.00207.x)
- Santhi, C., P.M. Allen, R.S. Muttiah, J.G. Arnold, and P. Tuppad. 2008b. Regional estimation of base flow for the conterminous United States by hydrologic landscape regions, *Journal of Hydrology*, 351:139–153. doi:10.1016/j.jhydrol.2007.12.018.
- Wang, X., S.R. Potter, J.R. Williams, J.D. Atwood, T. Pitts. 2006. Sensitivity analysis of APEX for national assessment. *Transactions of the American Society of Agricultural Engineers* 49(3):679-688.
- Williams, J. R., E. Wang, A. Meinardus, and W. L. Harman. 2003. APEX user's guide. Temple, Texas: Blackland Research and Extension Center.

